Journal Name

COMMUNICATION

Catalytic asymmetric aza-Michael addition of fumaric monoacids with multifunctional thiourea/boronic acids

Kenichi Michigami, Hiroki Murakami, Takeru Nakamura, Noboru Hayama, and Yoshiji Takemoto*

Received 00th January 20xx,
Accepted 00th January 20xx

DOI: 10.1039/x0xx00000x

www.rsc.org/

The first chemical enantioselective synthesis of *N*-hydroxyaspartic acid derivatives using chiral multifunctional thiourea/boronic acid organocatalysts was developed. A series of fumaric monoacids underwent an intermolecular asymmetric aza-Michael addition of *O*-alkyl hydroxylamines in excellent regioselectivity. The addition of another carboxylic acid raised the enantiomeric enrichment up to 97% ee. *O*-Deprotection of the aza-Michael adduct provided an aspartate-derived hydroxylamine fragment applicable for KAHA (α-keto acid-hydroxylamine) ligation.

Chemoselective peptide conjunction by enzymes is a ubiquitous process in nature, producing only recyclable phosphates as by-products.[1] Meanwhile, a general chemical approach for the amide C–N bond formation is based on stoichiometric activation of carboxylic acids by coupling reagents.[2] Though this method is highly reliable, reagent-derived non-recyclable side products are inevitably generated. In addition, protection of nucleophilic functional groups is required due to incompatibility with condensation reagents. The development of environmentally benign alternatives is thus highly demanded.[3] Among large numbers of strategies reported to circumvent these issues, elegant examples have been disclosed in recent years by Bode and co-workers. The protocol of simply mixing α-keto acids and hydroxylamines in aqueous solvent under mild conditions afford amides concomitant with the release of carbon dioxide (CO_2) and water.[4] This clean amide synthesis, KAHA ligation, has manifested significant advantages in polypeptide synthesis because the connection of peptide segments proceeds without protection of side chains and the loss of enantiopurity.[4a] However, low accessibility of both α-keto acids and hydroxylamines underlies a major problem that affects the practical convenience. In marked contrast to α-amino acid-derived α-keto acids,[5] synthetic research for hydroxylamine counterparts is still less exploited:[6] only a few simple derivatives including cyclic analogues of homoserine, serine, and aspartic acid semialdehyde (Asa) have been synthesised and applied to KAHA peptide ligation (Scheme 1A).[4b,6d,7] Since these nucleophiles require long-step routes for preparation, a straightforward and enantioselective synthesis of such hydroxylamines represents a major challenge for KAHA strategy in view of general peptide synthesis.

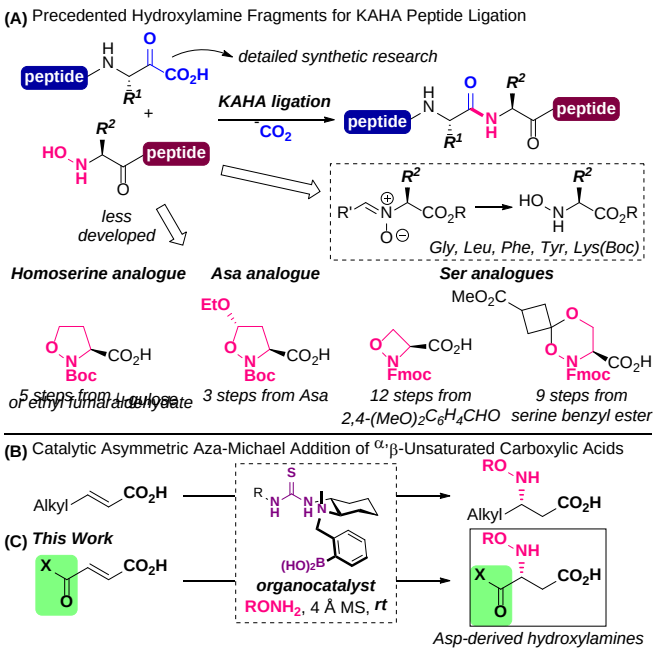

Scheme 1. Strategy for the Synthesis of α-Amino Acid-Derived Hydroxylamines for KAHA Peptide Ligation

We have recently focused on a direct catalytic asymmetric aza-Michael addition of $BnONH_2$ to α,β-unsaturated carboxylic acids using organocatalysts consisting of arylboronic acid and chiral *trans*-1,2-cyclohexanediamine-based aminothiourea (Scheme 1B).[8-10] Notably, our multifunctional catalysts only promoted 1,4-addition: The 1,2-adducts, *N*-benzyloxyamides, which are usually formed in organoboron-catalysed dehydrative amidation,[11] were

Graduate School of Pharmaceutical Sciences, Kyoto University, Yoshida, Sakyo-ku, Kyoto 606-8501, Japan. E-mail: takemoto@pharm.kyoto-u.ac.jp
†Electronic Supplementary Information (ESI) available: [experimental procedures, characterization data, copies of ^1H and ^{13}C NMR spectra, and copies of HPLC analyses (PDF)]. See DOI: 10.1039/x0xx00000x

not observed. Encouraged by the efficient protocols free from "pre-activation" and "protection" of carboxylic acids,[12] we targeted *N*-hydroxyaspartic acid derivatives to demonstrate synthetic versatility of our catalytic systems. Although biocatalytic synthesis of enantiopure *N*-hydroxy and *N*-alkoxyaspartates have been reported,[13] chemical methods are still under developed, and to the best of our knowledge, no example has emerged for catalytic asymmetric variant.[14] Herein, we report the asymmetric synthesis of *N*-hydroxyaspartic acid derivatives catalysed by multifunctional thiourea/boronic acids, which would offer a new, facile access to aspartate-derived hydroxylamine fragments suitable for KAHA peptide ligation.

First, initial investigations focused on catalytic asymmetric aza-Michael addition using mono-*tert*-butyl fumarate (**1a**) and *O*-benzylhydroxylamine (**2a**) as a nucleophile. In line with our previous studies, a chiral integrated thiourea/boronic acid catalyst **A** was employed in the presence of 4 Å molecular sieves (4 Å MS) at room temperature.[8c] Though no reaction took place in DMF and MeCN (Table 1, entries 1 and 2), the reaction in less polar solvents, Et_2O and CH_2Cl_2, furnished the corresponding *N*-benzyloxyaspartic acid diester **3aa** after treatment with $TMSCHN_2$ (entries 3 and 4). When the reaction was conducted in toluene, both the yield and ee drastically increased (entry 5). CCl_4 was found to be the optimal solvent, providing **3aa** in 80% yield and 88% ee (entry 6). Next, thiourea moiety of the catalyst was deviated. Loss of both yields and ees was observed with electron-withdrawing thioureas **B** and **C** (entries 7 and 8). The *ortho*-Me substituted catalyst **D** gave slightly higher ee, but the yield dropped to 59%. *N*-Methyl thiourea catalyst **E** also promoted the reaction, albeit in moderate yield and ee (entry 10). Therefore, we continued the following experiments with catalyst **A**. Afterwards, a range of carboxylic acid was employed as additives, since our previous works suggested three molecules of carboxylic acid were involved in catalytic cycle: Two of them bind to the catalyst and the other one works as a proton shuttle (*vide infra*).[8c] No reaction occurred with 1 equivalent of HCO_2H, and AcOH or $^tBuCO_2H$ did not exhibit beneficial effects. Meanwhile, both the yield and ee improved with $PhCO_2H$, affording **3aa** in 88% yield and 93% ee (entry 14). In sharp contrast, a highly acidic *p*-TsOH inhibited the reaction completely, probably due to the protonation of the nucleophile and/or the catalyst (entry 15). Control experiments revealed that both the catalyst and 4 Å MS were essential for the reaction (entries 16 and 17). All reactions proceeded at β position of the carboxylic acid exclusively, which indicates that the carboxylic acid was predominantly activated *in situ* by boronic acid over the alkyl ester moiety.[15]

Table 1. Optimisation of the Reaction Conditions.

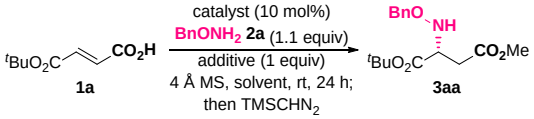

entry	catalyst	additive	solvent	**3aa** (%)[a]	ee (%)[b]
1	**A**	-	DMF	0	-
2	**A**	-	MeCN	0	-
3	**A**	-	Et_2O	22	28
4	**A**	-	CH_2Cl_2	10	47
5	**A**	-	toluene	60	69
6	**A**	-	CCl_4	80	88
7	**B**	-	CCl_4	66	80
8	**C**	-	CCl_4	72	76
9	**D**	-	CCl_4	59	90
10	**E**	-	CCl_4	62	80
11	**A**	HCO_2H	CCl_4	0	-
12	**A**	$MeCO_2H$	CCl_4	57	91
13	**A**	$^tBuCO_2H$	CCl_4	77	87
14	**A**	**$PhCO_2H$**	**CCl_4**	**88**	**93**
15	**A**	*p*-TsOH·H_2O	CCl_4	0	-
16	none	-	CCl_4	0	-
17[c]	**A**	-	CCl_4	0	-

Reaction conditions: **1a** (0.10 mmol), **2a** (0.11 mmol, 1.1 equiv), catalyst (0.010 mmol, 10 mol%), additive (0.10 mmol, 1.0 equiv), 4 Å MS (50 mg), solvent (1.0 mL, 0.1 M), rt, 24 h. [a]Isolated yields are shown. [b]Ees were estimated by chiral HPLC analysis. [c]The reaction was performed without 4 Å MS.

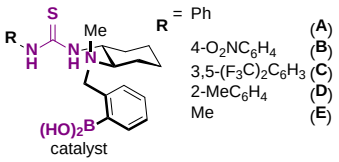

With the optimal conditions in hand, we next explored the substrate scope of the aza-Michael addition of fumaric acid monoesters with **2a** in the presence of catalyst **A**. (Figure 1). Benzyl ester **1b** and ethyl ester **1c** were converted into the corresponding aspartates **3ba** and **3ca**, respectively in moderate yields with high ees. Remarkably, in addition to fumaric acid monoesters, phenylalanine-derived fumaric acid monoamides **1d** and **1e** underwent the aza-Michael addition. By employing catalyst **A** with (*R*,*R*) configuration, D-Phe-D-Asp derivative **3ea** was furnished in higher diastereoselectivity than that of L-Phe-D-Asp derivative **3da**. The catalyst was switched to (*S*,*S*)-**A** (**ent-A**) for the reaction of *N*-fumaryl-L-amino esters **1f** and **1g**, producing Gly-L-Asp and L-Ser-L-Asp derivatives **3fa** and **3ga**, respectively. Even though the stereoselectivity is moderate, these results suggest the feasibility of the synthesis of *N*-hydroxyaspartate-derived peptides through this protocol.

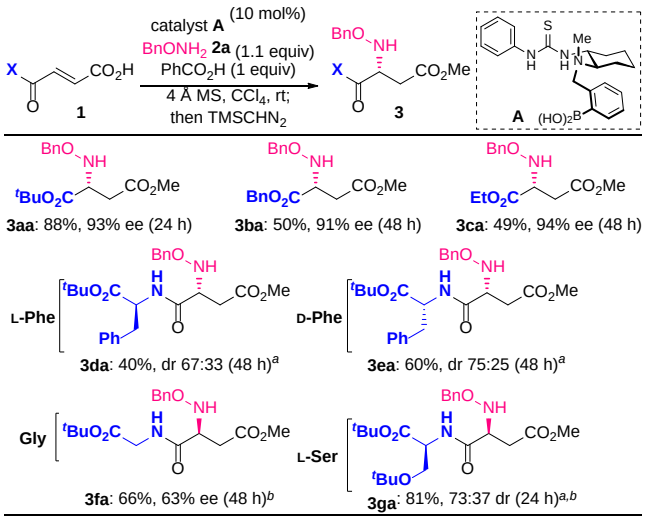

Figure 1. Substrate scope of fumaric monoacids (0.40 mmol). Isolated yields are shown. Ees were estimated by chiral HPLC analysis. [a]Dr was determined by ^{1}H NMR analysis. [b]**ent-A** was used as a catalyst.

The efficiency and high stereoselectivity of the aza-Michael addition of $BnONH_2$ led us to the examination of various *O*-substituted hydroxylamines. To evaluate *O*-substituent effect of nucleophiles **2a**-**2e** on ee, the aza-Michael addition of **1a** was examined under the optimal conditions (Figure 2). The use of electron-rich hydroxylamine **2b** resulted in lower yield and enantioselectivity, whereas electron-deficient *p*-CF_3 substituted nucleophile **2c** gave **3ac** in 96% ee. Besides, acetal-protected nucleophiles such as $BOMONH_2$ (**2d**) and $SEMONH_2$ (**2e**) were also competent nucleophiles, affording the corresponding adducts **3ad** and **3ae** in good yields and enantioselecitivies.

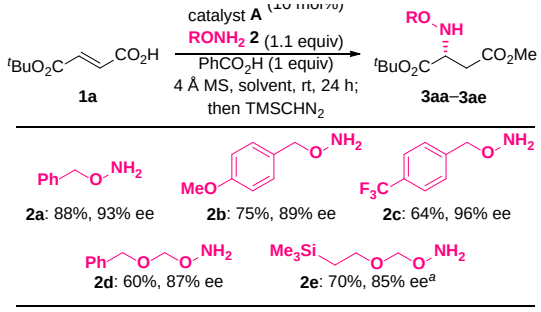

Figure 2. Screening of Nucleophiles (0.20–0.40 mmol). Isolated yields are shown. Ees were estimated by chiral HPLC analysis. [a]Ee was determined after *N*-benzoylation.

Based on the experimental results, including perfect regioselectivity and mechanistic studies performed previously,[8c] a proposed transition state of the addition of hydroxylamine is depicted in Figure 3. Since no reaction occurred in the absence of 4 Å MS (Table 1, entry 17), removal of water is indispensable for this reaction. In a plausible intermediate containing diacyloxyboronate, the hydrogen-bond interaction between the thiourea NH protons and one of the carboxy group facilitates conjugate addition of hydroxylamine. The high enantioselectivity would be attributed to an additional interaction between the nucleophile NH proton and another carboxy ligand, accelerating *Re*-face attack of hydroxylamine. The nucleophilic addition is accompanied with intermolecular proton transfer, which is promoted by the third molecule of carboxylic acid.

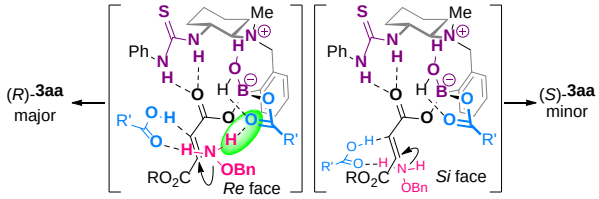

Figure 3. Proposed Transition State of Nucleophilic Addition.

A quick access to various chiral *N*-alkoxyaspartate derivatives prompted us to examine *O*-deprotection of the Michael adducts for the application to KAHA ligation. Various deprotection conditions tested revealed that compound **3be**, obtained from **1b** and **2e**, was the substrate of choice. First, treatment of **3be** with TFA and subsequent careful quenching with water gave an OH-free hydroxylamine **4b** in 42% yield.[15,16] The following KAHA ligation using α-keto acid **5** proceeded smoothly and the corresponding amide **6b** was obtained without significant loss of enantiomeric excess.[7a] The same reaction with Fmoc-L-leucine-derived α-keto acid **7**[17] also afforded dipeptide **8b** in moderate yield without epimerisation.

Scheme 3. *O*-Deprotection and KAHA Ligation of Asparatate-Derived Hydroxylamine Derivatives

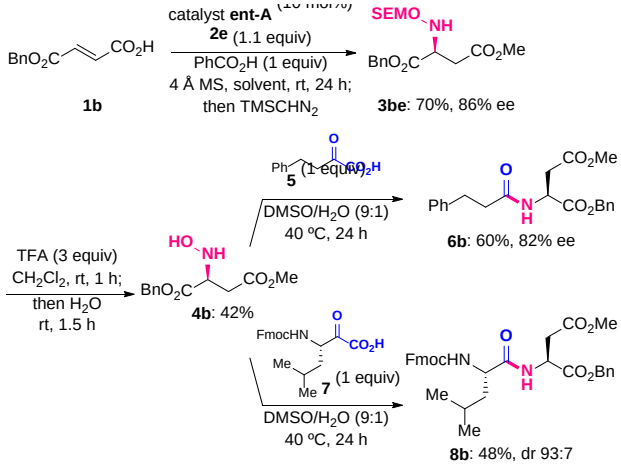

In summary, we have developed a direct aza-Michael addition of hydroxylamine derivatives to various fumaric monoacids catalysed by multifunctional thiourea/boronic acids. The process enables the first catalytic asymmetric chemical synthesis of *N*-hydroxyaspartic acid derivatives with perfect regioselectivity and high enantioselectivity. Deprotection of the $SEMONH_2$-adduct provides a new aspartate-derived hydroxylamine fragment for KAHA peptide ligation. Further research into the synthetic application is actively ongoing, and the results will be reported in due course.

Conflicts of interest

There are no conflicts to declare.

Acknowledgement

This paper is dedicated to the memory of our talented colleague, Mr. Takeru Nakamura, who passed away on 25 October, 2017. This work was financially supported by JSPS KAKENHI, Grant No. JP16H06384.

Notes and references

1 Recent reviews on enzymatic amide C–N bond formation: (a) K. Yazawa, K. Numata, *Molecules*, 2014, **19**, 13755; (b) A. Goswami, S. G. V. Lanen, *Mol. BioSyst.*, 2015, **11**, 338; (c) J. Pitzer, K. Steiner, *J. Biotechnol.*, 2016, **235**, 32; (d) M. Winn, J. K. Fyans, Y. Zhuo, J. Micklefield, *Nat. Prod. Rep.*, 2016, **33**, 317. (e) R. D. Süssmuth, A. Mainz, *Angew. Chem., Int. Ed.*, 2017, **56**, 3770.

2 Selected reviews on amide synthesis using coupling reagents: (a) C. A. G. N. Montalbetti, V. Falque, *Tetrahedron*, 2005, **61**, 10827; (b) E. Valeur, M. Bradley, *Chem. Soc. Rev.*, 2009, **38**, 606; (c) A. El-Faham, F. Albericio, *Chem. Rev.*, 2011, **111**, 6557.

3 A recent review on nonclassical amidation: (a) C. L. Allen, J. M. J. Williams, *Chem. Soc. Rev.*, 2011, **40**, 3405; (b) R. M. de Figueiredo, J.-S. Suppo, J.-M. Campagne, *Chem. Rev.*, 2016, **116**, 12029.

4 (a) J. W. Bode, R. M. Fox, K. D. Baucom, *Angew. Chem., Int. Ed.*, 2006, **45**, 1248; (b) A. K. Sanki, R. S. Talan, S. J. Sucheck, *J. Org. Chem.*, 2009, **74**, 1886; (c) I. Pusterla, J. W. Bode, *Angew. Chem., Int. Ed.*, 2012, **51**, 513.

5 (a) L. Ju, A. R. Lippert, J. W. Bode, *J. Am. Chem. Soc.*, 2008, **130**, 4253; (b) L. Ju, J. W. Bode, *Org. Biomol. Chem.*, 2009, **7**, 2259; (c) T. J. Harmand, S. S. Kulkarni, J. W. Bode, *Tetrahedron Lett.*, 2015, **56**, 3477.

6 Selected examples of the synthesis of α-amino acid-derived hydroxylamines. (a) G. Grundke, W. Keese, M. Rimper, *Synthesis*, 1987, 1115; (b) W. Oppolzer, O. Tamura, *Tetrahedron Lett.*, 1990, **31**, 991. (c) M. D. Wittman, R. L. Halcomb, S. J. Danishefsky, *J. Org. Chem.* 1990, **55**, 1981; (d) S. I. Medina, J. Wu, J. W. Bode, *Org. Biomol. Chem.*, 2010, **8**, 3405; (e) C. D. McCune, S. J. Chan, M. L. Beio, W. Shen, W. J. Chung, L. M. Szczesniak, C. Chai, S. Q. Koh, P. T.-H. Wong, D. B. Berkowitz, *ACS Cent. Sci.*, 2016, **2**, 242.

7 Selected examples of the synthesis and applications of α-amino acid-derived cyclic hydroxylamines: (a) V. R. Pattabiraman, A. O. Ogunkoya, J. W. Bode, *Angew. Chem., Int. Ed.*, 2012, **51**, 5114; (b) C. E. Murar, F. Thuaud, J. W. Bode, *J. Am. Chem. Soc.*, 2014, **136**, 18140; (c) I. Pusterla, J. W. Bode, *Nat. Chem.*, 2015, **7**, 668; (d) C. E. Murar, T. J. Harmand, J. W. Bode, *Bioorg. Med. Chem.*, 2017, **25**, 4996; (e) T. J Harmand, C. E. Murar, H. Takano, J. W. Bode, *Org. Synth.* 2018, **95**, 142; (f) C. E. Murar, T. J. Harmand, H. Takano, J. W. Bode, *Org. Synth.* 2018, **95**, 157. (g) S. Baldauf, J. W. Bode, *Synthesis*, 2019, DOI: 10.1055/s-0037-1611635.

8 (a) T. Azuma, A. Murata, Y. Kobayashi, T. Inokuma, Y. Takemoto, *Org. Lett.*, 2014, **16**, 4256; (b) N. Hayama, T. Azuma, Y. Kobayashi, Y. Takemoto, *Chem. Pharm. Bull.*, 2016, **64**, 704; (c) N. Hayama, R. Kuramoto, T. Földes, K. Nishibayashi, Y. Kobayashi, I. Pápai, Y. Takemoto, *J. Am. Chem. Soc.* 2018, **140**, 12216.

9 Selected examples of catalytic transformation of carboxylic acids without converting the acid moieties: (a) R. Giri, N. Maugel, J.-J. Li, D.-H. Wang, S. P. Breazzano, L. B. Saunders, J.-Q. Yu, *J. Am. Chem. Soc.*, 2007, **129**, 3510; (b) R. M. Al-Zoubi, O. Marion, D. G. Hall, *Angew. Chem., Int. Ed.*, 2008, **47**, 2876; (c) H. Zheng, R. McDonald, D. G. Hall, *Chem. Eur. J.*, 2010, **16**, 5454; (d) Y. Morita, T. Yamamoto, H. Nagai, Y. Shimizu, M. Kanai, *J. Am. Chem. Soc.*, 2015, **137**, 7075; (e) H. Nagai, Y. Morita, Y. Shimizu, M. Kanai, *Org. Lett.*, 2016, **18**, 2276; (f) M. Simonetti, D. M. Cannas, A. Panigrahi, S. Kujawa, M. Kryjewski, P. Xie, I. Larrosa, *Chem. Eur. J.*, 2017, **23**, 549 and references cited therein.

10 Recent reviews on aza-Michael Addition: (a) D. Enders, C. Wang, J. X. Liebich, *Chem. Eur. J.*, 2009, **15**, 11058; (b) P. R. Krishna, A. Sreeshailam, R. Srinivas, *Tetrahedron*, 2009, **65**, 9657; (c) Z. Amara, J. Caron, D. Joseph, *Nat. Prod. Rep.*, 2013, **30**, 1211; (d) J. Gmach, Ł. Joachimiak, K. M. Błażewska, *Synthesis*, 2016, **48**, 2681.

11 Selected examples of organoboron-catalysed dehydrative amidation: (a) K. Ishihara, S. Ohara, H. Yamamoto, *J. Org. Chem.*, 1996, **61**, 4196; (b) K. Arnold, B. Davies, D. Hérault, A. Whiting, *Angew. Chem., Int. Ed.*, 2008, **47**, 2673; (c) P. Starkov, T. D. Sheppard, *Org. Biomol. Chem.*, 2011, **9**, 1320; (d) N. Gernigon, R. M. Al-Zoubi, D. G. Hall, *J. Org. Chem.*, 2012, **77**, 8386; (e) T. M. E. Dine, W. Erb, Y. Berhault, J. Rouden, J. Blanchet, *J. Org. Chem.*, 2015, **80**, 4532; (f) H. Noda, M. Furutachi, Y. Asada, M. Shibasaki, N. Kumagai, *Nat. Chem.*, 2017, **9**, 571. (g) K. Wang, Y. Lu, K. Ishihara, *Chem. Commun.*, 2018, **54**, 5410. (h) D. N. Sawant, D. B. Bagal, S. Ogawa, K. Selvam, S. Saito, *Org. Lett.* 2018, **20**, 4397.

12 Selected examples of Michael addition of α,β-unsaturated carboxylic acid derivatives: (a) Y. Hamashima, H. Somei, Y. Shimura, T. Tamura, M. Sodeoka, *Org. Lett.*, 2004, **6**, 1861; (b) N. Yamagiwa, H. Qin, S. Matsunaga, M. Shibasaki, *J. Am. Chem. Soc.*, 2005, **127**, 13419; (c) S. Kikuchi, H. Sato, S. Fukuzawa, *Synlett*, 2006, 1023; (d) M. P. Sibi, K. Itoh, *J. Am. Chem. Soc.*, 2007, **129**, 8064; (e) M. Weiß, S. Borchert, E. Rémond, S. Jugé, H. Gröger, *Heteroatom. Chem.*, 2012, **23**, 202; (f) Y. Kobayashi, Y. Taniguchi, N. Hayama, T. Inokuma, Y. Takemoto, *Angew. Chem., Int. Ed.*, 2013, **52**, 11114 and references cited therein.

13 (a) M. S. Gulzar, M. Akhtar, D. Gani, *J. Chem. Soc., Chem. Commun.*, 1994, 1601; (b) B. Weiner, G. J. Poelarends, D. B. Janssen, B. L. Feringa, *Chem. Eur. J.*, 2008, **14**, 10094; (c) V. P. Veetil, H. Raj, M. de Villiers, P. G. Tepper, F. J. Dekker, W. J. Quax, G. J. Poelarends, *ChemCatChem*, 2013, **5**, 1325.

14 (a) J. E. Baldwin, L. M. Harwood, M. J. Lombard, *Tetrahedron*, 1984, **40**, 4363; (b) T. Kolasa, *Can. J. Chem.*, 1985, **63**, 2139; (c) R. W. Feenstra, E. H. M. Stokkingreef, R. J. F. Nivard, H. C. J. Ottenheijm, *Tetrahedron*, 1988, **44**, 5583; (d) S. B. McNabb, M. Ueda, T. Naito, *Org. Lett.*, 2004, **6**, 1911; (e) N. Tibrewal, G. I. Elliott, *Bioorg. Med. Chem. Lett.*, 2011, **21**, 517.

15 For the details of optimisations, see the Supporting Information.

16 R. H. Schlessinger, M. A. Poss, S. Richardson, *J. Am. Chem. Soc.*, 1986, **108**, 3112.

17 (a) F. Thuaud, F. Rohrbacher, A. Zwicky, J. W. Bode, *Helv. Chim. Acta*, 2016, **99**, 868. (b) T. Nanjo, N. Kato, Y. Takemoto, *Org. Lett.*, **2018**, *20*, 5766.

Catalytic asymmetric aza-Michael addition of fumaric monoacids with multifunctional thiourea/boronic acids

Kenichi Michigami, Hiroki Murakami, Takeru Nakamura, Noboru Hayama and Yoshiji Takemoto*

Graduate School of Pharmaceutical Sciences, Kyoto University, Yoshida Sakyo-ku, Kyoto 606-8501, Japan

takemoto@pharm.kyoto-u.ac.jp

Supporting Information

Table of Contents

(A) Supplemental Data

(A-1) Optimisation Details: Tables S1-S6 S3

(A-2) Determination of Stereochemistry S5

(B) General S6

(C) Materials and Methods

(C-1) Preparation of Substrates S7

(C-2) Preparation of Nucleophiles S10

(C-3) General Procedure for Catalytic Aza-Michael Addition S12

(D) *O*-Deprotection and KAHA Ligation S18

(E) References S20

(F) ^{1}H NMR and ^{13}C NMR Spectra S21

(G) HPLC Traces S87

(A) Supplemental Data

(A-1) Optimisation Details: Tables S1-S8

Several reaction parameters of the enantioselective aza-Michael addition were investigated. In each tables are described isolated yields.

Table S1. Investigation of Solvent Effect

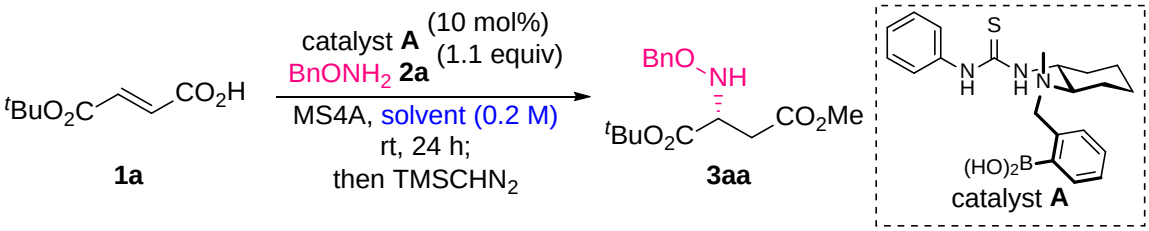

entry	solvent	**3aa** (%)	ee (%)	entry	solvent	**3aa** (%)	ee (%)
1	DMF	0	-	7	hexane	35	38
2	MeCN	0	-	***8***	***CCl_4***	***70***	***88***
3	EtOAc	0	-	9	C_2Cl_4	70	81
4	Et_2O	22	28	10	4-$F_3CC_6H_4Cl$	55	73
5	CH_2Cl_2	10	47	11	PhF	15	62
6	toluene	60	69	12	PhCl	29	7

Table S2. Deviation of Thioureas of Multifunctional Organoboron Catalysts

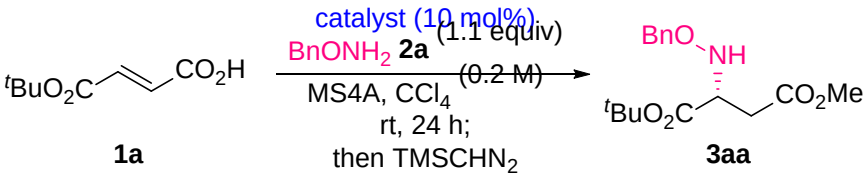

entry	catalyst	**3aa** (%)	ee (%)
1	***A***	***80***	***88***
2	**B**	66	80
3	**C**	72	76
4	**D**	59	90
5	**E**	62	80
6	**F**	54	51

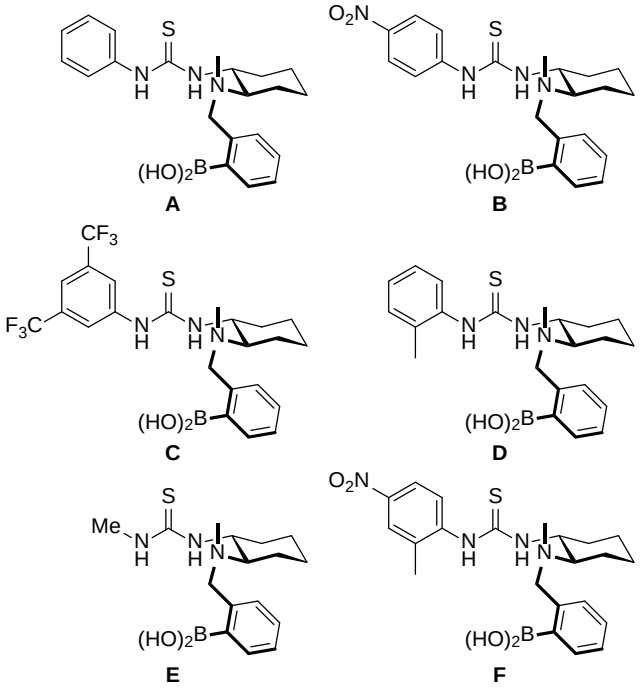

Table S3. Screening of Acid Additives

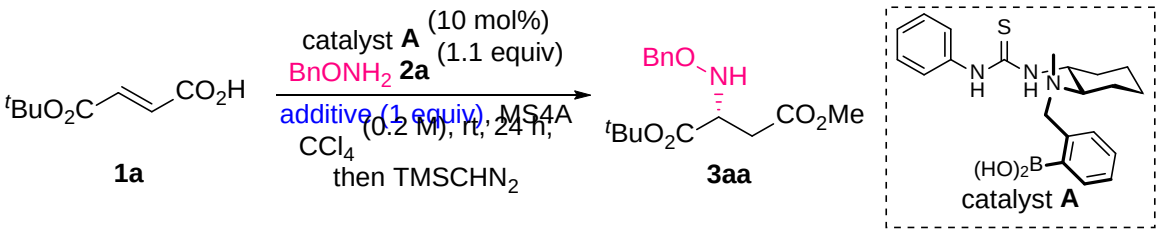

entry	additive	**3aa** (%)	ee (%)
1	none	80	88
2	HCO_2H	0	-
3	$MeCO_2H$	57	91
4	$^tBuCO_2H$	77	87
5	***$PhCO_2H$***	***76***	***93***
6	$TsOH·H_2O$	0	-

Table S4. Investigation of Nucleophiles

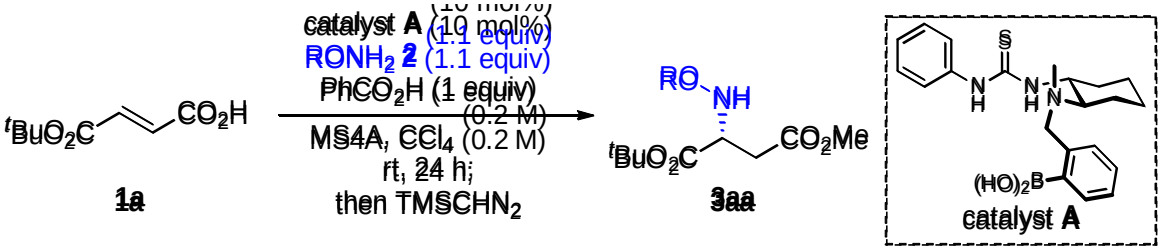

entry	nucleophile	**3aa** (%)	ee (%)
1	**2a**	76	93
2	**2b**	50	74
3	**2c**	64	96
4	**2d**	60	87
5[a]	**2e**	70	85
6	**S2a**	0	-

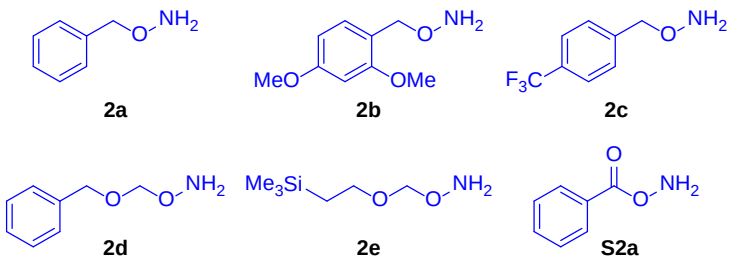

[a]Ee was determined after *N*-benzoylation.

Figure S1. Unsuccessful Substrates

Monomethyl fumarate (**S1a**) and fumaryl monoanilide (**S1b**) did not undergo the aza-Michael addition, probably due to low solubility in CCl_4.

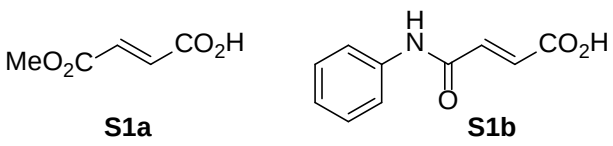

(A-2) Determination of Stereochemistry

The aza-Michael adduct **3aa** was converted into *N*-Fmoc-aspartic diester **S3aa** and the stereochemistry was determined as *R* configuration by comparison of HPLC charts and optical rotations with (*S*)-*N*-Fmoc-aspartic diester derived from the commercially available mono-*tert*-butyl-L-aspartate (Scheme S1).

Scheme S1

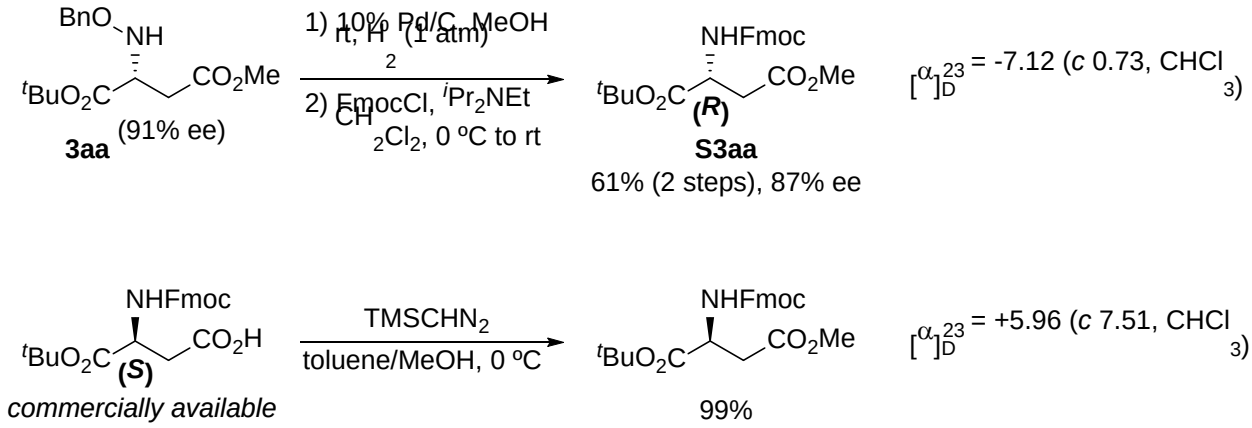

(B) General

All manipulations were carried out under argon atmosphere unless otherwise noted. Infrared (IR) spectra were recorded on a JASCO FT/IR-4100 Fourier transform infrared spectrophotometer. NMR spectra were recorded on a JEOL ECP-400 spectrometer and JEOL ECA-500 spectrometer, operating at 400 MHz (^{1}H) or 100 MHz (^{13}C) and 500 MHz (^{1}H) or 125 MHz (^{13}C), respectively. Chemical shifts in $CDCl_3$, DMSO-d_6, and CD_3OD were reported in the scale relative to $CHCl_3$ (7.26 ppm), DMSO (2.50 ppm), and MeOH (3.31 ppm) for ^{1}H NMR, and to $CDCl_3$ (77.0 ppm) for ^{13}C NMR as internal references, respectively. NMR data are reported as follows: chemical shifts, multiplicity (s: singlet, d: doublet, t: triplet, q: quartet, quin: quintet, m: multiplet, br: broad signal), coupling constant (Hz), and integration. ESI-HRMS spectra were measured on a Shimadzu LCMS-IT-TOF fitted with an ESI. Optical rotations were measured on a JASCO P-2200 digital polarimeter with a path length of 1 cm; concentrations are quoted in grams per 100 mL. $[\alpha]_D$values are measured in 10^{-1} deg cm^2/g. Chiral HPLC analyses were carried out using a SHIMADZU DGU-20A$_5$. Column chromatography was performed with Cica silica gel 60N (40-100 μm, spherical, neutral). Dry solvents were purchased from Wako Pure Chemical Industries, Ltd. and used as received. Organocatalysts **A**-**F** were prepared according to our developed procedures.[1]

(C) Materials and Methods

(C-1) Preparation of Substrates

Monoethyl fumarate (**1c**) was purchased from Tokyo Chemical Industry Co., Ltd. Monomethyl fumarate (**S1a**) was purchased from Sigma-Aldrich Co. LLC. mono-*tert*-butyl fumarate (**1a**)[2] and (*E*)-4-oxo-4-(phenylamino)but-2-enoic acid (**S1b**)[3] were prepared according to the reported procedures.

Mono-*tert*-butyl fumarate (1a)[2]: White solids.

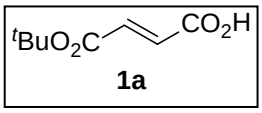

^{1}H NMR (400 MHz, $CDCl_3$) δ: 6.87 (d, J = 15.6 Hz, 1H), 6.76 (d, J = 15.6 Hz, 1H), 1.52 (s, 9H) ppm.

(*E*)-4-Oxo-4-(phenylamino)but-2-enoic acid (S1b)[3]: White solids.

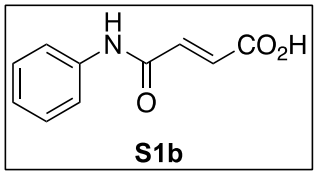

IR (neat) $\tilde{\nu}$: 1696, 1654 cm^{-1}; ^{1}H NMR (400 MHz, DMSO-d_6) δ: 12.99 (br s, 1H), 10.51 (s, 1H), 7.67 (d, J = 8.0 Hz, 2H), 7.34 (t, J = 7.6 Hz, 2H), 7.14 (d, J = 15.2 Hz, 1H), 7.09 (t, J = 7.6 Hz, 1H), 6.65 (d, J = 15.2 Hz, 1H) ppm; ^{13}C NMR (100 MHz, DMSO-d_6) δ: 166.4, 161.6, 138.6, 137.2, 130.8, 128.9, 124.0, 119.4 ppm; HRMS (ESI) *m/z* calcd. for $[M-H]^-$: 190.0510, found: 190.0521.

Monobenzyl fumarate (1b)[4]: To a solution of benzyl *tert*-butyl fumarate[5] (262.1 mg, 1.0 mmol, 1 equiv) in CH_2Cl_2 (4.0 mL) was added TFA (1.8 mL) and stirred at room temperature for 7 h. The mixture was concentrated, and the resulting solids were recrystallised from CH_2Cl_2 and hexane to afford **1b** as white solids (138.4 mg, 0.67 mmol, 67%).

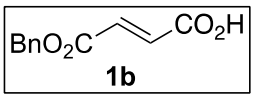

IR (neat) $\tilde{\nu}$: 2940, 1719, 1694 cm^{-1}; ^{1}H NMR (400 MHz, $CDCl_3$) δ: 7.39-7.34 (m, 5H), 6.99 (d, J = 16.0 Hz, 1H), 6.88 (d, J = 16.0 Hz, 1H), 5.25 (s, 2H) ppm.

Ethyl (*S*,*E*)-4-((1-(*tert*-butoxy)-1-oxo-3-phenylpropan-2-yl)amino)-4-oxobut-2-enoate (S1d):

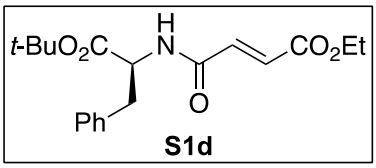

A mixture of L-phenylalanine *tert*-butyl ester hydrochloride[6] (1.32 g, 6.0 mmol, 1.0 equiv), monoethyl fumarate (944.0 mg, 6.6 mmol, 1.1 equiv), HOBt (972.0 mg, 7.2 mmol, 1.2 equiv), Et_3N (1.82 g, 18.0 mmol, 3.0 equiv) and EDCI (1.38 g, 7.2 mmol, 1.2 equiv) in DMF (30 mL) was stirred at room temperature for 20 h. The solution was diluted with brine (20 mL) and extracted with Et_2O (20 mL, 2 times). The combined organic phase was dried over Na_2SO_4 followed by filtration and concentration under reduced pressure. The residue was then purified by silica-gel column chromatography (eluent: hexane/EtOAc, 3:1) to afford **S1d** as white solids (1.43 g, 4.12 mmol, 67%).

m.p. 139.3-140.0 ˚C; $[\alpha]_D^{19}$ 106.9 (*c* 0.89, $CHCl_3$); IR (neat) $\tilde{\nu}$: 3312, 1734, 1716, 1637 cm^{-1}; ^{1}H NMR (500 MHz, $CDCl_3$) δ: 7.29-7.22 (m, 3H), 7.14 (d, J = 6.0 Hz, 2H), 6.92 (d, J = 15.5 Hz, 1H), 6.80 (d, J = 15.5 Hz, 1H), 6.45 (d, J = 7.5 Hz, 1H), 4.84 (dt, J = 7.0, 6.0 Hz, 1H), 4.22 (q, J = 7.5 Hz, 2H), 3.14 (d, J = 6.0 Hz, 2H), 1.42 (s, 9H), 1.30 (t, J = 7.5 Hz, 3H), ^{13}C NMR (125 MHz, $CDCl_3$) δ: 170.2, 165.5, 163.0, 135.9, 130.9, 129.6, 128.5, 127.2, 82.9, 61.3, 53.9, 37.9, 28.0, 14.2 ppm; HRMS (ESI) *m/z* calcd. for $C_{19}H_{25}NO_5$ $[M+Na]^+$: 370.1625, found: 370.1588.

(*S*,*E*)-4-((1-(*tert*-Butoxy)-1-oxo-3-phenylpropan-2-yl)amino)-4-oxobut-2-enoic acid (1d): To a solution

of **S1d** (1.43 g, 4.12 mmol, 1.0 equiv) in THF (20 mL) and water (8.0 mL) was added LiOH (172.8 mg, 4.12 mmol, 1.0 equiv) and stirred at room temperature for 12 h. The mixture was washed with Et_2O, and the aqueous phase was acidified with 1 M HCl aq. The solution was extracted with EtOAc (20 mL, 2 times) and the combined organic layer was washed with brine. After drying over Na_2SO_4 followed by filtration, the solvent wasremoved under reduced pressure to afford **1d** as white solids (565.3 mg, 1.77 mmol, 43%).

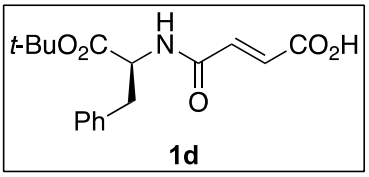

1d

m.p. 118.7-119.1˚C; $[\alpha]_D^{20}$ 105.8 (*c* 0.68, $CHCl_3$); IR (neat) $\tilde{\nu}$: 3350, 1726, 1659, 1642cm^{-1}; ^{1}H NMR (500 MHz, $CDCl_3$) δ: 7.29-7.24 (m, 3 H), 7.15-7.14 (m, 2 H), 7.00 (d, *J* = 15.5 Hz, 1H), 6.83 (d, *J* = 7.5 Hz, 1H), 6.82 (d, *J* = 15.0 Hz, 1H), 4.89 (dt, *J* = 8.0, 7.0 Hz, 1H), 3.13 (d, *J* = 6.0 Hz, 2H), 1.42 (s, 9H) ppm; ^{13}C NMR (125 MHz, $CDCl_3$) δ: 170.9, 169.4, 163.1, 137.6, 135.7, 130.3, 129.6, 128.6, 127.3, 83.4, 54.0, 38.1, 28.0 ppm; HRMS (ESI) *m/z* calcd. for $C_{17}H_{21}NO_5$ $[M+Na]^+$: 342.1312, found: 342.1295.

Ethyl (*R*,*E*)-4-((1-(*tert*-butoxy)-1-oxo-3-phenylpropan-2-yl)amino)-4-oxobut-2-enoate (S1e):

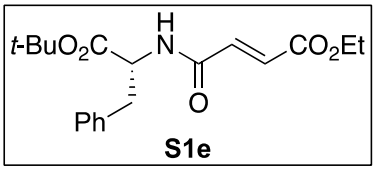

S1e

A mixture of D-phenylalanine *t*-butyl ester hydrochloride[6] (1.32 g, 6.0 mmol, 1.0 equiv), monoethyl fumarate (944.0 mg, 6.6 mmol, 1.1 equiv), HOBt (972.0 mg, 7.2 mmol, 1.2 equiv), Et_3N (1.82 g, 18.0 mmol, 3.0 equiv) and EDCI (1.38 g, 7.2 mmol, 1.2 equiv) in DMF (30 mL) was stirred at room temperature for 20 h. The solution was diluted with brine (20 mL) and extracted with Et_2O (20 mL, 2 times). The combined organic phase was dried over Na_2SO_4 followed by filtration and concentration under reduced pressure. The residue was then purified by silica-gel column chromatography (eluent: hexane/EtOAc, 3:1) to afford **S1d** as white solids (1.46 g, 4.23 mmol, 70%).

m.p. 135.5-137.8 ˚C; $[\alpha]_D^{18}$ -91.3 (*c* 0.94, $CHCl_3$); IR (neat) $\tilde{\nu}$: 3310, 1734, 1716, 1636 cm^{-1}; ^{1}H NMR (500 MHz, $CDCl_3$) δ: 7.27-7.22 (m, 3H), 7.15-7.13 (m, 2H), 6.94 (d, *J* = 15.5 Hz, 1H), 6.81 (d, *J* = 14.5 Hz, 1H), 6.54 (d, *J* = 7.5 Hz, 1H), 4.85 (dt, *J* = 7.5, 6.0 Hz, 1H), 4.21 (q, *J* = 7.0 Hz, 2H), 3.14 (d, *J* = 6.0 Hz, 2H), 1.41 (s, 9H), 1.29 (t, *J* = 7.5 Hz, 3H), ^{13}C NMR (125 MHz, $CDCl_3$) δ: 170.3, 165.5, 163.0, 135.95, 135.91, 130.9, 129.5, 128.5, 127.1, 82.8, 61.3, 53.9, 37.9, 28.0, 14.2 ppm; HRMS (ESI) *m/z* calcd. for $C_{19}H_{25}NO_5$ $[M+Na]^+$: 370.1625, found: 370.1576.

(*R*,*E*)-4-((1-(*tert*-Butoxy)-1-oxo-3-phenylpropan-2-yl)amino)-4-oxobut-2-enoic acid (1e): To a solution of **S1e** (1.46 g, 4.23 mmol, 1.0 equiv) in THF (20 mL) and water (8.0 mL) was added LiOH. (177.4 mg, 4.23 mmol, 1.0 equiv) and stirred at room temperature for 12 h. The mixture was washed with Et_2O, and the aqueous phase was acidified with 1 M HCl aq. The solution was extracted with EtOAc (20 mL, 2 times) and the combined organic layer was washed with brine. After drying over Na_2SO_4 followed by filtration, the solvent was removed under reduced pressure to afford **1e** as white solids (855.0 mg, 2.67 mmol, 65 %).

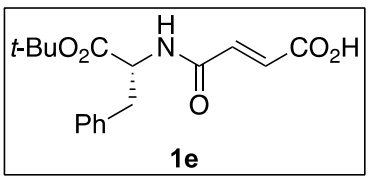

1e

m.p. 118.6-119.2˚C; $[\alpha]_D^{21}$ -95.0 (*c* 0.48, $CHCl_3$); IR (neat) $\tilde{\nu}$: 3351, 1726, 1660, 1642cm^{-1}; ^{1}H NMR (500 MHz, $CDCl_3$) δ: 7.29-7.24 (m, 3 H), 7.14 (d, *J* = 7.0 Hz, 2 H), 6.99 (d, *J* = 15.5 Hz, 1H), 6.81 (d, *J* = 15.0 Hz, 1H), 6.74 (d, *J* = 8.0 Hz, 1H), 4.88 (dt, *J* = 8.0, 6.0 Hz, 1H), 3.14 (d, *J* = 6.5 Hz, 2H), 1.42 (s, 9H) ppm; ^{13}C NMR (125 MHz, $CDCl_3$) δ: 170.9, 169.4, 163.0, 137.6, 130.2, 129.6, 128.6, 127.3, 83.4, 54.0, 38.0,

28.0 ppm; HRMS (ESI) *m/z* calcd. for $C_{17}H_{21}NO_5$ $[M+Na]^+$: 342.1312, found: 342.1291.

Ethyl (*E*)-4-((*tert*-butoxycarbonylmethyl)amino)-4-oxobut-2-enoate (S1f): A mixture of glycine *tert*-butyl ester hydrochloride (835.0 mg, 4.98 mmol, 1.0 equiv), monoethyl fumarate (788.4 mg, 5.47 mmol, 1.1 equiv), HOBt (1.01 g, 7.47 mmol, 1.5 equiv), and EDCI (1.43 g, 7.47 mmol, 1.5 equiv) in DMF (13.5 mL) was stirred at room temperature for 20 h. The solution was diluted with brine (30 mL) and extracted with Et_2O (50 mL, 3 times). The combined organic phase was dried over Na_2SO_4 followed by filtration and concentration under reduced pressure. The residue was then purified by silica-gel column chromatography (eluent: hexane/EtOAc, 1:1) to afford **S1f** as yellow oil (716.7 mg, 2.78 mmol, 56%).

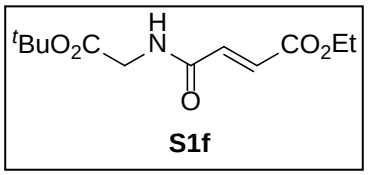

S1f

IR (neat) $\tilde{\nu}$: 3301, 2980, 1724, 1668 cm^{-1}; ^1H NMR (500 MHz, $CDCl_3$) δ: 6.94 (d, J = 15.0 Hz, 1H), 6.82 (d, J =15.0 Hz, 1H), 4.24 (q, J = 7.0 Hz, 2H), 4.03 (d, J = 4.5 Hz, 2H), 1.47 (s, 9H), 1.31 (t, J = 6.5 Hz, 3H) ppm; ^{13}C NMR (125 MHz, $CDCl_3$) δ: 168.6, 165.5, 163.6, 135.5, 131.1, 82.9, 61.3, 42.4, 28.1, 14.2 ppm; HRMS (ESI) *m/z* calcd. for $[M+Na]^+$: 280.1155, found: 280.1157.

(*E*)-4-((*tert*-Butoxycarbonylmethyl)amino)-4-oxobut-2-enoic acid (1f): A solution of **S1f** (716.0 mg, 2.78 mmol, 1 equiv) in THF (14 mL) was treated with 1 M LiOH aq. (2.78 mL, 2.78 mmol, 1.0 equiv) and stirred at ambient temperature for 4 h. The mixture was acidified with 1 M HCl aq. and extracted with $CHCl_3$ (30 mL, 3 times). After drying over Na_2SO_4 followed by filtration, the solvent was removed under reduce pressure to afford **1f** as white solids (366.7 mg, 1.60 mmol, 60%).

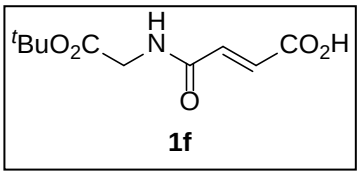

1f

m.p. 229.4 ˚C (decomp.); IR (neat) $\tilde{\nu}$: 3339, 2868, 1732, 1689, 1658, 1637 cm^{-1}; ^1H NMR (500 MHz, $CDCl_3$) δ: 7.02 (d, J = 15.5 Hz, 1H), 6.84 (d, J = 15.5 Hz, 1H), 6.54 (br s, 1H), 4.06 (d, J = 4.5 Hz, 2H), 1.48 (s, 9H) ppm; ^{13}C NMR (125 MHz, CD_3OD) δ: 168.6, 166.9, 165.3, 135.6, 130.5, 81.7, 41.6, 26.9 ppm; HRMS (ESI) *m/z* calcd. for $[M-H]^-$: 228.0877, found: 228.0868.

Ethyl (*S*,*E*)-4-((1,3-bis(*tert*-butoxy)-1-oxopropan-2yl)amino)-4-oxobut-2-enoate (S1g): A mixture of *O*-*tert*-butyl-L-serine *tert*-butyl ester hydrochloride (2.53 g, 10.0 mmol, 1.0 equiv), monoethyl fumarate (1.72 g, 12.0 mmol, 1.2 equiv), HOBt (1.62 g, 12.0 mmol, 1.2 equiv), and EDCI (2.87 g, 15.0 mmol, 1.5 equiv) in DMF (27 mL) was stirred at room temperature for 12 h. The solution was diluted with brine (50 mL) and extracted with Et_2O (50 mL, 3 times). The combined organic phase was dried over Na_2SO_4 followed by filtration and concentration under reduced pressure. The residue was then purified by silica-gel column chromatography (eluent: hexane/EtOAc, 1:1) to afford **S1g** as white solids (3.06 g, 8.91 mmol, 89%).

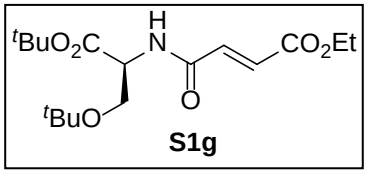

S1g

m.p. 79.4- 80.5 ˚C; $[\alpha]_D^{25}$ 43.2 (*c* 0.45, $CHCl_3$); IR (neat) $\tilde{\nu}$: 3309, 2981, 1741, 1715, 1656 cm^{-1}; ^1H NMR (125 MHz, $CDCl_3$) δ: 6.99 (d, J = 15.5 Hz, 1H), 6.96 (d, J = 8.5 Hz, 1H), 4.60 (dt, J = 8.0, 3.0 Hz, 1H), 4.13 (q, J = 7.0 Hz, 2H), 3.69 (dd, J = 8.0, 3.0 Hz, 1H), 3.46 (dd, J = 8.0, 3.0 Hz, 1H), 1.35 (s, 9H), 1.18 (t, J = 7.0 Hz, 3H), 1.01 (s, 9H) ppm; ^{13}C NMR (125 MHz, $CDCl_3$) δ: 169.0, 165.5, 163.2, 136.3, 130.5, 81.9, 73.0, 62.1, 61.1, 53.5, 27.9, 27.2, 14.1 ppm; HRMS (ESI) *m/z* calcd. for $C_{17}H_{29}NO_6$ $[M+Na]^+$: 366.1887,

found: 366.1861.

(*S*,*E*)-4-((1,3-Bis(*tert*-butoxy)-1-oxopropan-2-yl)amino)-4-oxobut-2-enoic acid (1g): A solution of **S1g** (1.03 g, 3.0 mmol, 1.0 equiv) in THF (15 mL) was treated with 1 M LiOH aq. (3.0 mL, 3.0 mmol, 1.0 equiv) and stirred at ambient temperature for 4 h. The mixture was acidified with 1 M HCl aq. and extracted with $CHCl_3$ (20 mL, 3 times). After drying over Na_2SO_4 followed by filtration, the solvent was removed to afford **1g** as white solids (836.9 mg, 2.65 mmol, 88%).

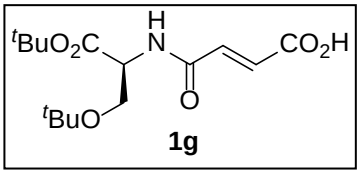

1g

m.p. 165.5-167.9˚C; $[\alpha]_D^{23}$ 25.6 (*c* 0.42, $CHCl_3$); IR (neat) $\tilde{\nu}$: 3331, 3074, 1720, 1706, 1631 cm^{-1}; ^1H NMR (500 MHz, $CDCl_3$) δ: 7.19 (d, *J* = 8.5 Hz, 1H), 7.07 (d, *J* = 15.5 Hz, 1H), 6.88 (d, *J* = 15.5 Hz, 1H), 4.73 (dt, *J* = 9.0, 3.0 Hz, 1H), 3.80 (dd, *J* = 9.0, 3.0 Hz, 1H), 3.56 (dd, *J* = 9.0, 3.0 Hz, 1H), 1.45 (s, 9H), 1.12 (s, 9H) ppm; ^{13}C NMR (125 MHz, $CDCl_3$) δ: 169.7, 168.8, 137.3, 130.5, 82.8, 73.5, 62.2, 53.6, 28.0, 27.3 ppm; HRMS (ESI) *m/z* calcd. for $C_{15}H_{25}NO_6[M+Na]^+$: 338.1574, found: 338.1554.

(C-2) Preparation of Nucleophiles

O-benzylhydroxylamine (**2a**) was prepared by neutralization of $BnONH_2 \cdot HCl$ by 4 M NaOH aq. After extraction with $CHCl_3$, general work up and dried under vacuum to afford **2a**. *O*-Benzoylhydroxylamine (**S2a**) was prepared according to the reported procedure.[8]

***O*-(4-Methoxybenzyl)hydroxylamine (2b)**: A mixture of *N*-hydroxyphthalimide (1.80 g, 11.0 mmol, 1.1 equiv), 4-methoxybenzyl chloride (1.86 g, 10.0 mmol, 1.0 equiv), and Et_3N (1.22 g, 12.1 mmol, 1.1 equiv) in CH_2Cl_2 (25 mL) was stirred at room temperature for 4 h. The suspension was washed with brine (20 mL, 3 times) and the combined organic phase was dried over Na_2SO_4. After the solvent was removed under reduced pressure, the residue was dissolved in $CHCl_3$/MeOH = 3:1 (50 mL). To the solution was added to $N_2H_4 \cdot H_2O$ (750.9 mg, 15.0 mmol, 1.5 equiv) and stirred at room temperature for 2 h. The mixture was filtered through a pad of Celite® and the filtrate was concentrated under reduced pressure. The residue was purified by silica-gel column chromatography (eluent: hexane/EtOAc, 1:1) to afford **2b** as colorless oil (1.10 g, 6.2 mmol, 62%).

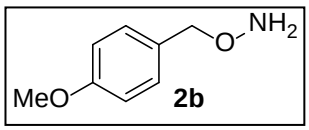

2b

IR (neat) $\tilde{\nu}$: 2977, 2917 cm^{-1}; ^1H NMR (500 MHz, $CDCl_3$) δ: 7.29 (d, *J* = 9.0 Hz, 2H), 6.89 (d, *J* = 9.0 Hz, 2H), 5.33 (br s, 2H), 4.61 (s, 2H), 3.80 (s, 3H) ppm; ^{13}C NMR (125 MHz, $CDCl_3$) δ: 159.5, 130.1, 129.4, 113.9,113.7, 77.7, 53.3 ppm; HRMS (ESI) *m/z* calcd. for C_8H_9NO, $[M]^+$: 176.0682, found: 176.0556.

***O*-(4-Trifluoromethylbenzyl)hydroxylamine (2c)**: **2c** was prepared through the procedure analogous to that of **2b**. Alkylation was performed using *N*-hydroxyphthalimide (1.35 g, 7.0 mmol, 1.4 equiv), 4-(trifluoromethyl)benzyl chloride (815.0 mg, 5.0 mmol, 1.0 equiv), and Et_3N (708.3 mg, 7.0 mmol, 1.4 equiv) in CH_2Cl_2 (20 mL). Deprotection of phthalimide was conducted with $N_2H_4 \cdot H_2O$ (525.6 mg, 10.5 mmol, 1.5 equiv) in CH_3Cl/MeOH = 3:1 (15 mL), which afforded **2c** as colorless oil (810.0 mg, 4.2 mmol, 84%).

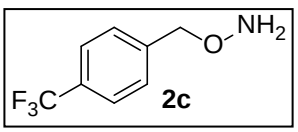

2c

IR (neat) $\tilde{\nu}$: 2940, 1323 cm^{-1}; ^1H NMR (500 MHz, $CDCl_3$) δ: 7.63 (d, *J* = 8.0 Hz, 2H), 7.48 (d, *J* = 8.0 Hz, 2H), 5.48 (br s, 2H), 4.75 (s, 2H) ppm; ^{13}C NMR (125 MHz, $CDCl_3$) δ: 141.7, 130.0 (q, *J* = 32.5 Hz), 128.3,

125.4 (q, J = 3.9 Hz), 76.9 ppm; HRMS (ESI) *m/z* calcd. for C_8H_8FNO, $[M+H]^+$: 192.0631, found: 192.0579.

***O*-(Benzyloxymethyl)hydroxylamine (2d)**: **2d** was prepared through the procedure analogous to that of **2b**. Alkylation was performed using *N*-hydroxyphthalimide (322.6 mg. 2.0 mmol, 1.0 equiv), chloromethyl benzyl ether (439.1 mg, 2.8 mmol, 1.4 equiv), and Et_3N (286.0 mg, 2.8 mmol, 1.4 equiv) in CH_2Cl_2 (4.5 mL). Deprotection of phthalimide was conducted with $N_2H_4{\cdot}H_2O$ (150.2 mg, 3.0 mmol, 1.5 equiv) in CH_3Cl/MeOH = 3:1 (5 mL), which afforded **2d** as colorless oil (213.4 mg, 1.4 mmol, 70%).

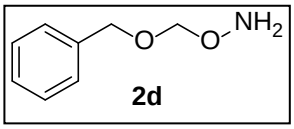

2d

IR (neat) $\tilde{\nu}$: 2871 cm^{-1}; ^1H NMR (500 MHz, $CDCl_3$) δ: 7.38-7.34 (m, 4H), 7.32-7.29 (m, 1H), 5.51 (br s, 2H), 4.85 (s, 2H), 4.67 (s, 2H) ppm; ^{13}C NMR (125 MHz, $CDCl_3$) δ: 137.1, 128.4, 127.7, 98.5, 69.9 ppm; HRMS (ESI) *m/z* calcd. for $C_8H_{12}NO_2$, $[M]^+$: 154.0865, found: 154.0805.

***O*-((2-Trimethylsilylethoxy)methyl)hydroxylamine (2e)**: **2e** was prepared through the procedure analogous to that of **2b**. Alkylation was performed using *N*-hydroxyphthalimide (815.5 mg. 5.0 mmol, 1.0 equiv), chloromethyl 2-(trimethylsilyl)ethyl ether (1.16 g, 7.0 mmol, 1.4 equiv), and Et_3N (708.3 mg, 7.0 mmol, 1.4 equiv) in CH_2Cl_2 (11.4 mL). Deprotection of phthalimide was conducted with $N_2H_4{\cdot}H_2O$ (375.5 mg, 7.5 mmol, 1.5 equiv) in CH_3Cl/MeOH = 3:1 (10 mL), which afforded **2e** as colorless oil (550.5 mg, 3.1 mmol, 62%).

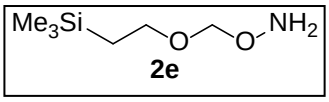

2e

IR (neat) $\tilde{\nu}$: 2953 cm^{-1}; ^1H NMR (500 MHz, $CDCl_3$) δ: 5.47 (br s, 2H), 4.73 (s, 2H), 3.64 (t, J = 8.0 Hz, 2H), 0.96 (t, J = 8.0 Hz, 2H), 0.01 (s, 9H) ppm; ^{13}C NMR (125 MHz, $CDCl_3$) δ: 98.8, 65.7, 18.3 ppm; HRMS (ESI) *m/z* calcd. for $C_6H_{17}NO_2Si$, $[M+H]^+$: 164.1107, found: 164.1018.

***O*-Benzoylhydroxylamine (S2a)**[7]: Colorless oil.

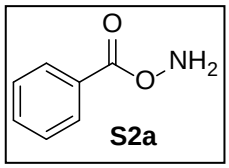

S2a

^1H NMR (400 MHz, $CDCl_3$) δ: 8.00 (d, J = 2.0 Hz, 2H), 7.58 (t, J = 7.6 Hz, 1H), 7.45 (t, J = 7.6 Hz, 2H), 6.60 (br s, 2H) ppm.

(C-3) General Procedure for Catalytic Aza-Michael Addition

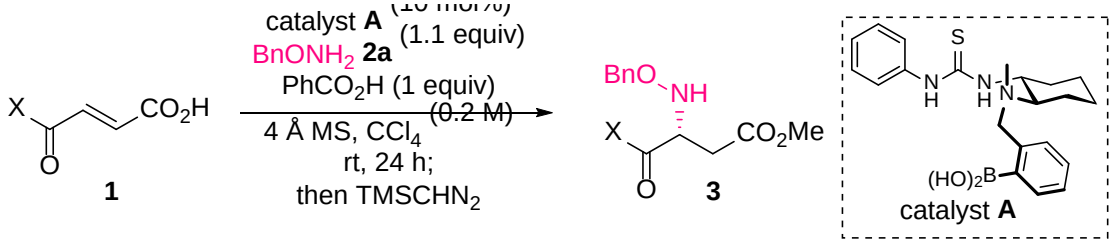

Prior to the reaction, 4 Å MS was dried by heat-gun (>300 ºC, 15 min) under vacuum (*ca*. 2 Torr). To an oven-dried 10 mL screw tube were placed an organocatalyst (10 mol%), substrate **1** (1.0 equiv), and benzoic acid (1.0 equiv), which were suspended in CCl_4 (0.2 M) and sealed with a Teflon-coated screw cap. After stirring at room temperature for 10 min, pre-heated 4 Å MS (500 mg/mmol) was added and the tube was capped and further stirred for 5 min. Hydroxylamine **2** (1.1 equiv) was then added and the system was closed again followed by stirring at ambient temperature for the indicated time. After the reaction progress was monitored by ^{1}H NMR analysis (a small amount of the mixture was transferred into an NMR tube). The reaction mixture was diluted in toluene/MeOH (3:1, 1 mL) and treated with $TMSCHN_2$ (10% in hexane, 1 mL) and stirred for 30 min. The excess $TMSCHN_2$ was quenched with AcOH, then the mixture was filtered through Celite® and the cake was washed with MeOH. After the solvent was removed under reduced pressure, the residue was purified by silica-gel column chromatography (eluent: hexane/EtOAc, 1:1) to afford the product **3**. The ee of **3** was estimated by chiral HPLC analysis.

1-*tert*-Butyl 4-methyl *N*-benzyloxy-D-aspartate (3aa): The reaction was carried out using **1a** (34.4 mg, 200 µmol, 1.0 equiv) and **2a** (27.0 mg, 220 µmol, 1.1 equiv) in the presence of catalyst **A** (7.9 mg, 20 µmol, 10 mol%), benzoic acid (24.4 mg, 200 µmol, 1.0 equiv) and 4 Å MS (100.0 mg) for 24 h. The crude product was purified by silica-gel column chromatography (eluent: hexane/EtOAc, 3:1) afforded **3aa** as colorless oil (40.5 mg, 164 µmol, 80%, 93% ee).

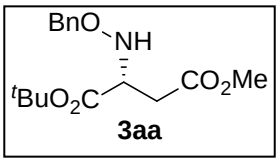

$[\alpha]_D^{24}$ +5.4 (*c* 1.00, $CHCl_3$); IR (neat) $\tilde{\nu}$: 3275, 1731 cm^{-1}; ^{1}H NMR (400 MHz, $CDCl_3$) δ: 7.31 (m, 5H), 6.18 (br s, 1H), 4.69 (s, 2H), 3.92 (br s, 1H), 3.68 (s, 3H), 2.76 (dd, *J* = 16.0, 6.4 Hz, 1H), 2.63 (dd, *J* = 16.0, 6.4 Hz, 1H), 1.47 (s, 9H) ppm; ^{13}C NMR (125 MHz, $CDCl_3$) δ: 171.3, 170.6, 137.5, 128.3, 128.2 127.7, 76.3, 64.2, 60.1, 51.8, 34.3, 27.9 ppm; HRMS (ESI) *m/z* calcd. for $C_{16}H_{23}NO_5$, $[M+Na]^+$: 332.1468, found: 332.1470. The enantiomeric excess was estimated by chiral HPLC analysis (DAICEL CHIRALPAK IB, eluent: hexane/2-propanol = 99/1, flow rate: 1.0 mL/min. detector: UV at 220 nm), t_R = 12.0 min (minor), 10.5 min (major).

1-Benzyl 4-methyl *N*-benzyloxy-D-aspartate (3ba): The reaction was carried out using **1b** (82.4 mg, 400 µmol, 1.0 equiv) and **2a** (54.2 mg, 440 µmol, 1.1 equiv) in the presence of catalyst **A** (15.9 mg, 40 µmol, 10 mol%), benzoic acid (48.8 mg, 400 µmol, 1.0 equiv) and 4 Å MS (200.0 mg) for 24 h. The crude product was purified by silica-gel column chromatography (eluent: hexane/EtOAc, 2:1) afforded **3ba** as colorless oil (69.6 mg, 201 µmol, 50%, 91% ee).

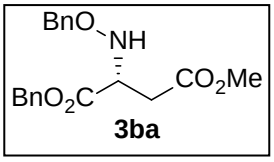

$[\alpha]_D^{26}$ +4.2 (*c* 0.94, $CHCl_3$); IR (neat) $\tilde{\nu}$: 1738 cm^{-1}; ^{1}H NMR (500 MHz, $CDCl_3$) δ: 7.34 (m, 10H), 6.26 (br s, 1H), 5.23 (d, *J* = 12.0 Hz, 1H), 5.19 (d, *J* = 12.0 Hz, 1H), 4.71 (d, *J* = 12.0 Hz, 1H), 4.68 (d, *J* = 12.0

Hz, 1H), 4.09 (t, *J* = 7.0 Hz, 1H), 3.64 (s, 3H), 2.85 (dd, *J* = 16.0, 6.0 Hz, 1H), 2.70 (dd, *J* =16.0, 6.0 Hz, 1H) ppm; ^{13}C NMR (125 MHz, $CDCl_3$) δ: 171.5, 171.2, 137.4, 135.4, 128.68, 128.60, 128.4, 128.3, 128.0, 76.6, 67.2, 60.2, 52.0, 34.2 ppm; HRMS (ESI) *m/z* calcd. for $C_{19}H_{21}NO_5$, $[M+Na]^+$: 366.1312, found: 366.1290. The enantiomeric excess was estimated by chiral HPLC analysis (DAICEL CHIRALPAK IB, eluent: hexane/2-propanol = 98/2, flow rate: 1.0 mL/min. detector: UV at 254 nm), t_R = 16.1 min (major), 17.4 min (minor).

1-Ethyl 4-methyl *N*-benzyloxy-D-aspartate (3ca): The reaction was carried out using **1c** (57.6 mg, 400 μmol, 1.0 equiv) and **2a** (54.2 mg, 440 μmol, 1.1 equiv) in the presence of catalyst **A** (15.9 mg, 40 μmol, 10 mol%), benzoic acid (48.8 mg, 400 μmol, 1.0 equiv) and 4 Å MS (200.0 mg) for 24 h. The crude product was purified by silica-gel column chromatography (eluent: hexane/EtOAc, 2:1) afforded **3ca** as colorless oil (55.2 mg, 197.6 μmol, 49%, 94% ee).

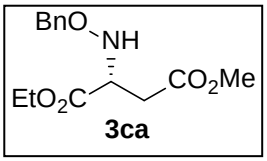

3ca

$[\alpha]_D^{26}$ 6.1 (*c* 1.04, $CHCl_3$); IR (neat) $\tilde{\nu}$: 3265, 1732 cm^{-1}; ^{1}H NMR (400 MHz, $CDCl_3$) δ: 7.31 (m, 5H), 6.22 (br s, 1H), 4.69 (s, 2H), 4.23 (q, *J* = 6.8 Hz, 2H), 4.01 (t, *J* = 6.4 Hz, 1H), 3.68 (s, 3H), 2.81 (dd, *J* = 16.4, 6.4 Hz, 1H), 1.28 (t, *J* = 6.8 Hz, 3H) ppm; ^{13}C NMR (100 MHz, $CDCl_3$) δ: 171.5, 171.2, 137.4, 128.4, 128.3, 127.8, 76.5, 61.4, 60.0, 51.9, 34.1, 14.0 ppm; HRMS (ESI) *m/z* calcd. for $C_{14}H_{19}NO_5$, $[M+Na]^+$: 304.1155, found: 304.1140. The enantiomeric excess was estimated by chiral HPLC analysis (DAICEL CHIRALPAK @, eluent: hexane/2-propanol = 99/1, flow rate: 1.0 mL/min. detector: UV at 254 nm), t_R = 16.9 min (major), 20.1 min (minor).

Methyl (*R*)-3-((benzyloxy)amino)-4-(((*S*)-1-(*tert*-butoxy)-1-oxo-3-phenylpropan-2-yl)amino)-4-oxobutanoate (3da): The reaction was carried out using **1d** (133.2 mg, 400 μmol, 1.0 equiv) and **2a** (54.2 mg, 440 μmol, 1.1 equiv) in the presence of catalyst **A** (15.9 mg, 40 μmol, 10 mol%), benzoic acid (48.8 mg, 400 μmol, 1.0 equiv) and and 4 Å MS (200.0 mg) for 24 h. The crude product was purified by silica-gel column chromatography (eluent: hexane/EtOAc, 2:1) afforded **3da** as colorless oil (120.0 mg, 263 μmol, 66%, 67:33 dr).

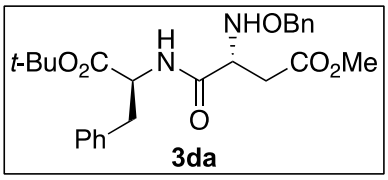

3da

For major diastereomer: $[\alpha]_D^{21}$ 39.8 (*c* 0.51, $CHCl_3$); IR (neat) $\tilde{\nu}$: 3381, 1730, 1675 cm^{-1}; ^{1}H NMR (500 MHz, $CDCl_3$) δ: 7.34-7.14 (m, 10H), 6.19 (d, *J* = 5.5 Hz, 1H), 4.73 (dt, *J* = 7.5, 6.0 Hz, 1H), 4.68 (d, *J* = 12.0 Hz, 1H), 4.61 (d, *J* = 12.0 Hz, 1H), 3.81 (m, 1H), 3.66 (s, 3H), 3.11 (dd, *J* = 15.0, 6.0 Hz, 1H), 3.07 (dd, *J* = 15.0, 6.0 Hz, 1H), 2.87 (dd, *J* = 17.5, 9.0 Hz, 1H), 2.77 (dd, *J* = 17.0, 9.0 Hz, 1H), 1.40 (s, 9H) ppm; ^{13}C NMR (125 MHz, $CDCl_3$) δ: 172.5, 170.4, 170.2, 137.2, 136.3, 129.6, 128.57, 128.52, 128.4, 128.1, 127.0, 82.4, 76.3, 60.5, 53.6, 52.0, 38.2, 32.2, 28.0 ppm; HRMS (ESI) *m/z* calcd. for $C_{25}H_{32}N_2O_6$, $[M+H]^+$: 457.2333, found: 457.2353.

For minor diastereomer: $[\alpha]_D^{21}$ 19.7 (*c* 0.60, $CHCl_3$); IR (neat) $\tilde{\nu}$: 3388, 1732, 1674 cm^{-1}; ^{1}H NMR (500 MHz, $CDCl_3$) δ: 7.33-7.17 (m, 10H), 6.18 (d, *J* = 6.0 Hz, 1H), 4.73 (dt, *J* = 7.5, 6.0 Hz, 1H), 4.62 (d, *J* = 11.5 Hz, 1H), 4.59 (d, *J* = 11.5 Hz, 1H),3.82 (ddd, *J* = 8.0, 7.0, 4.5 Hz, 1H), 3.65 (s, 3H), 3.11 (dd, *J* = 14.0, 6.5 Hz, 1H), 3.08 (dd, *J* = 14.0, 6.0 Hz, 1H), 2.83 (dd, *J* = 12.0, 4.5 Hz, 1H), 2.71 (dd, *J* = 12.0, 8.0 Hz, 1H), 1.44 (s, 9H) ppm; ^{13}C NMR (125 MHz, $CDCl_3$) δ: 172.3, 170.47, 170.42, 137.1, 136.2, 129.7, 128.4, 128.1, 127.0, 82.4, 76.2, 60.6, 53.6, 52.0, 38.1, 32.5, 28.0 ppm; HRMS (ESI) *m/z* calcd. for $C_{25}H_{32}N_2O_6$,

$[M+H]^+$: 457.2333, found: 457.2354.

Methyl (*R*)-3-((benzyloxy)amino)-4-(((*R*)-1-(*tert*-butoxy)-1-oxo-3-phenylpropan-2-yl)amino)-4-oxobutanoate (3ea): The reaction was carried out using **1e** (133.2 mg, 400 μmol, 1.0 equiv) and **2a** (54.2 mg, 440 μmol, 1.1 equiv) in the presence of catalyst **A** (15.9 mg, 40 μmol, 10 mol%), benzoic acid (48.8 mg, 400 μmol, 1.0 equiv) and 4 Å MS (200.0 mg) for 24 h. The crude product was purified by silica-gel column chromatography (eluent: hexane/EtOAc, 2:1) afforded **3ea** as colorless oil (128.2 mg, 280 μmol, 70%, 75:25 dr).

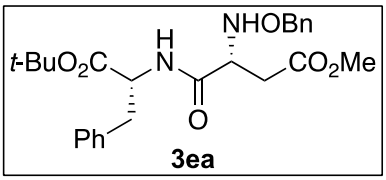

3ea

For major diastereomer: $[\alpha]_D^{21}$ -15.0 (*c* 0.66, $CHCl_3$); IR (neat) $\tilde{\nu}$: 3381, 1731, 1674 cm^{-1}; ^1H NMR (500 MHz, $CDCl_3$) δ: 7.34-7.16 (m, 10H), 6.19 (br s, 1H), 4.73 (dt, *J* = 7.5, 6.0 Hz, 1H), 4.61 (d, *J* = 11.5 Hz, 1H), 4.59 (d, *J* = 11.5 Hz, 1H), 3.82 (m, 1H), 3.66 (s, 3H), 3.11 (dd, *J* = 14.0, 6.5 Hz, 1H), 3.08 (dd, *J* = 14.0, 6.5 Hz, 1H), 2.83 (dd, *J* = 12.0, 4.5 Hz, 1H), 2.71 (dd, *J* = 17.0, 8.0 Hz, 1H), 1.41 (s, 9H) ppm; ^{13}C NMR (125 MHz, $CDCl_3$) δ: 172.3, 170.47, 170.42, 137.1, 136.2, 129.7, 128.5, 128.4, 128.1, 127.0, 82.4, 76.2, 60.6, 53.6, 52.0, 38.1, 32.5, 28.0 ppm; HRMS (ESI) *m/z* calcd. for $C_{25}H_{32}N_2O_6$, $[M+H]^+$: 457.2333, found: 457.2328.

For minor diastereomer: $[\alpha]_D^{22}$ -43.9 (*c* 0.57, $CHCl_3$); IR (neat) $\tilde{\nu}$: 3383, 1729, 1674 cm^{-1}; ^1H NMR (500 MHz, $CDCl_3$) δ: 7.32-7.14 (m, 10H), 6.19 (d, *J* = 6.0 Hz, 1H), 4.74 (dt, *J* = 7.5, 6.5 Hz, 1H), 4.65 (d, *J* = 11.5 Hz, 1H), 4.59 (d, *J* = 11.5 Hz, 1H), 3.81 (m, 1H), 3.66 (s, 3H), 3.12 (dd, *J* = 14.0, 6.0 Hz, 1H), 3.07 (dd, *J* = 14.0, 6.0 Hz, 1H), 2.87 (dd, *J* = 17.0, 5.0 Hz, 1H), 2.77 (dd, *J* = 17.5, 8.0 Hz, 1H), 1.40 (s, 9H) ppm; ^{13}C NMR (125 MHz, $CDCl_3$) δ: 172.5, 170.4, 170.2, 137.1, 136.3, 129.5, 128.5, 128.49, 128.46, 128.0, 127.0, 82.3, 76.2, 60.4, 53.6, 51.9, 38.1, 32.2, 28.0 ppm; HRMS (ESI) *m/z* calcd. for $C_{25}H_{32}N_2O_6$, $[M+H]^+$: 457.2333, found: 457.2355.

Methyl (*S*)-3-((benzyloxy)amino)-4-((*tert*-butoxycarbonylmethyl)amino)-4-oxobutanoate (3fa): The reaction was carried out using **1f** (91.6 mg, 400 μmol, 1.0 equiv) and **2a** (54.2 mg, 440 μmol, 1.1 equiv) in the presence of catalyst **ent-A** (15.9 mg, 40 μmol, 10 mol%), benzoic acid (48.8 mg, 400 μmol, 1.0 equiv) and 4 Å MS (200.0 mg) for 24 h. The crude product was purified by silica-gel column chromatography (eluent: hexane/EtOAc, 2:1) afforded **3fa** as colorless oil (241.4 mg, 266 μmol, 66%, 63% ee).

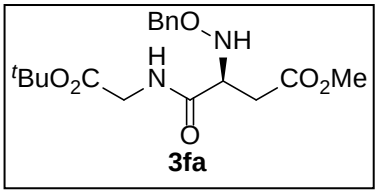

3fa

$[\alpha]_D^{24}$ 4.6 (*c* 1.46, $CHCl_3$); IR (neat) $\tilde{\nu}$: 1733, 1669 cm^{-1}; ^1H NMR (500 MHz, $CDCl_3$) δ: 7.34-7.28 (m, 4H), 7.19 (m, 1H), 6.46 (br s, 1H), 4.73 (s, 2H), 4.03 (d, *J* = 5.5 Hz, 1H), 3.88 (dd, *J* = 5.0, 2.0 Hz, 1H), 3.85 (dd, *J* = 5.0, 2.0 Hz, 1H), 3.66 (s, 3H), 2.89 (dd, *J* = 17.0, 8.0 Hz), 2.78 (dd, *J* = 17.0, 8.0 Hz), 1.46 (s, 9H) ppm; ^{13}C NMR (125 MHz, $CDCl_3$) δ: 172.5, 170.8, 168.7, 130.6, 128.7, 128.5, 128.1, 82.3, 76.2, 60.4, 52.0, 42.0, 32.3, 28.1 ppm; HRMS (ESI) *m/z* calcd. for $C_{18}H_{26}N_2O_6$, $[M+H]^+$: 367.1864, found: 367.1789. The enantiomeric excess was estimated by chiral HPLC analysis (DAICEL CHIRALPAK IB, eluent: hexane/2-propanol = 96/4, flow rate: 1.0 mL/min. detector: UV at 254 nm), t_R = 29.6 min (major), 27.7 min (minor).

Methyl (*R*)-3-((benzyloxy)amino)-4-(((*S*)-1,3-di-*tert*-butoxy-1-oxopropan-2-yl)amino)-4-oxobutanoate (3ga): The reaction was carried out using **1g** (126 mg, 400 μmol, 1.0 equiv) and **2a** (54.2 mg, 440 μmol, 1.1 equiv) in the presence of catalyst **ent-A** (15.9 mg, 40 μmol, 10 mol%), benzoic acid (48.8 mg, 400 μmol, 1.0 equiv) and 4 Å MS (200.0 mg) for 24 h. The crude product was purified by silica-gel column chromatography (eluent: hexane/EtOAc, 2:1) afforded **3da** as colorless oil (366.6 mg, 322 μmol, 81%, 73:27 dr).

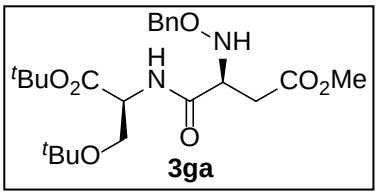

3ga

For major diastereomer: $[\alpha]_D^{21}$ 33.2 (*c* 1.02, $CHCl_3$); IR (neat) $\tilde{\nu}$: 3403, 1735, 1679 cm^{-1}; ^1H NMR (500 MHz, $CDCl_3$) δ: 7.66 (d, *J* = 8.0 Hz, 1H), 7.37-7.31 (m, 5H), 6.26 (d, *J* = 10.0 Hz, 1H), 4.80 (dd, *J* = 15.0, 11.5 Hz, 2H), 4.60 (dt, *J* = 9.0, 2.5 Hz, 1H), 3.90 (dt, *J* = 7.5, 4.5 Hz, 1H), 3.81 (dd, *J* = 17.0, 4.5 Hz, 1H), 3.67 (s, 3H), 3.54 (dd, *J* = 8.5, 3.0 Hz, 1H), 2.91 (dd, *J* = 17.0, 4.5 Hz, 1H), 2.76 (dd, *J* = 17.0, 9.0 Hz, 1H), 1.47 (s, 9H), 1.13 (s, 9H) ppm; ^{13}C NMR (125 MHz, $CDCl_3$) δ: 172.4, 170.5, 169.2, 137.3, 128.6, 128.5, 128.0, 81.8, 76.4, 73.1, 60.7, 53.2, 52.0, 32.6, 28.1, 27.4 ppm; HRMS (ESI) *m/z* calcd. for $C_{25}H_{32}N_2O_6$, $[M+H]^+$: 453.2595, found: 453.2570.

For minor diastereomer: $[\alpha]_D^{21}$ 1.0 (*c* 0.96, $CHCl_3$); IR (neat) $\tilde{\nu}$: 3405, 1737, 1679 cm^{-1}; ^1H NMR (500 MHz, $CDCl_3$) δ: 7.61 (d, *J* = 8.5 Hz, 1H), 7.34-7.26 (m, 5H), 6.26 (d, *J* = 6.5 Hz, 1H), 4.78 (dd, *J* = 17.0, 11.0 Hz, 2H), 4.61 (dt, *J* = 8.5, 2.5 Hz, 1H), 3.91 (ddd, *J* = 9.0, 6.5, 3.0 Hz, 1H), 3.81 (dd, *J* = 9.0, 3.0 Hz, 1H), 3.67 (s, 3H), 3.54 (dd, *J* = 9.0, 3.0 Hz, 1H), 2.93 (dd, *J* = 17.5, 5.0 Hz, 1H), 2.80 (dd, *J* = 17.5, 9.0 Hz, 1H), 1.47 (s, 9H), 1.12 (s, 9H) ppm; ^{13}C NMR (125 MHz, $CDCl_3$) δ: 172.4, 170.5, 169.3, 137.3, 128.58, 128.51, 128.0, 81.9, 76.4, 73.1, 62.2, 60.5, 53.2, 51.9, 32.3, 28.1, 27.4 ppm; HRMS (ESI) *m/z* calcd. for $C_{25}H_{32}N_2O_6$, $[M+H]^+$: 453.2595, found: 453.2524.

1-*tert*-Butyl 4-methyl *N*-(4-methoxybenzyl)oxy-D-aspartate (3ab): The reaction was carried out using **1a** (68.8 mg, 400 μmol, 1.0 equiv) and **2b** (67.4 mg, 440 μmol, 1.1 equiv) in the presence of catalyst **A** (15.9 mg, 40 μmol, 10 mol%), benzoic acid (48.8 mg, 400 μmol, 1.0 equiv) and 4 Å MS (200.0 mg) for 24 h. The crude product was purified by silica-gel column chromatography (eluent: hexane/EtOAc, 2:1) afforded **3ab** as colorless oil (101.8 mg, 300 μmol, 75%, 89% ee).

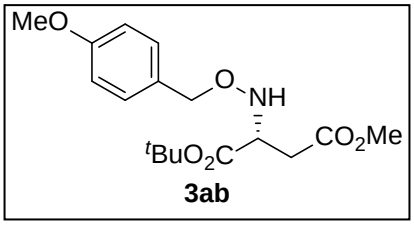

3ab

$[\alpha]_D^{23}$ 8.2 (*c* 0.68, $CHCl_3$); IR (neat) $\tilde{\nu}$: 1732 cm^{-1}; ^1H NMR (500 MHz, $CDCl_3$) δ: 7.26 (t, *J* = 7.0 Hz, 2H), 6.86 (d, *J* = 7.0 Hz, 2H), 6.12 (br s, 1H), 4.61 (s, 2H), 3.80 (s, 3H), 3.68 (s, 3H), 2.75 (dd, *J* = 16.0, 7.5 Hz, 1H), 2.62 (dd, *J* = 16.0, 7.5 Hz, 1H), 1.46 (s, 9H) ppm; ^{13}C NMR (125 MHz, $CDCl_3$) δ: 171.4, 170.7, 159.4, 130.1, 129.7, 113.7, 82.1, 76.1, 60.7, 55.3, 51.9, 34.4, 28.0 ppm; HRMS (ESI) *m/z* calcd. for $C_{17}H_{25}NO_6$, $[M+H]^+$: 340.1755, found: 340.1744. The enantiomeric excess was estimated by chiral HPLC analysis (DAICEL CHIRALPAK IB, eluent: hexane/2-propanol = 98/2, flow rate: 1.0 mL/min. detector: UV at 254 nm), t_R = 13.3 min (major), 14.1 min (minor).

1-*tert*-Butyl 4-methyl *N*-(4-trifluoromethyl)benzyloxy-D-aspartate (3ac): The reaction was carried out using **1a** (34.4 mg, 200 μmol, 1.0 equiv) and **2c** (42.0 mg, 220 μmol, 1.1 equiv) in the presence of catalyst **A** (7.9 mg, 20 μmol, 10 mol%) and benzoic acid (48.8 mg, 400 μmol, 1.0 equiv) and 4 Å MS (200.0 mg) for 24 h. The crude product was purified by silica-gel column chromatography (eluent: hexane/EtOAc, 3:1) afforded **3ac** as colorless oil (48.2 mg, 128 μmol, 64%, 96% ee).

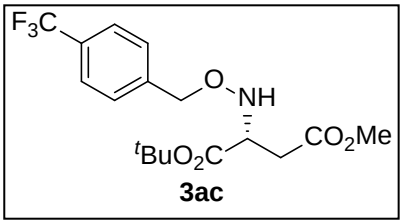

3ac

$[\alpha]_D^{25}$ 6.6 (*c* 1.90, $CHCl_3$); IR (neat) $\tilde{\nu}$: 1732, 1324 cm^{-1}; ^1H NMR (400 MHz, $CDCl_3$) δ: 7.60 (d, *J* = 8.0 Hz, 1H), 7.44 (d, *J* = 8.0 Hz, 1H), 6.25 (d, *J* = 6.0 Hz, 1H), 4.75 (s, 2H), 3.93 (dt, *J* = 6.0 Hz, 1H), 3.67 (s, 3H), 2.75 (dd, *J* = 16.0, 6.5 Hz, 1H), 2.61 (dd, *J* = 16.0, 6.5 Hz, 1H), 1.48 (s, 9H) ppm; ^{13}C NMR (125 MHz, $CDCl_3$) δ: 171.1, 170.5, 141.7, 129.9 (q, *J* = 32.6 Hz), 128.2, 125.2 (q, *J* = 3.7 Hz), 124.1 (q, *J* = 270 Hz), 82.2, 75.4, 60.7, 51.8, 51.7, 34.2, 27.9 ppm; HRMS (ESI) *m/z* calcd. for $C_{17}H_{22}NO_5F_3$, $[M+Na]^+$: 400.1342, found: 400.1333. The enantiomeric excess was estimated by chiral HPLC analysis (DAICEL CHIRALPAK IB, eluent: hexane/2-propanol = 99/1, flow rate: 1.0 mL/min. detector: UV at 254 nm), t_R = 15.8 min (minor), 20.2 min (major).

1-*tert*-Butyl 4-methyl *N*-(benzyloxy)methoxy-D-aspartate (3ad): The reaction was carried out using **1a** (34.4 mg, 200 μmol, 1.0 equiv) and **2d** (36.7 mg, 220 μmol, 1.1 equiv) in the presence of catalyst **A** (7.9 mg, 20 μmol, 10 mol%) and benzoic acid (48.8 mg, 400 μmol, 1.0 equiv) and 4 Å MS (200.0 mg) for 24 h. The crude product was purified by silica-gel column chromatography (eluent: hexane/EtOAc, 3:1) afforded **3ad** as colorless oil (40.0 mg, 122 μmol, 60%, 87% ee).

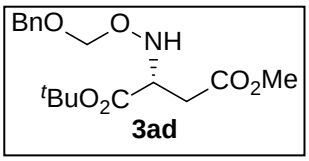

3ad

$[\alpha]_D^{25}$ 4.4 (*c* 1.06, $CHCl_3$); IR (neat) $\tilde{\nu}$: 1731 cm^{-1}; ^1H NMR (400 MHz, $CDCl_3$) δ: 7.31 (m, 5H), 6.43 (d, *J* = 6.4 Hz, 1H), 4.86 (s, 2H), 4.65 (s, 2H), 3.98 (dt, *J* = 10.0, 6.4 Hz, 1H), 3.69 (s, 3H), 2.77 (dd, *J* = 16.4, 6.4 Hz, 1H), 2.67 (dd, *J* = 16.4, 6.4 Hz, 1H), 1.48 (s, 9H) ppm; ^{13}C NMR (100 MHz, $CDCl_3$) δ: 171.2, 170.6, 137.7, 128.4, 127.79, 127.67, 82.1, 69.9, 60.8, 51.8, 34.4, 27.9 ppm; HRMS (ESI) *m/z* calcd. for $C_{17}H_{25}NO_6$, $[M+Na]^+$: 362.1574, found: 362.1588. The enantiomeric excess was estimated by chiral HPLC analysis (DAICEL CHIRALPAK IB, eluent: hexane/2-propanol = 98/2, flow rate: 1.0 mL/min. detector: UV at 220 nm), t_R = 16.1 min (major), 17.4 min (minor).

1-*tert*-Butyl 4-methyl *N*-(2-trimethylsilylethoxy)methoxy-D-aspartate (3ae): The reaction was carried out using **1a** (34.4 mg, 200 μmol, 1.0 equiv) and **2e** (33.6 mg, 220 μmol, 1.1 equiv) in the presence of catalyst **A** (7.9 mg, 20 μmol, 10 mol%), benzoic acid (48.8 mg, 400 μmol, 1.0 equiv) and 4 Å MS (200.0 mg) for 24 h. The crude product was purified by silica-gel column chromatography (eluent: hexane/EtOAc, 3:1) afforded **3ae** as colorless oil (48.9 mg, 142 μmol, 70%). Since **3ae** was not detectable on HPLC, *N*-benzoylation was conducted to estimate the ee of **3ae**.

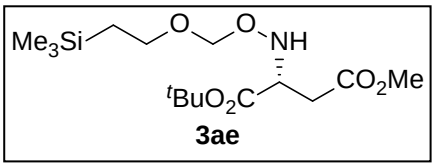

3ae

$[\alpha]_D^{25}$ +4.3 (*c* 1.00, $CHCl_3$); IR (neat) $\tilde{\nu}$: 1738 cm^{-1}; ^1H NMR (400 MHz, $CDCl_3$) δ: 6.36 (d, *J* = 6.4 Hz, 1H), 4.75 (s, 2H), 3.94 (dt, *J* = 12.8 Hz, 6.4 Hz), 3.68 (s, 3H), 3.62 (t, *J* = 8.4 Hz, 2H), 1.45 (s, 9H), 0.94 (t, *J* = 8.4 Hz, 2H) ppm; ^{13}C NMR (125 MHz, $CDCl_3$) δ: 171.2, 170.6, 97.7, 82.0, 65.7, 60.8, 51.8, 34.4, 27.9, 18.1 ppm; HRMS (ESI) *m/z* calcd. for $C_{15}H_{31}NO_6Si$, $[M+Na]^+$: 372.1813, found: 372.1820.

1-*tert*-Butyl 4-methyl *N*-benzoyl-*N*-(2-trimethylsilylethoxy)methoxy-D-aspartate (3ae'): To a solution of **3ae** (34.9 mg, 100 μmol, 1.0 equiv) in EtOAc (1mL) were added BzCl (21.1 mg, 150 μmol, 1.5 equiv) and sat. $NaHCO_3$ aq. (1 mL) at 0 °C. The mixture was allowed to warm to room temperature and stirred for 3 h. Added brine (2 mL) and extracted with EtOAc (5 mL, 2 times). The crude product was purified by silica-gel column chromatography (eluent: hexane/EtOAc, 5:1) afforded **3ae'** as colorless oil (38.8 mg, 85 μmol, 85%).

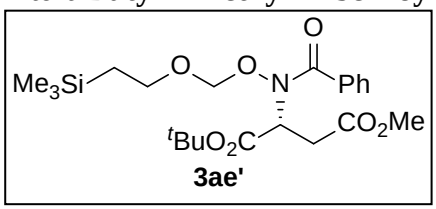

3ae'

$[\alpha]_D^{25}$ 0.71 (*c* 5.84, $CHCl_3$); IR (neat) $\tilde{\nu}$: 1736, 1648 cm^{-1}; ^1H NMR (500 MHz, $CDCl_3$) δ: 7.67 (d, *J* = 7.0 Hz, 2H), 7.46 (t, *J* = 7.0 Hz, 1H), 7.41 (t, *J* = 7.0 Hz, 2H) 5.06 (br, 1H), 4.85 (br, 2H), 3.73 (s, 3H), 3.49 (s, 2H), 3.21 (dd, *J* = 17.0, 7.0 Hz, 1H), 2.97 (dd, *J* = 17.0, 7.0 Hz, 1H), 1.48 (s, 9H), 0.85 (t, *J* = 8.0 Hz, 2H), 0.018 (s, 9H) ppm; ^{13}C NMR (125 MHz, $CDCl_3$) δ: 198.7, 171.3, 167.6, 134.2, 130.9, 128.3, 128.2, 99.6, 82.9, 67.7, 61.1, 52.0, 34.0, 27.9, 17.9 ppm; HRMS (ESI) *m/z* calcd. for $C_{22}H_{35}NO_7Si$, $[M+H]^+$: 453.2111, found: 453.2183. The enantiomeric excess was estimated by chiral HPLC analysis (DAICEL CHIRALPAK IB, eluent: hexane/2-propanol = 1, flow rate: 1.0 mL/min. detector: UV at 254 nm), t_R = 18.9 min (major), 23.7 min (minor).

1-Benzyl 4-methyl *N*-(2-trimethylsilylethoxy)methoxy-L-aspartate (3be): The reaction was carried out using **1b** (82.5 mg, 400 μmol, 1.0 equiv) and **2e** (67.3 mg, 440 μmol, 1.1 equiv) in the presence of catalyst **ent-A** (15.9 mg, 40 μmol, 10 mol%), benzoic acid (48.8 mg, 400 μmol, 1.0 equiv) and 4 Å MS (200.0 mg) for 24 h. The crude product was purified by silica-gel column chromatography (eluent: hexane/EtOAc, 3:1) afforded **3be** as colorless oil (268.4 mg, 284 μmol, 70%, 86% ee).

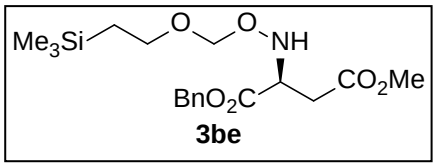

3be

$[\alpha]_D^{26}$ +4.7 (*c* 1.00, $CHCl_3$); IR (neat) $\tilde{\nu}$: 1739 cm^{-1}; ^1H NMR (500 MHz, $CDCl_3$) δ: 7.35 (m, 5H), 6.42 (d *J* = 7.0 Hz, 1H), 5.21 (s, 2H), 4.76 (s, 2H), 4.12 (dt, *J* = 7.0, 6.0Hz, 1H), 3.65 (s, 3H), 3.62 (dt, *J* = 8.5, 1.0 Hz, 1H), 2.85 (dd, *J* = 16.0, 6.0Hz, 1H) 2.74 (dd, *J* = 16.0, 6.0 Hz, 1H), 0.94 (dt, *J* = 8.5, 1.2 Hz, 2H), 0.01 (s, 9H) ppm; ^{13}C NMR (125 MHz, $CDCl_3$) δ: 171.4, 170.9, 135.2, 128.5, 128.3, 128.2, 97.8, 67.1, 65.8, 60.2, 51.9, 34.1, 18.0 ppm; HRMS (ESI) *m/z* calcd. for $C_{18}H_{29}NO_6Si$, $[M+Na]^+$: 406.1656, found: 406.1643. The enantiomeric excess was estimated by chiral HPLC analysis (DAICEL CHIRALPAK IB, eluent: hexane/2-propanol = 99/1, flow rate: 1.0 mL/min. detector: UV at 254 nm), t_R = 16.4 min (major), 18.2 min (minor).

1-*tert*-Butyl 4-methyl 9*H*-fluoren-9-ylmethoxycarbonyl-D-aspartate (S3aa): **3aa** (25.3 mg 100 μmol, 1.0 equiv) was dissolved in MeOH (30 mL) and added to 10% Pd/C (80 mg) under an atmosphere of argon. The reaction was carefully flushed with hydrogen gas and stirred at room temperature for 5 h. The atmosphere was replaced with argon before filtration through a pad of Celite®. The filtrate was concentrated under reduced pressure and the residue was dissolved in CH_2Cl_2 (1.0 mL). To the solution were added $^iPr_2NEt$ (64.6 mg, 500 μmol, 5.0 equiv) and FmocCl (25.8 mg, 120 μmol, 1.2 equiv). The resulting mixture was stirred at ambient temperature for 17 h, then the solvent was evaporated. The residue was purified by silica-gel column chromatography (eluent:

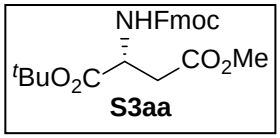

S3aa

hexane/EtOAc, 1:1) to afford **S3aa** as colorless oil (26.0 mg, 61 μmol, 61%).

$[\alpha]_D^{23}$ -7.1 (*c* 0.73, $CHCl_3$); IR (neat) $\tilde{\nu}$: 3368, 1721 cm^{-1}; ^1H NMR (500 MHz, $CDCl_3$) δ: 7.75 (d, *J* = 7.5 Hz, 2H), 7.60 (d, *J* = 7.5 Hz, 2H), 7.40 (t, *J* = 7.5 Hz, 2H), 5.80 (d, *J* = 8.5 Hz, 1H), 4.54 (dt, *J* = 8.5, 4.5 Hz, 1H), 4.38 (dt, *J* = 17.0, 7.0 Hz, 2H), 4.23 (t, *J* = 7.0 Hz, 1H), 3.71 (s, 3H), 3.00 (dd, *J* = 17.0, 4.0 Hz, 1H), 2.84 (dd, *J* = 17.0, 4.0 Hz, 1H), 1.48 (s, 9H) ppm; ^{13}C NMR (125 MHz, $CDCl_3$) δ: 171.3, 169.6, 156.0, 143.9, 143.8, 141.3, 127.8, 127.1, 125.2, 120.0, 82.7, 67.2, 52.0, 51.0, 47.2, 36.8, 27.9 ppm; HRMS (ESI) *m/z* calcd. for 448.1731, $[M+Na]^+$ found: 448.1757. The enantiomeric excess was estimated by chiral HPLC analysis (DAICEL CHIRALPAK IA, eluent: hexane/2-propanol = 96/4, flow rate: 1.0 mL/min. detector: UV at 254 nm), t_R = 20.3 min (major), 26.6 min (minor).

(D) *O*-Deprotection and KAHA Ligation

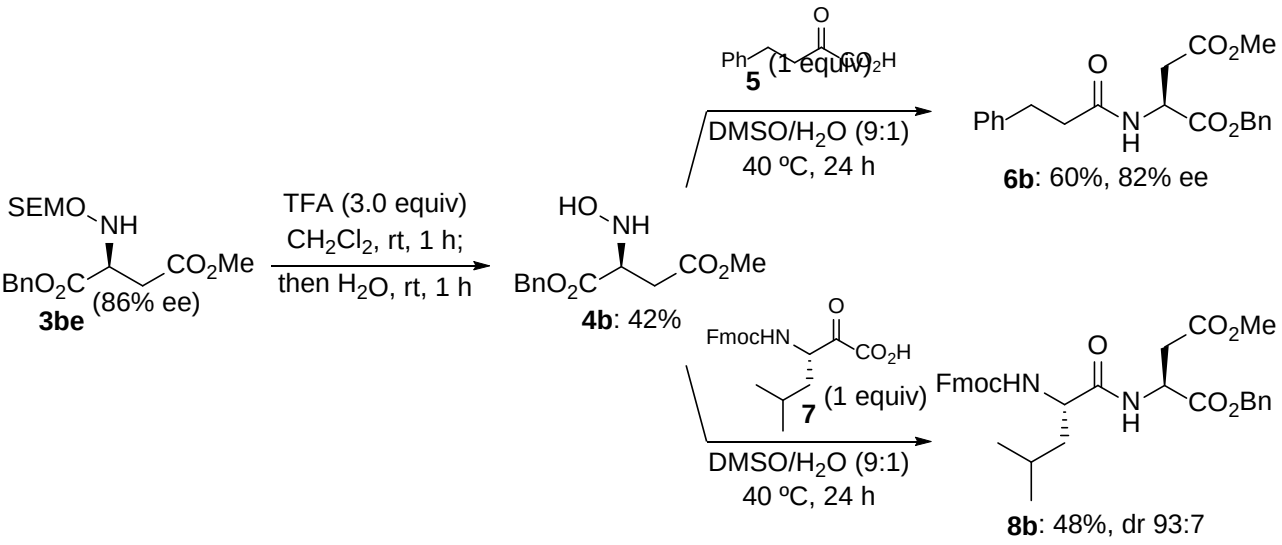

1-Benzyl 4-methyl *N*-hydroxy-L-aspartate (4b): To a solution of **3be** (192.7 mg, 500 μmol, 1.0 equiv) in CH_2Cl_2 (5 mL) was added TFA (172.5 mg, 1.5 mmol, 3.0 equiv) at room temperature and stirred for 1 h. H_2O (5 mL) was added and further stirred at ambient temperature for 1 h, and the mixture was dried over Na_2SO_4. The solids were filtered off and the solvent was removed under reduced presssure. The residue was then purified by silica-gel column chromatography (eluent: hexane/EtOAc, 1:2) to afford **4b** as colorless oil (53.1 mg, 210 μmol, 42%). Since **4b** was gradually degraded on standing, **4b** was used for KAHA ligation soon after purification.

^1H NMR (500 MHz, $CDCl_3$) δ: 7.32 (m, 5H), 5.22 (s, 2H), 4.06 (dt, *J* = 8.0, 5.0 Hz, 1H), 3.66 (s, 3H), 2.87 (dd, *J* = 16.0, 5.0 Hz, 1H), 2.80 (dd, *J* = 16.0, 5.0 Hz, 1H) ppm.

1-Benzyl 4-methyl (3-phenylpropanoyl)-L-aspartate (6b): A mixture of **4b** (23.3 mg, 92 μmol, 1.0 equiv) and 2-oxo-4-phenylbutanoic acid (**5**) (16.3 mg, 92 μmol, 1.0 equiv) in DMSO/H_2O (9:1, 200 μL) was stirred at 40 ºC for 24 h. The crude mixture was extracted with EtOAc (2 mL, 3 times) and then purified by silica-gel column chromatography (eluent: hexane/EtOAc, 1:2) to afford to **6b** as yellow oil (26.1 mg, 70 μmol, 60%, 82% ee).

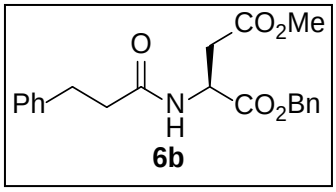

$[\alpha]_D^{24}$ -13.2 (*c* 1.75, $CHCl_3$); IR (neat) $\tilde{\nu}$: 3311, 1732, 1652 cm^{-1}; ^1H NMR (500 MHz, $CDCl_3$) δ: 7.38-7.30

(m, 6H), 7.27-7.24 (m, 1H), 7.19-7.17 (m, 3H), 6.42 (d, *J* = 8.0 Hz, 1H), 5.17 (dd, *J* = 28.0, 12.5 Hz, 2H), 4.88 (dt, *J* = 8.0, 4.0 Hz, 1H), 3.00 (dd, *J* = 17.5, 4.0 Hz, 1H), 2.95 (t, *J* = 8.0 Hz, 2H), 2.75 (dd, *J* = 17.5, 4.0 Hz, 1H), 2.59 (ddd, *J* = 18.0, 15.0, 8.0 Hz, 1H), 2.49 (ddd, *J* = 18.0 Hz, 15.0, 8.0 Hz) ppm; ^{13}C NMR (125 MHz, $CDCl_3$) δ: 171.8, 171.4, 170.5, 140.5, 135.1, 128.55, 128.45, 128.26, 126.1, 67.5, 51.9, 48.3, 38.0, 36.0, 31.4 ppm; HRMS (ESI) *m/z* calcd. For $C_{21}H_{23}NO_5$, $[M+H]^+$: 370.1649, found: 370.1676. The enantiomeric excess was estimated by chiral HPLC analysis (DAICEL CHIRALPAK IB, eluent: hexane/2-propanol = 99/1, flow rate: 1 mL/min. detector: UV at 254 nm), t_R = 18.2 min (minor), 16.4 min (major).

1-Benzyl 4-methyl 9*H*-fluoren-9-ylmethoxycarbonyl-L-leucyl-L-aspartate (8b): A mixture of **4b** (60.1 mg, 156 µmol, 1.0 equiv) and (*S*)-3-(9*H*-fluoren-9-ylmethoxycarbonyl)amino)-5-methyl-2-oxohexanoic acid (**7**) (57.1 mg, 150 µmol, 1.0 equiv) in DMSO/H_2O (9:1, 15 mL) was stirred at 40 ºC for 15 h. The crude mixture was extracted with EtOAc (2 mL, 3 times) and then purified by silica-gel column chromatography (eluent: hexane/EtOAc, 1:2) to afford to **8b** as yellow oil (41.2 mg, 72 µmol, 50%, 93:7 dr).

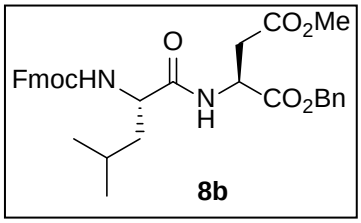

8b

$[\alpha]_D^{23}$ -3.20 (*c* 1.20, $CHCl_3$); IR (neat) $\tilde{\nu}$: 3314, 1738, 1661 cm^{-1}; ^{1}H NMR (500 MHz, $CDCl_3$) δ: 7.75 (d, *J* = 7.0 Hz, 2H), 7.57 (d, *J* = 5.5 Hz, 2H), 7.39-7.29 (m, 9H), 6.95 (d, *J* = 8.0 Hz, 1H), 5.34 (d, *J* = 8.0 Hz, 1H), 5.15 (dd, *J* = 21.0, 12.0 Hz, 2H), 4.91 (t, *J* = 4.0 Hz, 1H), 4.36 (m, 2H) 4.21 (m, 2H), 3.58 (s, 3H), 3.05 (dd, *J* = 17.0, 3.5 Hz, 1H), 2.81 (dd, *J* = 17.0, 3.5 Hz, 1H), 1.63 (m, 2H), 1.50 (m, 1H), 0.89 (s, 6H) ppm; ^{13}C NMR (125 MHz, $CDCl_3$) δ: 172.2, 171.5, 170.3, 156.1, 143.9, 143.8, 141.3, 135.1, 128.69, 128.60, 128.4, 127.8, 127.1, 125.1, 120.0, 67.7, 67.1, 53.4, 52.1, 48.5, 41.9, 36.0, 24.6, 22.9, 22.0 ppm; HRMS (ESI) *m/z* calcd. For $C_{33}H_{36}N_2O_7$, $[M+Na]^+$: 595.2415, found: 595.2396.

(E) References

[1] N. Hayama, T. Azuma, Y. Kobayashi, Y. Takemoto, *Chem. Pharm. Bull.*, 2016, **64**, 704.

[2] S. E. Denmark, A. Thorarensen, D. S. Middleton, *J. Am. Chem. Soc.*, 1996, **118**, 8266.

[3] D. Hadjipavlou-Litina, G. E. Magoulas, M. Krokidis, D. Papaioannou, *Eur. J. Med. Chem.*, 2010, **45**, 298.

[4] J. P. D. van Veldhoven, C. C. Blad, A. C. Klopman, D. R. Wolfram, M. J. Abdelkadir, J. R. Lane, J. Brussee, A. P. IJzerman, *Bioorg. Med. Chem. Lett.*, 2011, **21**, 2736.

[5] Ö. D. Ekici, Z. Z. Li, A. J. Campbell, K. E. James, J. L. Asgian, J. Mikolajczyk, G. S. Salvesen, R. Ganesan, S. Jelakovic, M. G. Grütter, J. C. Powers, *J. Med. Chem.*, 2006, **49**, 5728.

[6] A. Odriozola, M. Oiarbide, C. Palomo, *Chem. Eur. J.*, 2017, **23**, 12758.

[7] L. A. Carpino, C. A. Giza, B. A. Carpino, *J. Am. Chem. Soc.*, 1959, **81**, 955.

(F) ^{1}H NMR and ^{13}C NMR Spectra

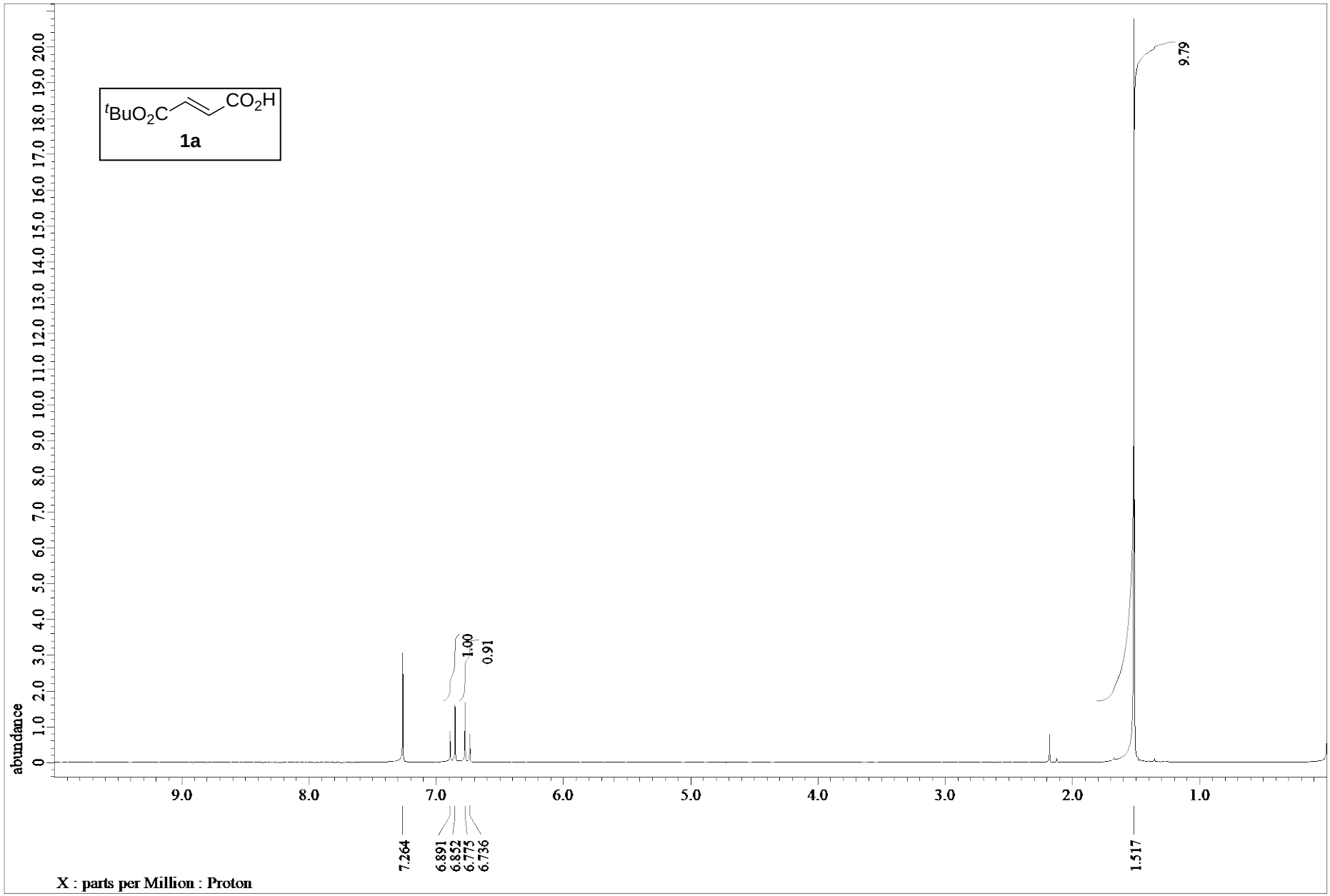

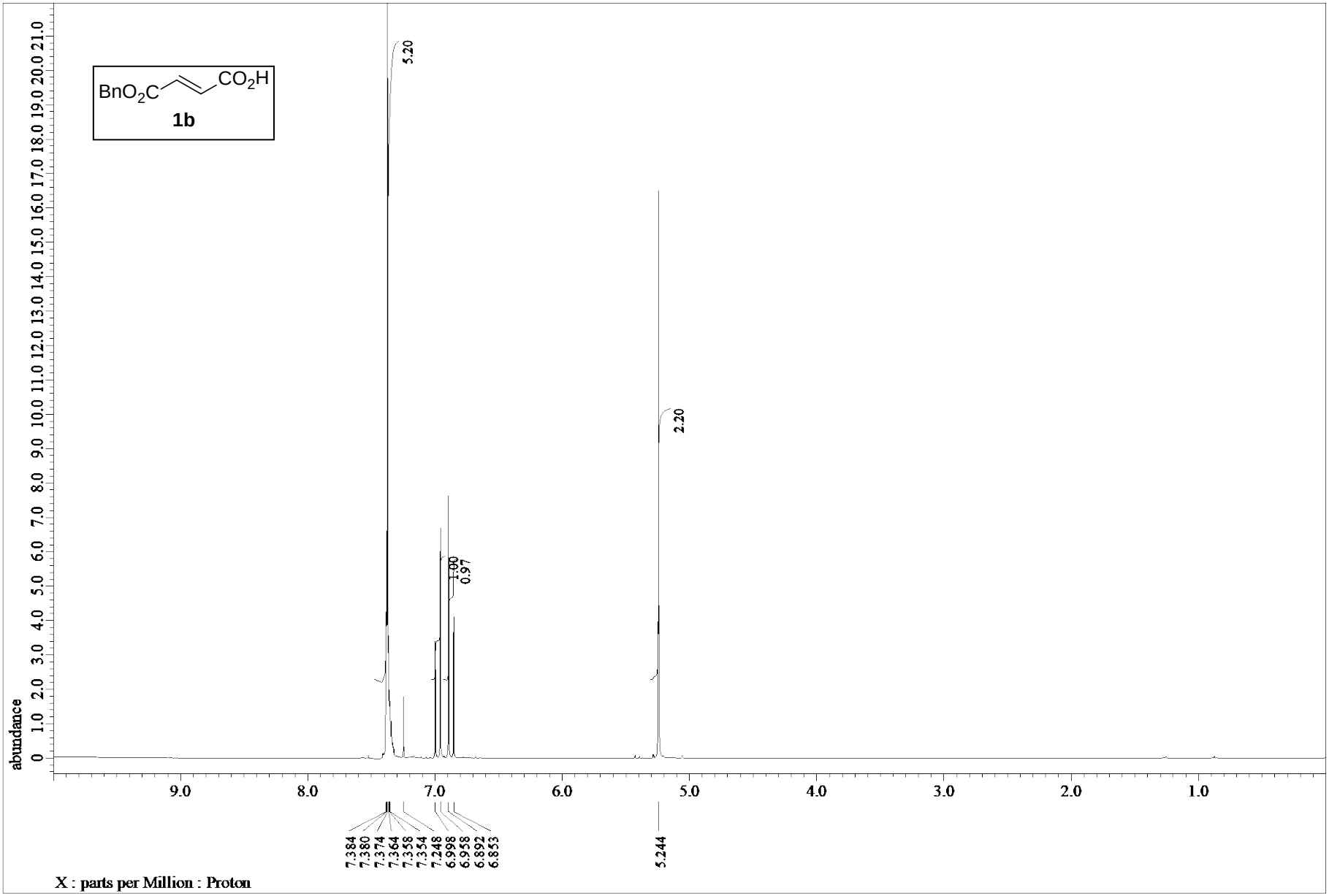
BnO2C
CO2H
1b
5.20
2.20
1.00
0.97
abundance
7.384
7.380
7.374
7.364
7.358
7.354
7.248
6.998
6.958
6.892
6.853
5.244
X : parts per Million : Proton

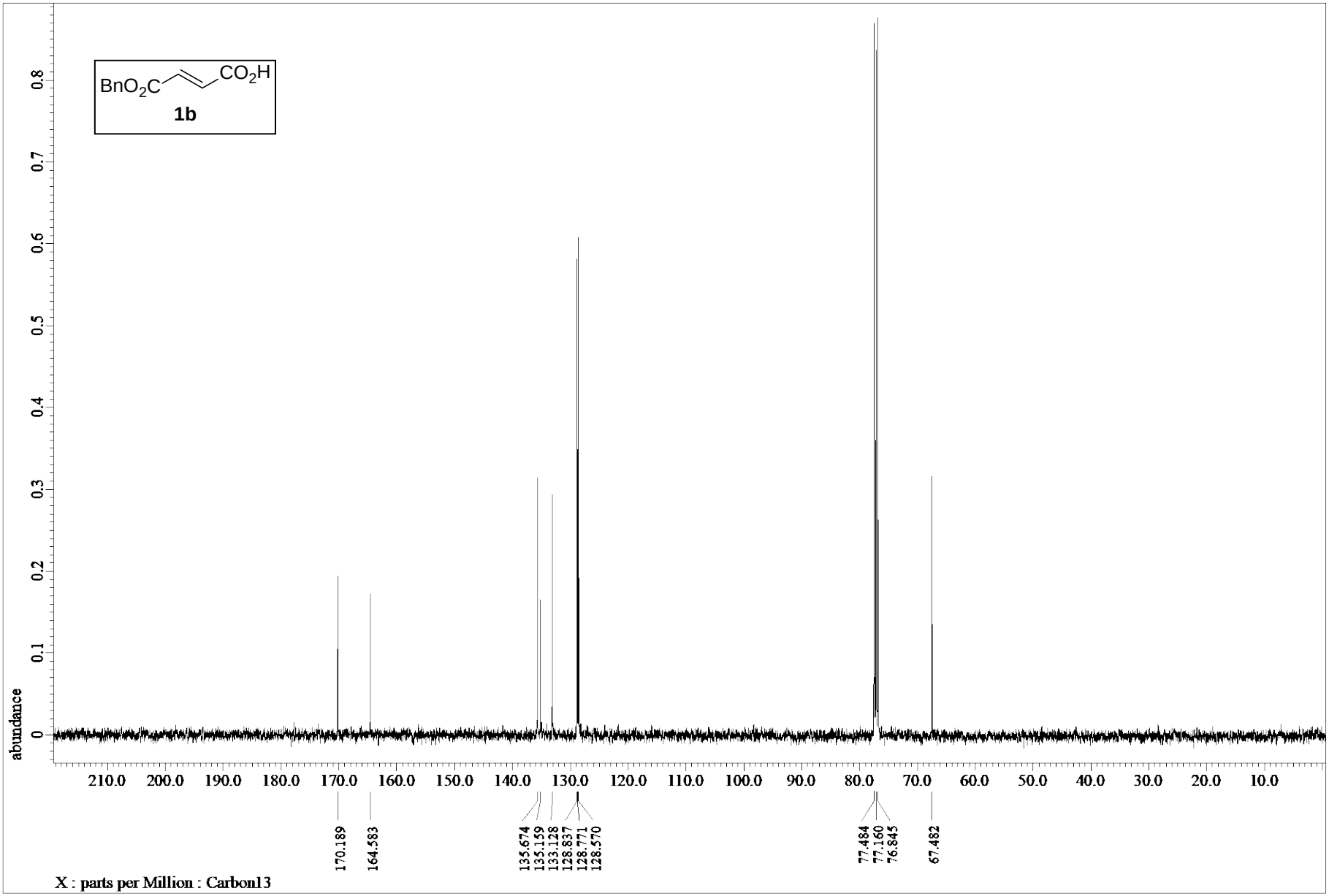
BnO2C
CO2H
1b
abundance
0
0.1
0.2
0.3
0.4
0.5
0.6
0.7
0.8
210.0
200.0
190.0
180.0
170.0
160.0
150.0
140.0
130.0
120.0
110.0
100.0
90.0
80.0
70.0
60.0
50.0
40.0
30.0
20.0
10.0
170.189
164.583
135.674
135.159
133.128
128.837
128.771
128.570
77.484
77.160
76.845
67.482
X : parts per Million : Carbon13

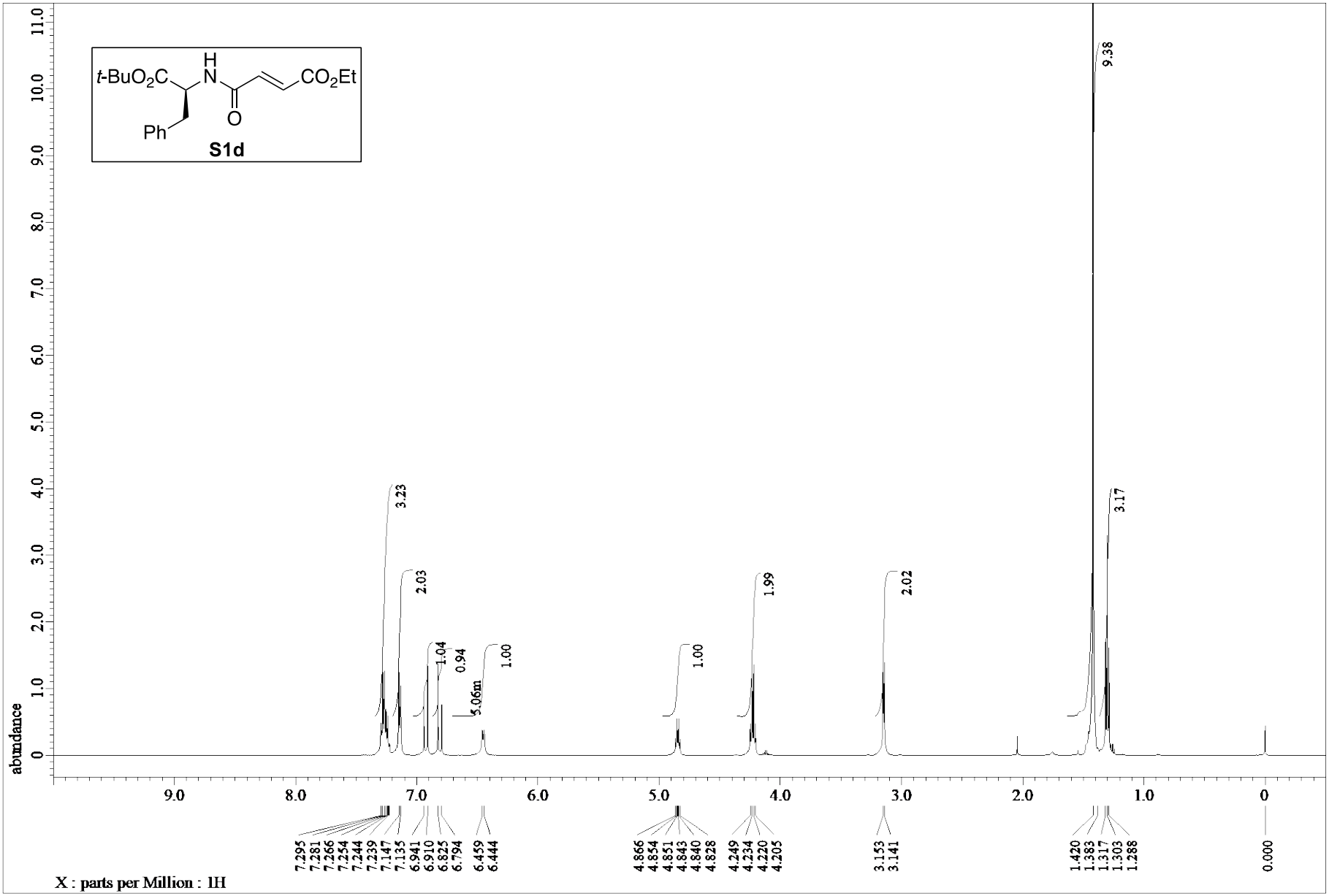
t-BuO2C
H
N
CO2Et
O
Ph
S1d
abundance
X : parts per Million : 1H
9.38
3.23
2.03
1.04
0.94
5.06m
1.00
1.00
1.99
2.02
3.17
7.295
7.281
7.266
7.254
7.244
7.239
7.147
7.135
6.941
6.910
6.825
6.794
6.459
6.444
4.866
4.854
4.851
4.843
4.840
4.828
4.249
4.234
4.220
4.205
3.153
3.141
1.420
1.383
1.317
1.303
1.288
0.000

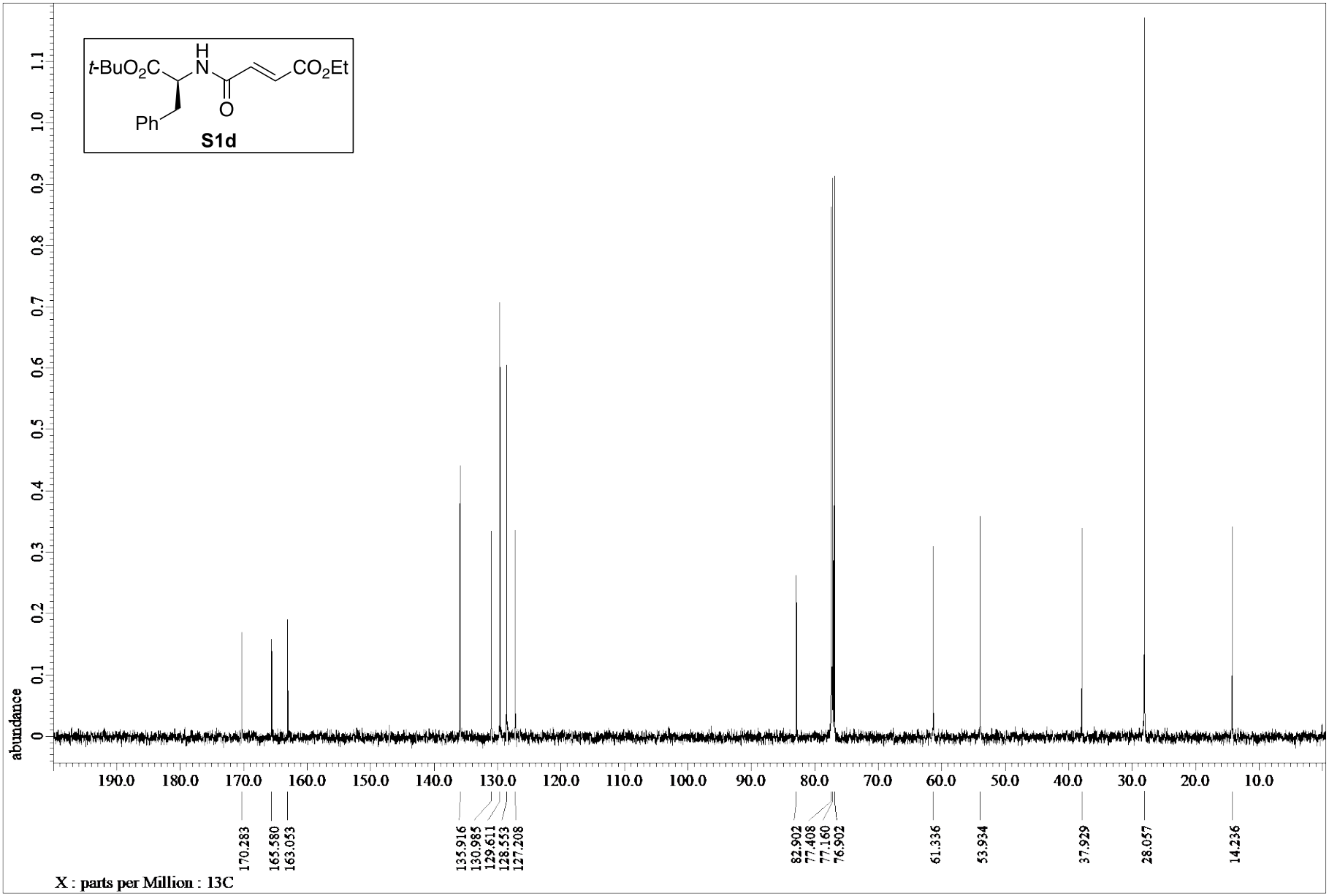
t-BuO2C
H
N
CO2Et
O
Ph
S1d
abundance
0
0.1
0.2
0.3
0.4
0.5
0.6
0.7
0.8
0.9
1.0
1.1
190.0
180.0
170.0
160.0
150.0
140.0
130.0
120.0
110.0
100.0
90.0
80.0
70.0
60.0
50.0
40.0
30.0
20.0
10.0
170.283
165.580
163.053
135.916
130.985
129.611
128.553
127.208
82.902
77.408
77.160
76.902
61.336
53.934
37.929
28.057
14.236
X : parts per Million : 13C

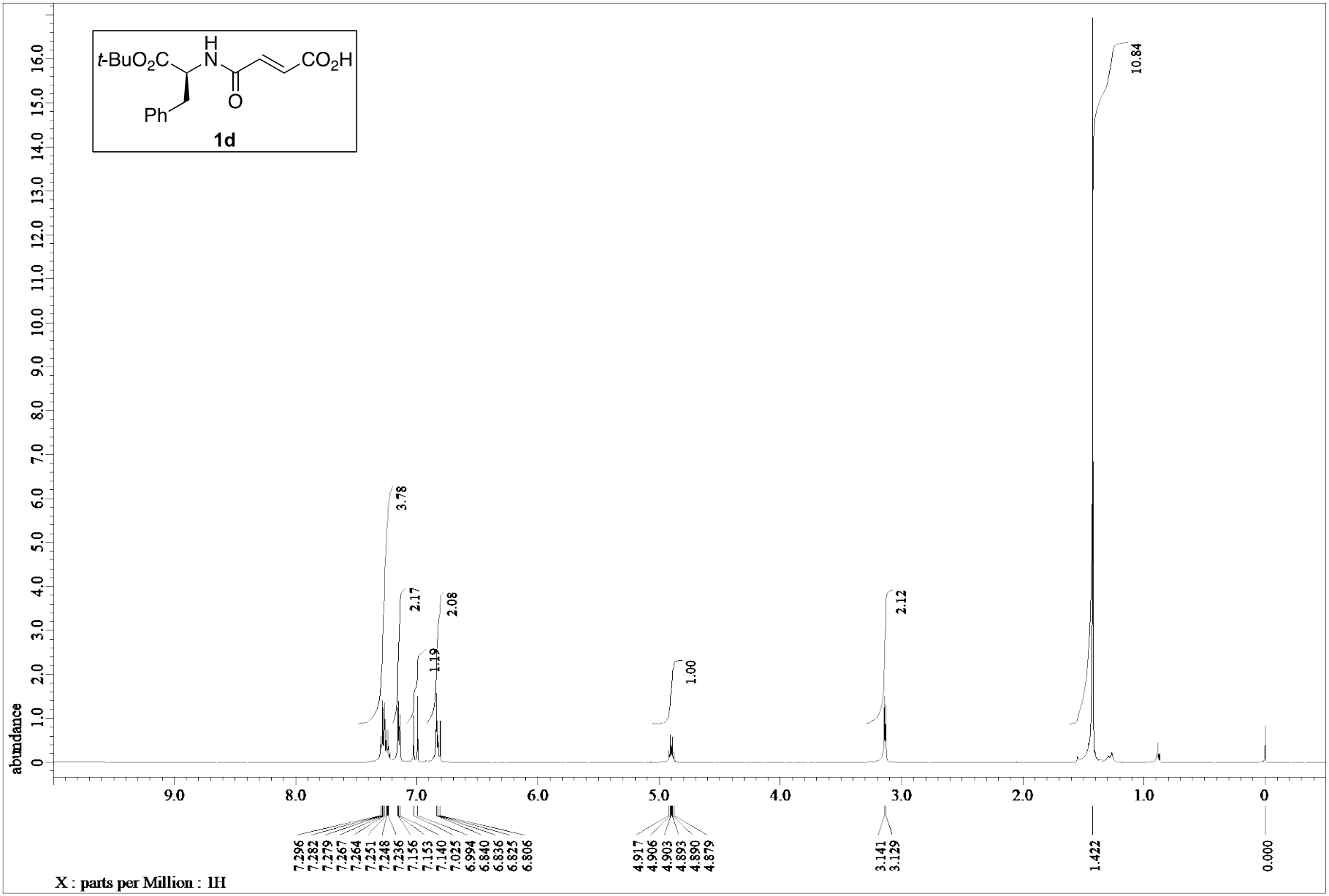
t-BuO2C
H
N
O
CO2H
Ph
1d
abundance
3.78
2.17
1.19
2.08
1.00
2.12
10.84
9.0
8.0
7.0
6.0
5.0
4.0
3.0
2.0
1.0
0
7.296
7.282
7.279
7.267
7.264
7.251
7.248
7.236
7.156
7.153
7.140
7.025
6.994
6.840
6.836
6.825
6.806
4.917
4.906
4.903
4.893
4.890
4.879
3.141
3.129
1.422
0.000
X : parts per Million : 1H

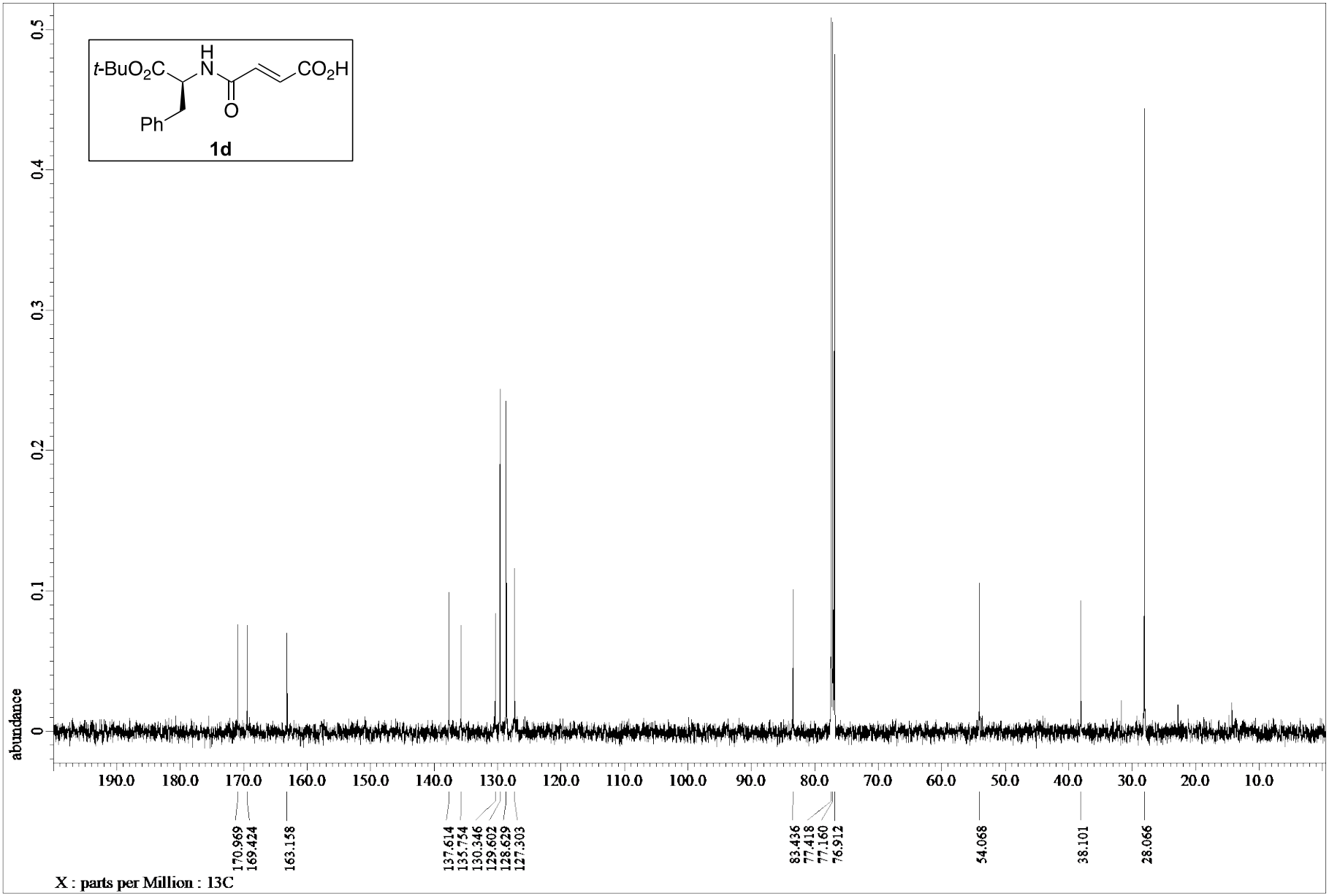
t-BuO2C
H
N
CO2H
O
Ph
1d
abundance
0.5
0.4
0.3
0.2
0.1
0
190.0
180.0
170.0
160.0
150.0
140.0
130.0
120.0
110.0
100.0
90.0
80.0
70.0
60.0
50.0
40.0
30.0
20.0
10.0
170.969
169.424
163.158
137.614
135.754
130.346
129.602
128.629
127.303
83.436
77.418
77.160
76.912
54.068
38.101
28.066
X : parts per Million : 13C

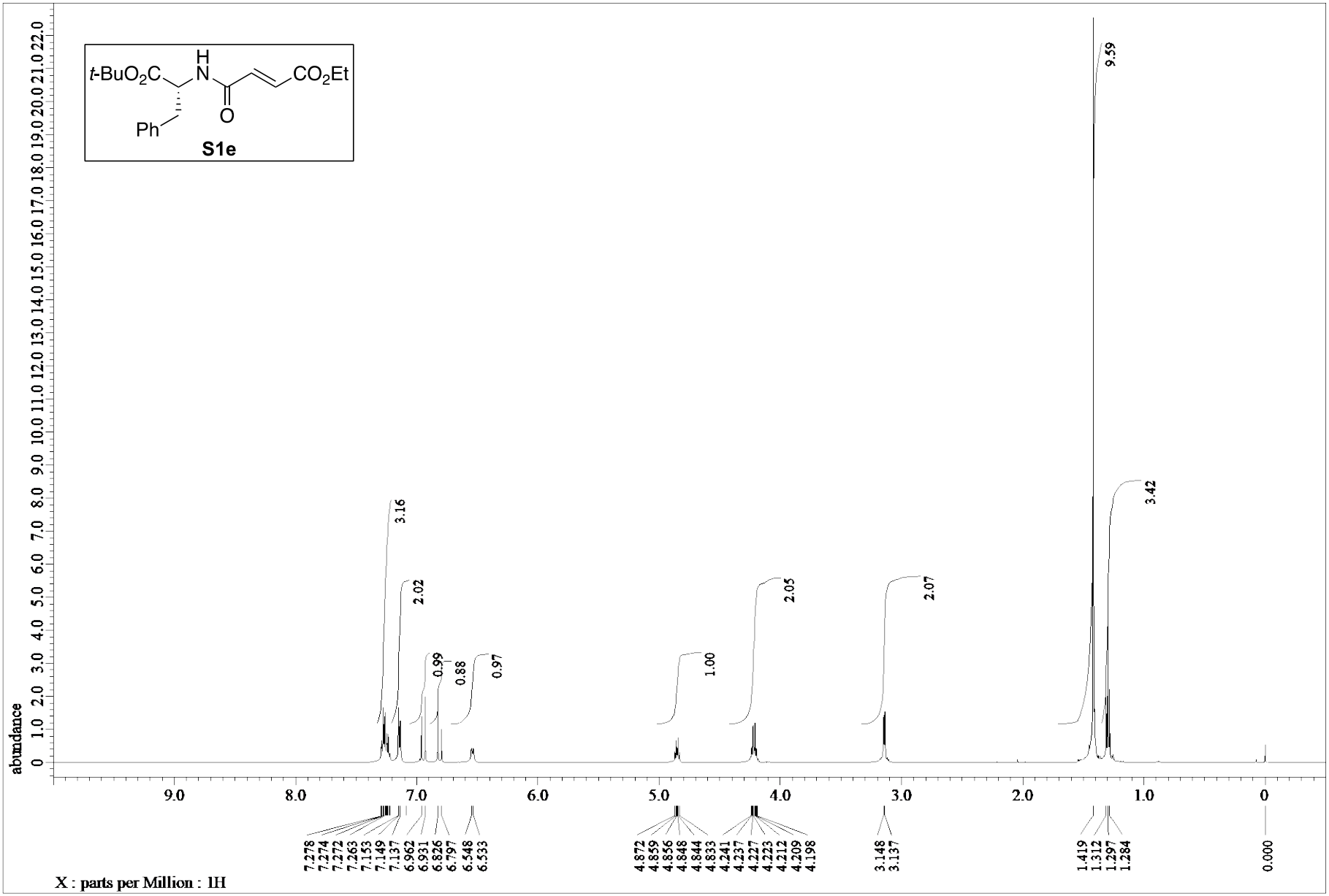
t-BuO2C
H
N
CO2Et
O
Ph
S1e
abundance
3.16
2.02
0.99
0.88
0.97
1.00
2.05
2.07
9.59
3.42
7.278
7.274
7.272
7.263
7.153
7.149
7.137
6.962
6.931
6.826
6.797
6.548
6.533
4.872
4.859
4.856
4.848
4.844
4.833
4.241
4.237
4.227
4.223
4.212
4.209
4.198
3.148
3.137
1.419
1.312
1.297
1.284
0.000
X : parts per Million : 1H

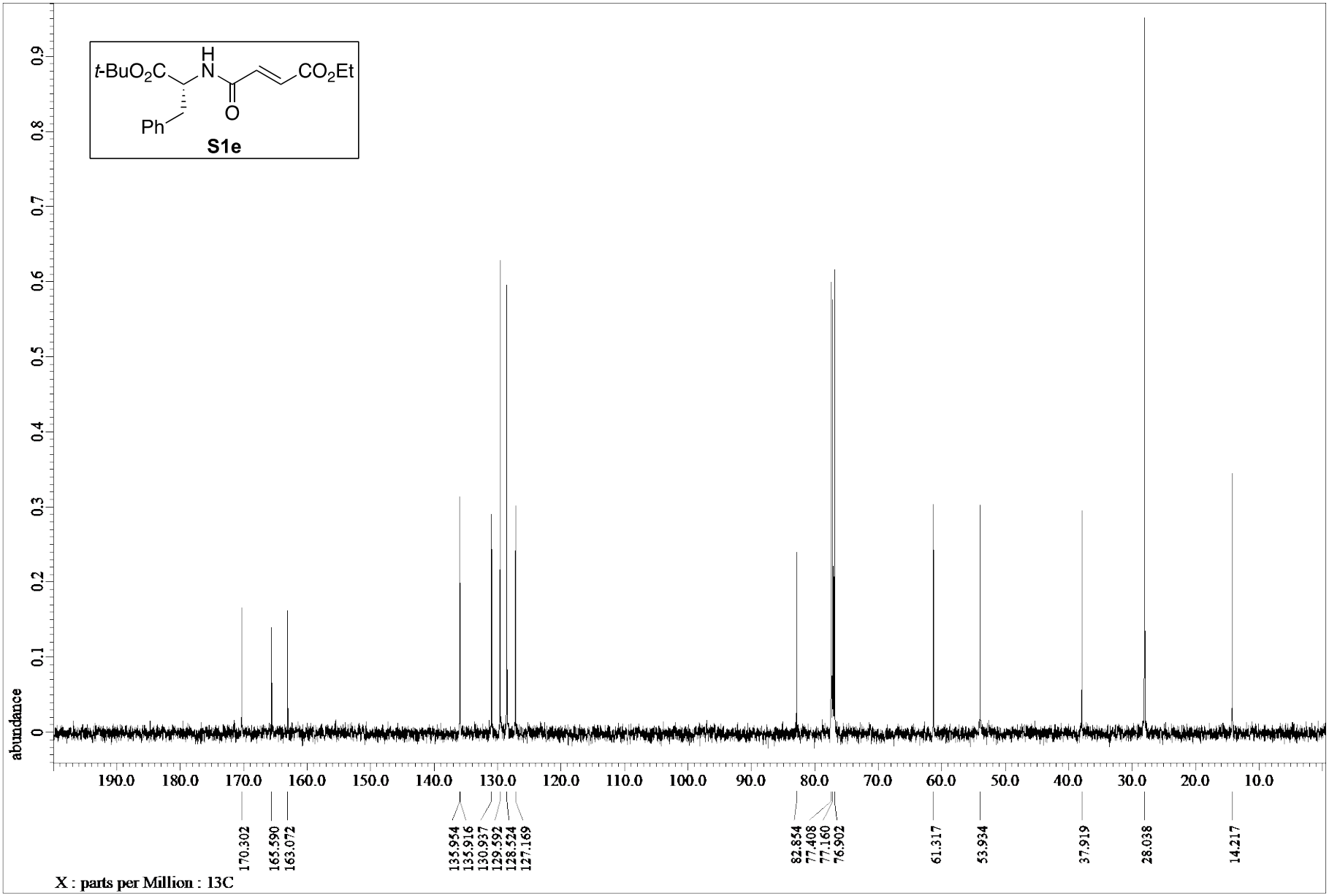
t-BuO2C
H
N
CO2Et
O
Ph
S1e
abundance
0
0.1
0.2
0.3
0.4
0.5
0.6
0.7
0.8
0.9
190.0
180.0
170.0
160.0
150.0
140.0
130.0
120.0
110.0
100.0
90.0
80.0
70.0
60.0
50.0
40.0
30.0
20.0
10.0
170.302
165.590
163.072
135.954
135.916
130.937
129.592
128.524
127.169
82.854
77.408
77.160
76.902
61.317
53.934
37.919
28.038
14.217
X : parts per Million : 13C

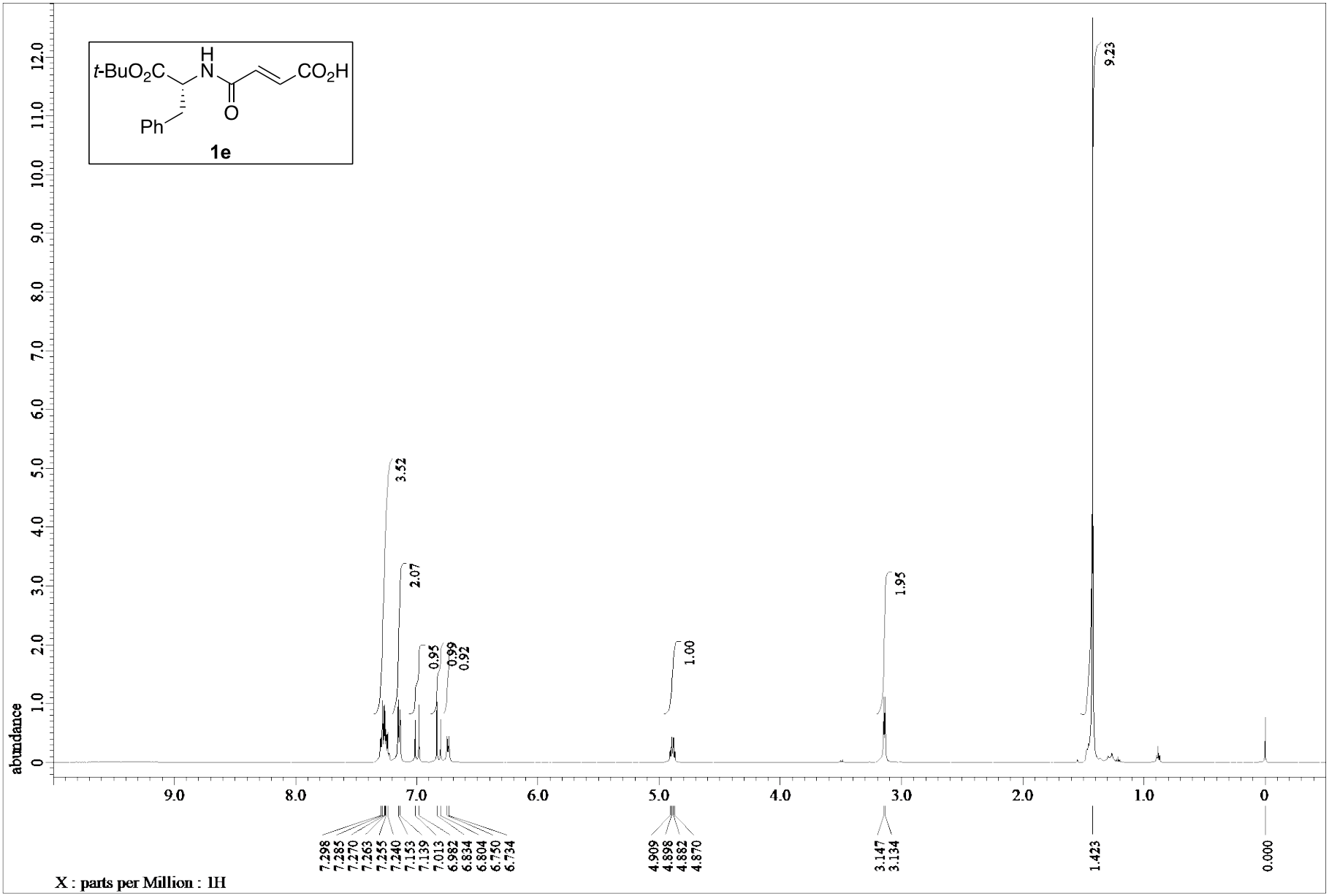
t-BuO2C
H
N
CO2H
O
Ph
1e
abundance
X : parts per Million : 1H
9.23
3.52
2.07
1.95
1.00
0.95
0.99
0.92
7.298
7.285
7.270
7.263
7.255
7.240
7.153
7.139
7.013
6.982
6.834
6.804
6.750
6.734
4.909
4.898
4.882
4.870
3.147
3.134
1.423
0.000

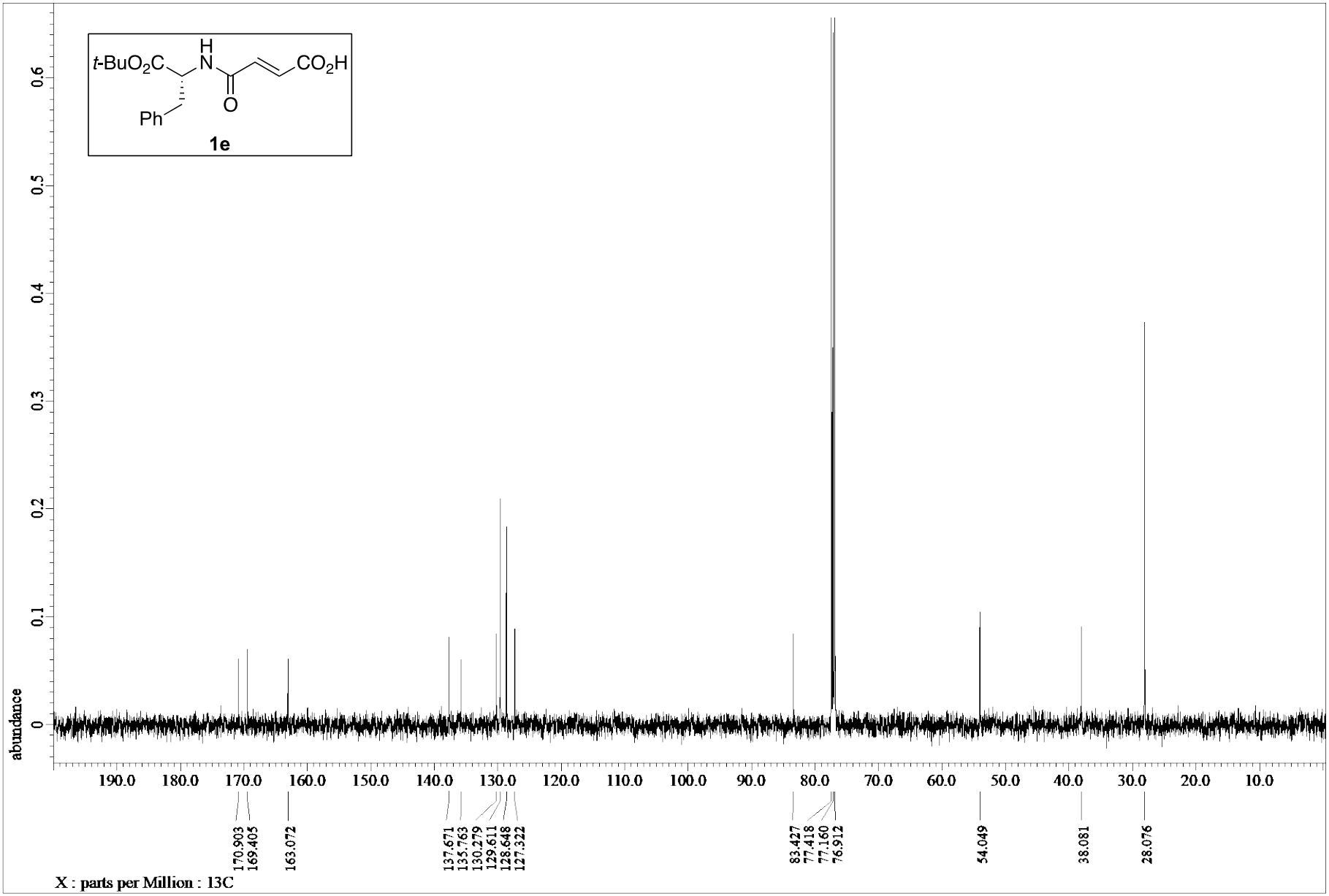
t-BuO2C
H
N
CO2H
O
Ph
1e
abundance
0
0.1
0.2
0.3
0.4
0.5
0.6
190.0
180.0
170.0
160.0
150.0
140.0
130.0
120.0
110.0
100.0
90.0
80.0
70.0
60.0
50.0
40.0
30.0
20.0
10.0
170.903
169.405
163.072
137.671
135.763
130.279
129.611
128.648
127.322
83.427
77.418
77.160
76.912
54.049
38.081
28.076
X : parts per Million : 13C

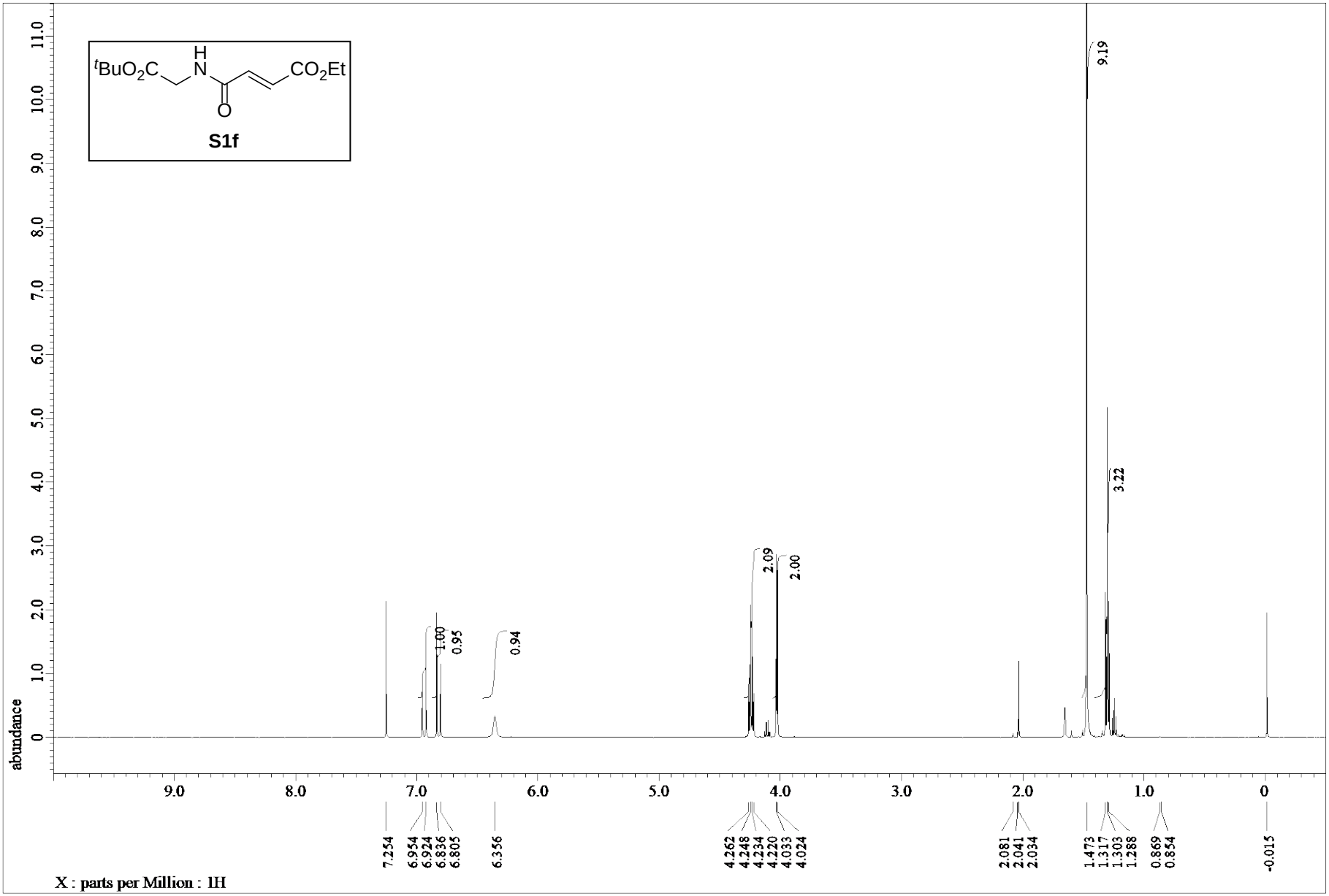
S1f
abundance
X : parts per Million : 1H
9.19
3.22
2.09
2.00
1.00
0.95
0.94
7.254
6.954
6.924
6.836
6.805
6.356
4.262
4.248
4.234
4.220
4.033
4.024
2.081
2.041
2.034
1.473
1.317
1.303
1.288
0.869
0.854
-0.015

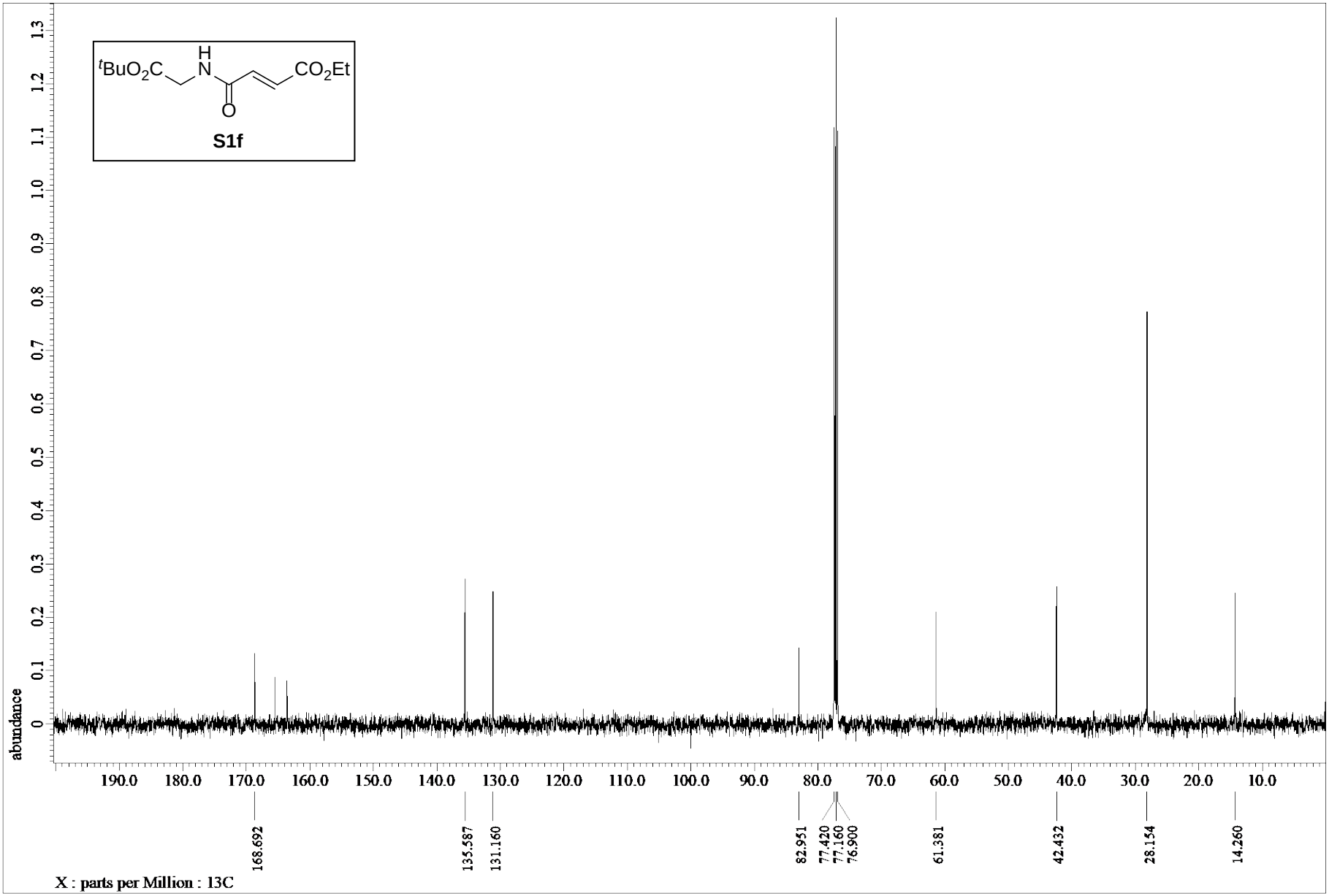
S1f
abundance
X : parts per Million : 13C
168.692
135.587
131.160
82.951
77.420
77.160
76.900
61.381
42.432
28.154
14.260

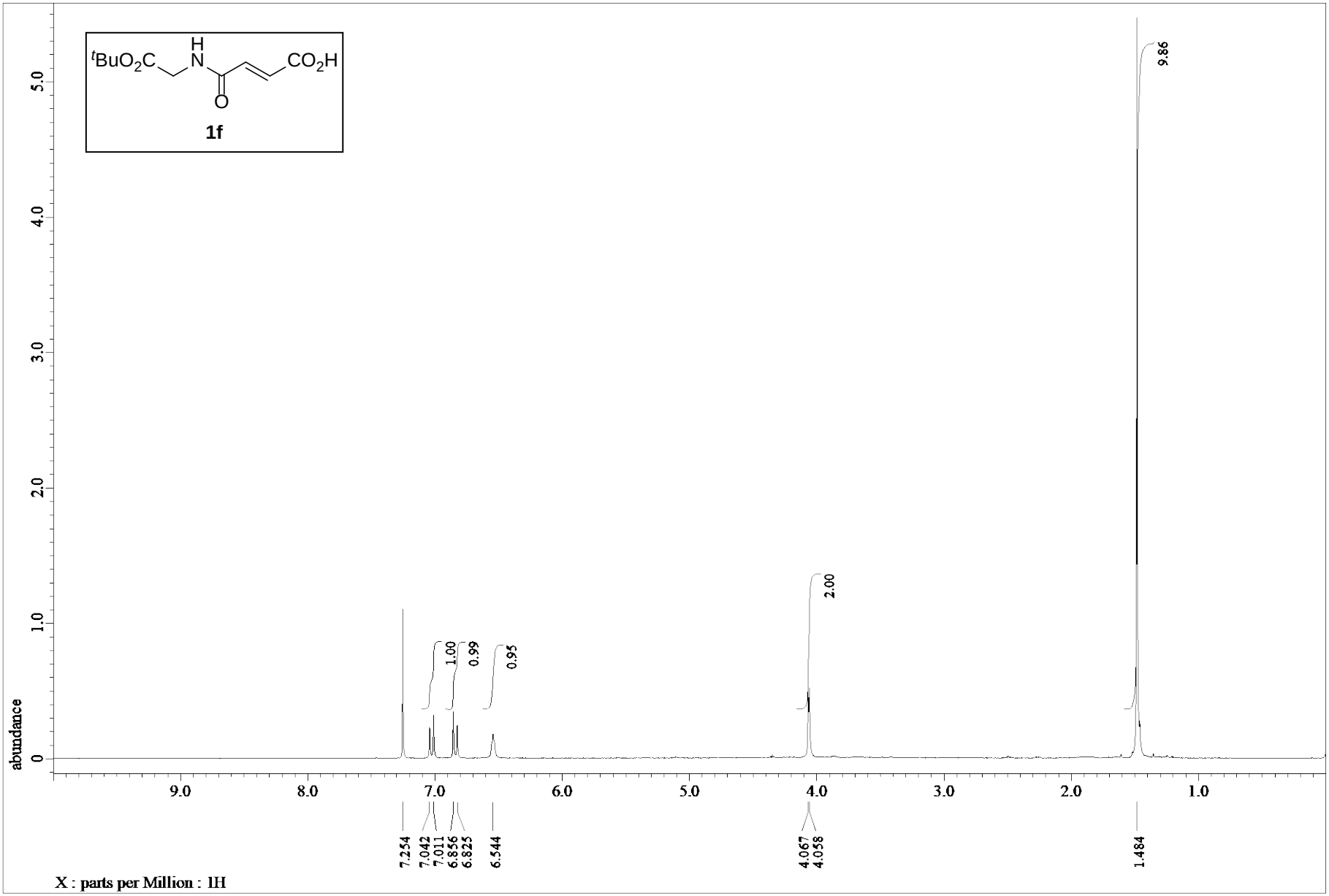
tBuO2C
H
N
CO2H
O
1f
9.86
2.00
1.00
0.99
0.95
abundance
5.0
4.0
3.0
2.0
1.0
0
9.0
8.0
7.0
6.0
5.0
4.0
3.0
2.0
1.0
7.254
7.042
7.011
6.856
6.825
6.544
4.067
4.058
1.484
X : parts per Million : 1H

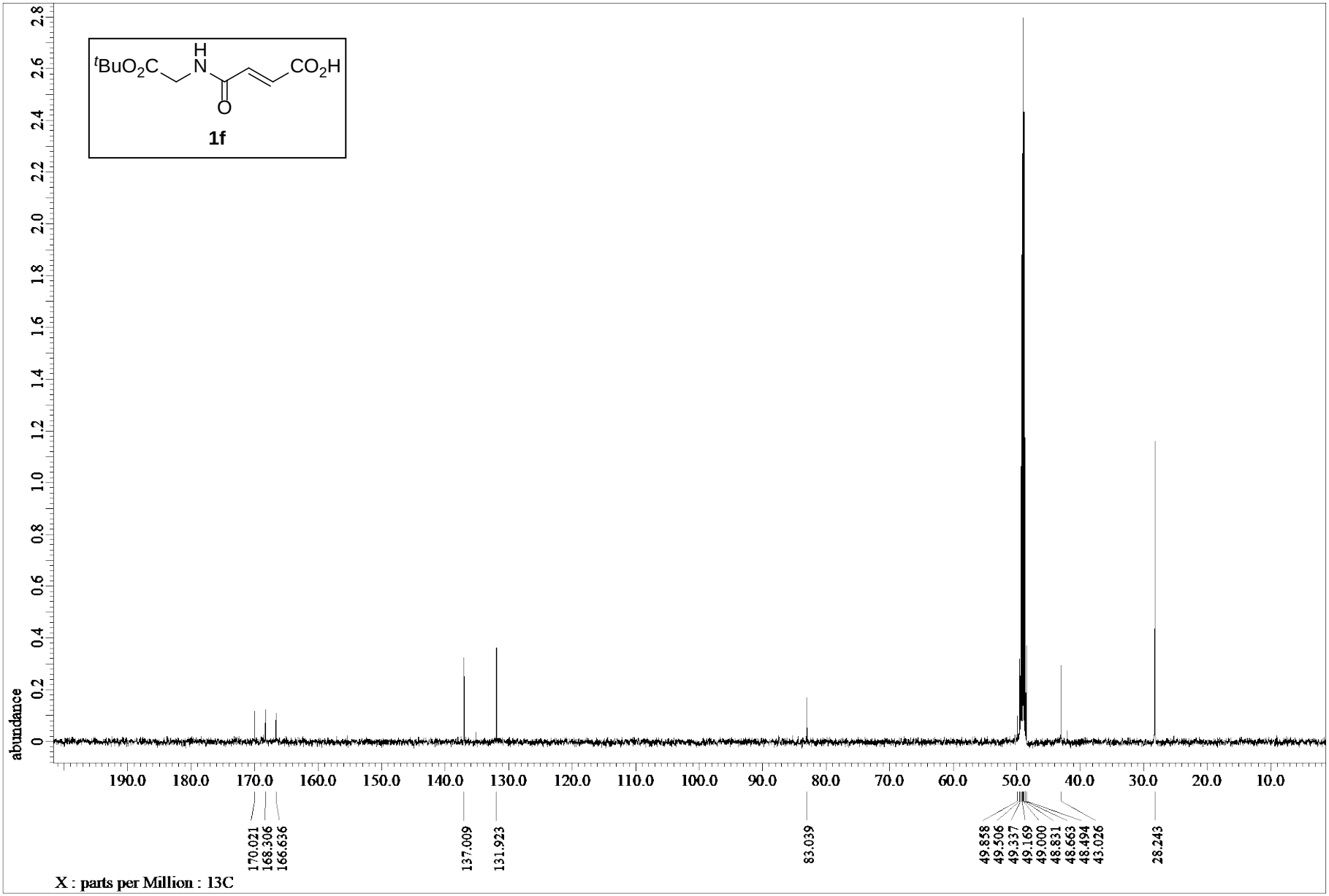
tBuO2C
H
N
CO2H
O
1f
abundance
0
0.2
0.4
0.6
0.8
1.0
1.2
1.4
1.6
1.8
2.0
2.2
2.4
2.6
2.8
190.0
180.0
170.0
160.0
150.0
140.0
130.0
120.0
110.0
100.0
90.0
80.0
70.0
60.0
50.0
40.0
30.0
20.0
10.0
170.021
168.306
166.636
137.009
131.923
83.039
49.858
49.506
49.337
49.169
49.000
48.831
48.663
48.494
43.026
28.243
X : parts per Million : 13C

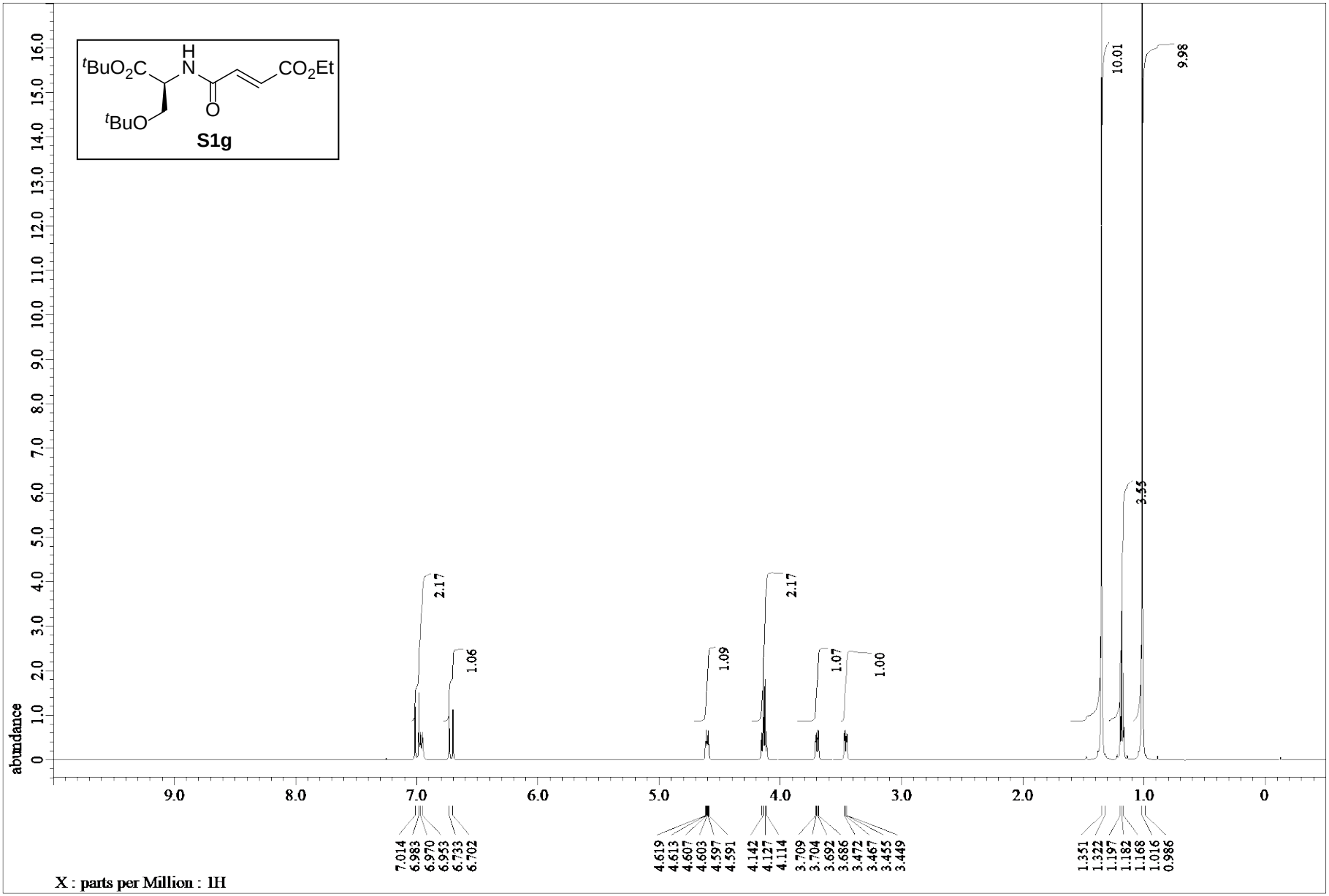
S1g
abundance
X : parts per Million : 1H
10.01
9.98
3.55
2.17
1.06
1.09
2.17
1.07
1.00
7.014
6.983
6.970
6.953
6.733
6.702
4.619
4.613
4.607
4.603
4.597
4.591
4.142
4.127
4.114
3.709
3.704
3.692
3.686
3.472
3.467
3.455
3.449
1.351
1.322
1.197
1.182
1.168
1.016
0.986

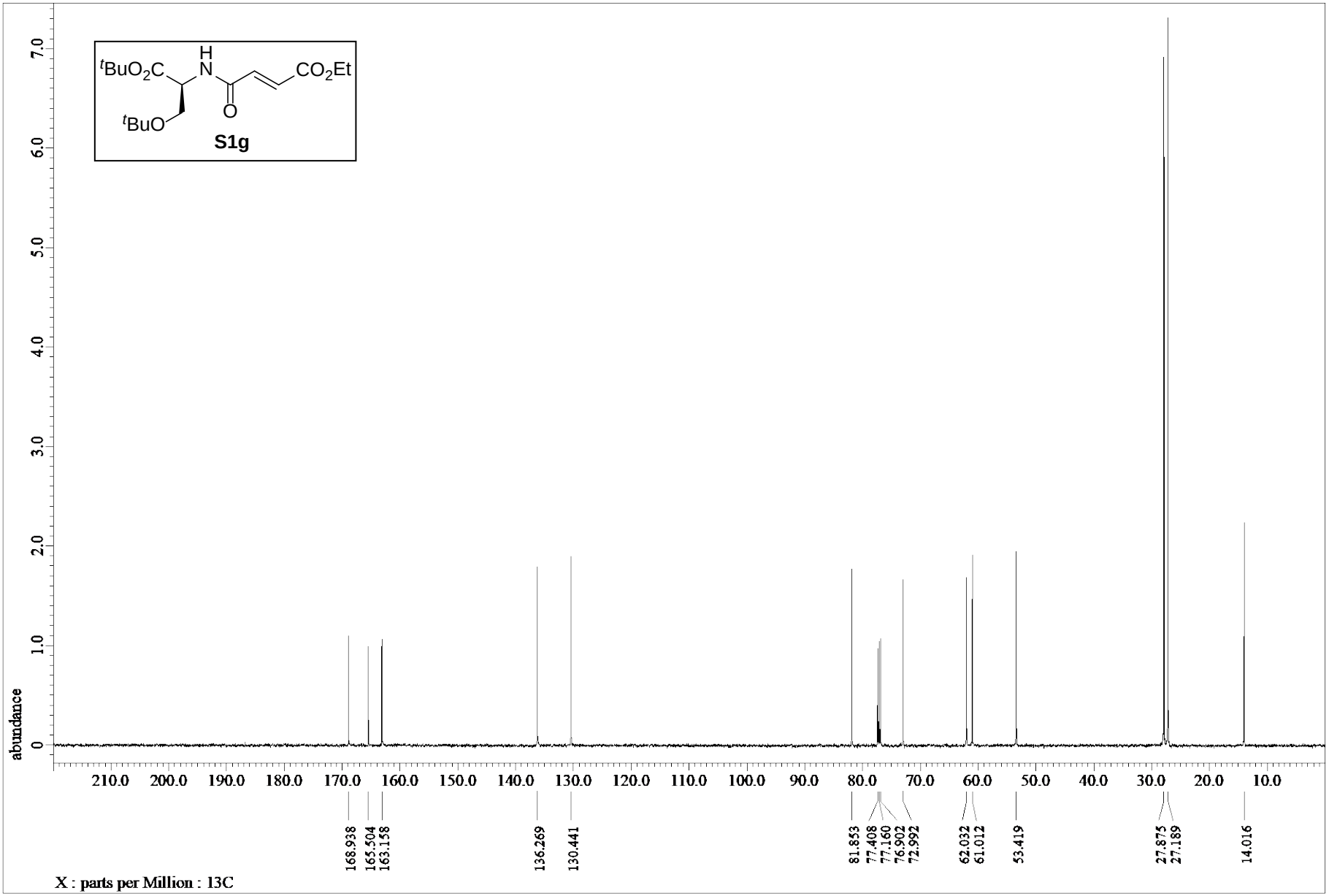
S1g
abundance
X : parts per Million : 13C
168.938
165.504
163.158
136.269
130.441
81.853
77.408
77.160
76.902
72.992
62.032
61.012
53.419
27.875
27.189
14.016

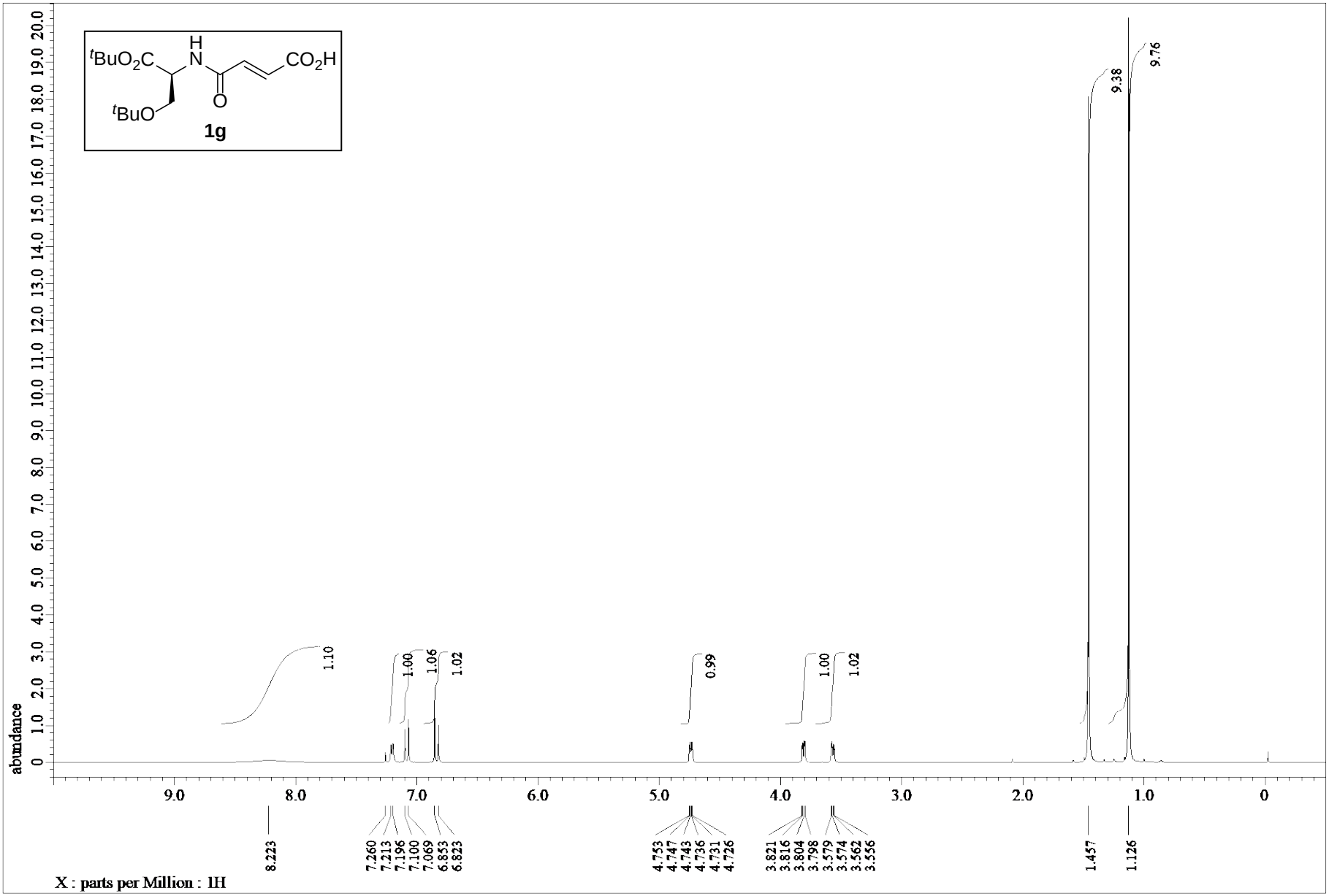
1g
abundance
X : parts per Million : 1H
1.10
1.00
1.06
1.02
0.99
1.00
1.02
9.38
9.76
8.223
7.260
7.213
7.196
7.100
7.069
6.853
6.823
4.753
4.747
4.743
4.736
4.731
4.726
3.821
3.816
3.804
3.798
3.579
3.574
3.562
3.556
1.457
1.126

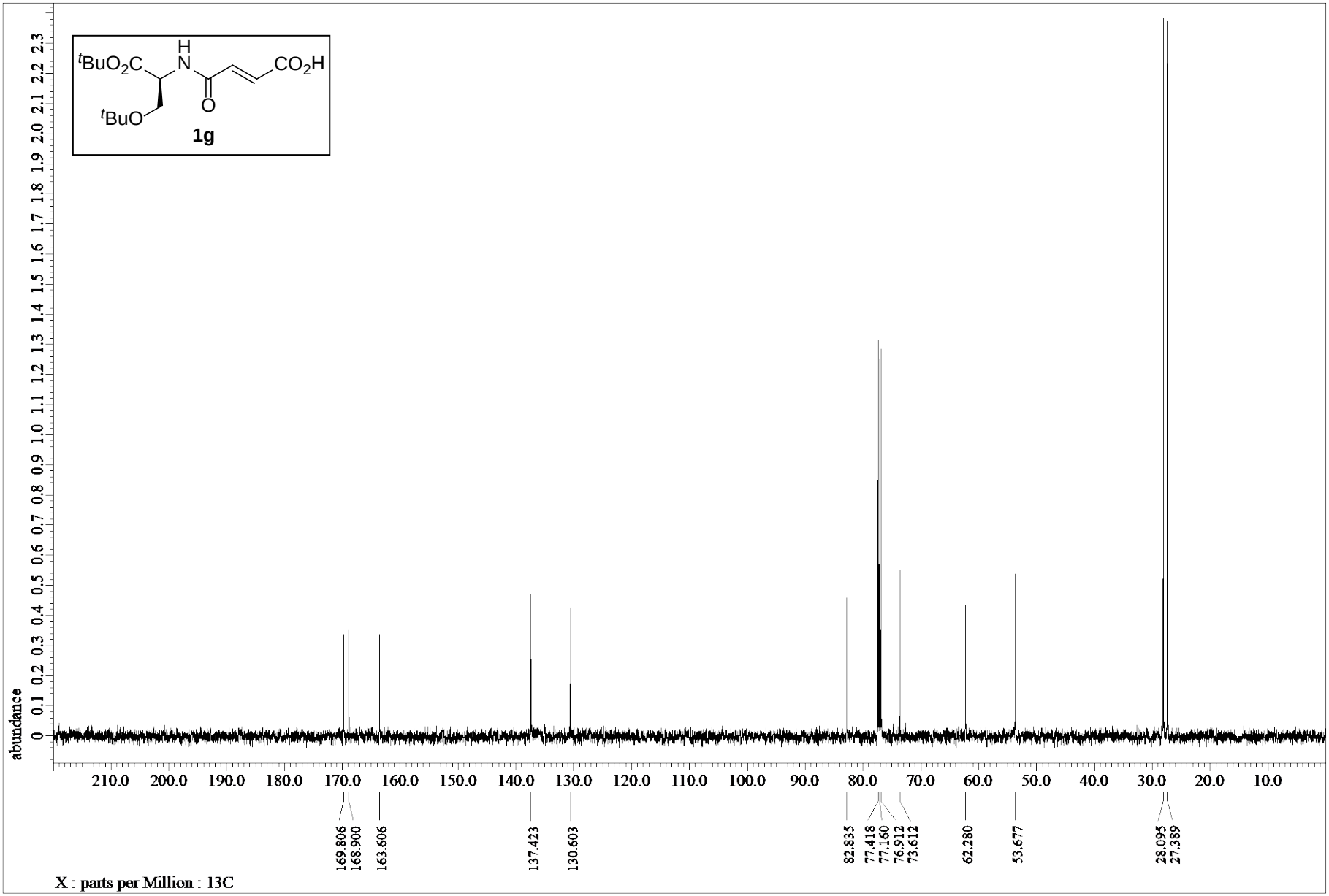
^{t}BuO$_2$C
H
N
CO$_2$H
O
^{t}BuO
1g
abundance
0 0.1 0.2 0.3 0.4 0.5 0.6 0.7 0.8 0.9 1.0 1.1 1.2 1.3 1.4 1.5 1.6 1.7 1.8 1.9 2.0 2.1 2.2 2.3
210.0 200.0 190.0 180.0 170.0 160.0 150.0 140.0 130.0 120.0 110.0 100.0 90.0 80.0 70.0 60.0 50.0 40.0 30.0 20.0 10.0
169.806
168.900
163.606
137.423
130.603
82.835
77.418
77.160
76.912
73.612
62.280
53.677
28.095
27.389
X : parts per Million : 13C

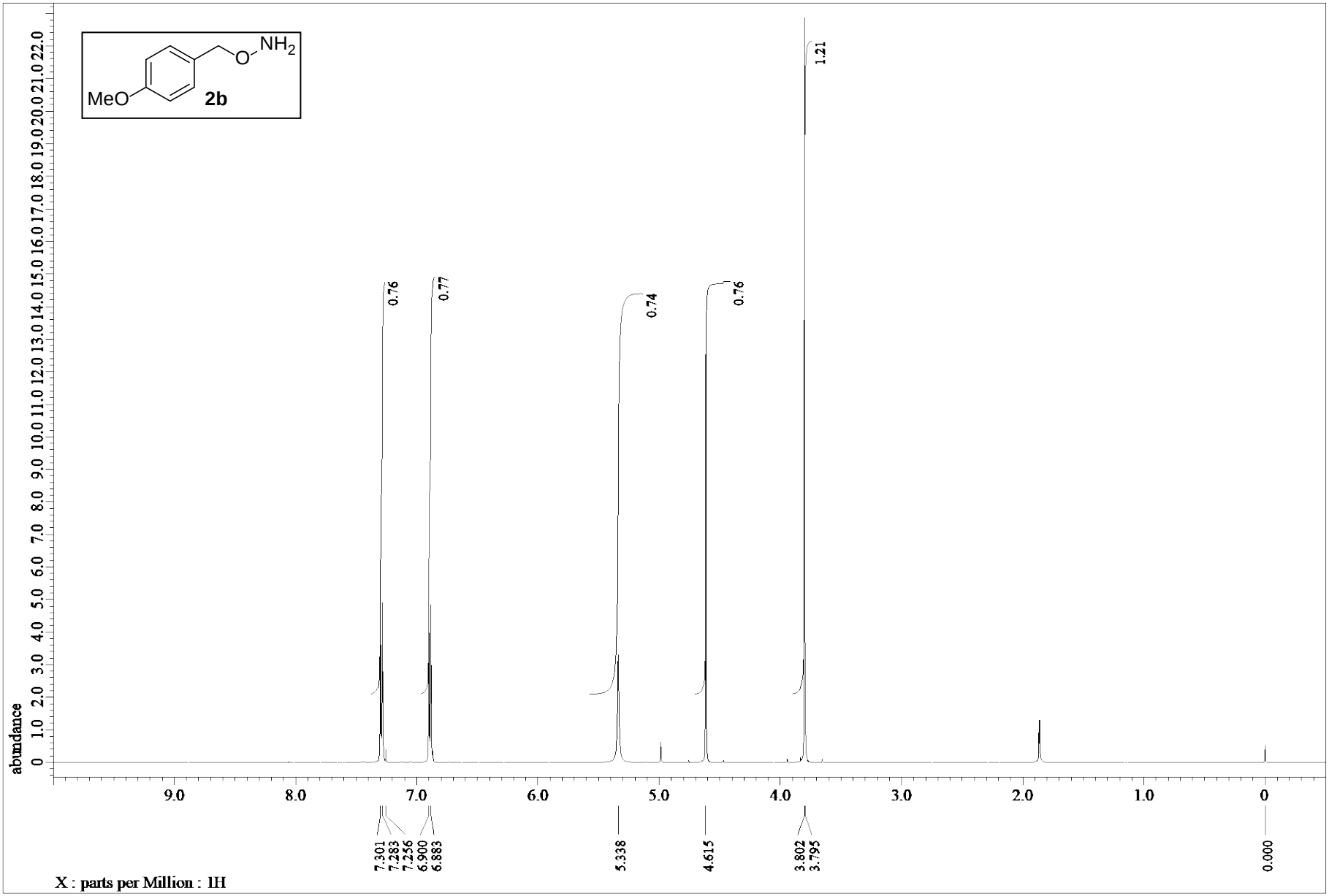
MeO
NH2
O
2b
abundance
0
1.0
2.0
3.0
4.0
5.0
6.0
7.0
8.0
9.0
10.0
11.0
12.0
13.0
14.0
15.0
16.0
17.0
18.0
19.0
20.0
21.0
22.0
0.76
0.77
0.74
0.76
1.21
9.0
8.0
7.0
6.0
5.0
4.0
3.0
2.0
1.0
0
7.301
7.283
7.256
6.900
6.883
5.338
4.615
3.802
3.795
0.000
X : parts per Million : 1H

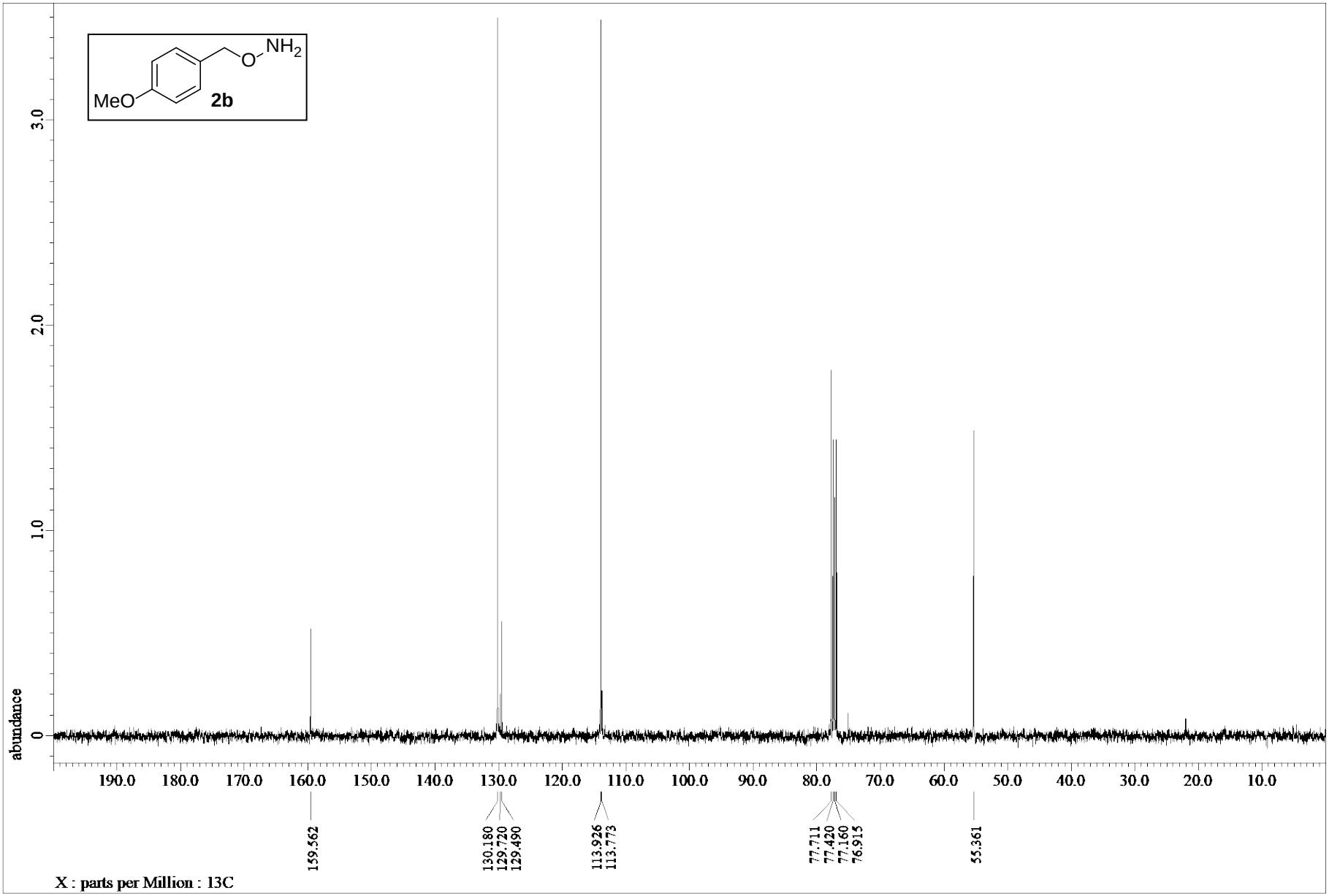
NH2
O
MeO
2b
abundance
3.0
2.0
1.0
0
190.0
180.0
170.0
160.0
150.0
140.0
130.0
120.0
110.0
100.0
90.0
80.0
70.0
60.0
50.0
40.0
30.0
20.0
10.0
159.562
130.180
129.720
129.490
113.926
113.773
77.711
77.420
77.160
76.915
55.361
X : parts per Million : 13C

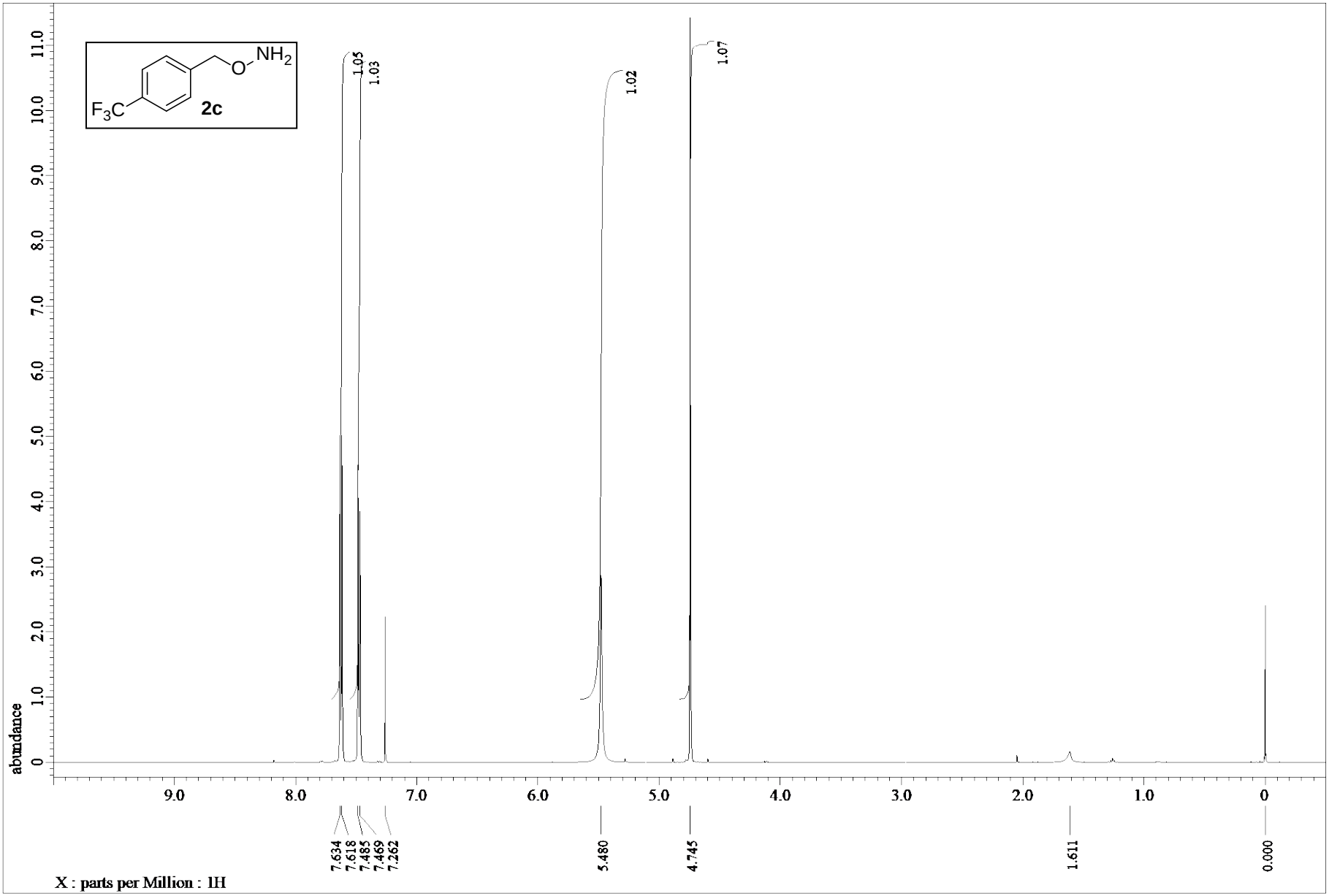
NH2
O
F3C
2c
1.05
1.03
1.02
1.07
abundance
11.0
10.0
9.0
8.0
7.0
6.0
5.0
4.0
3.0
2.0
1.0
0
9.0
8.0
7.0
6.0
5.0
4.0
3.0
2.0
1.0
0
7.634
7.618
7.485
7.469
7.262
5.480
4.745
1.611
0.000
X : parts per Million : 1H

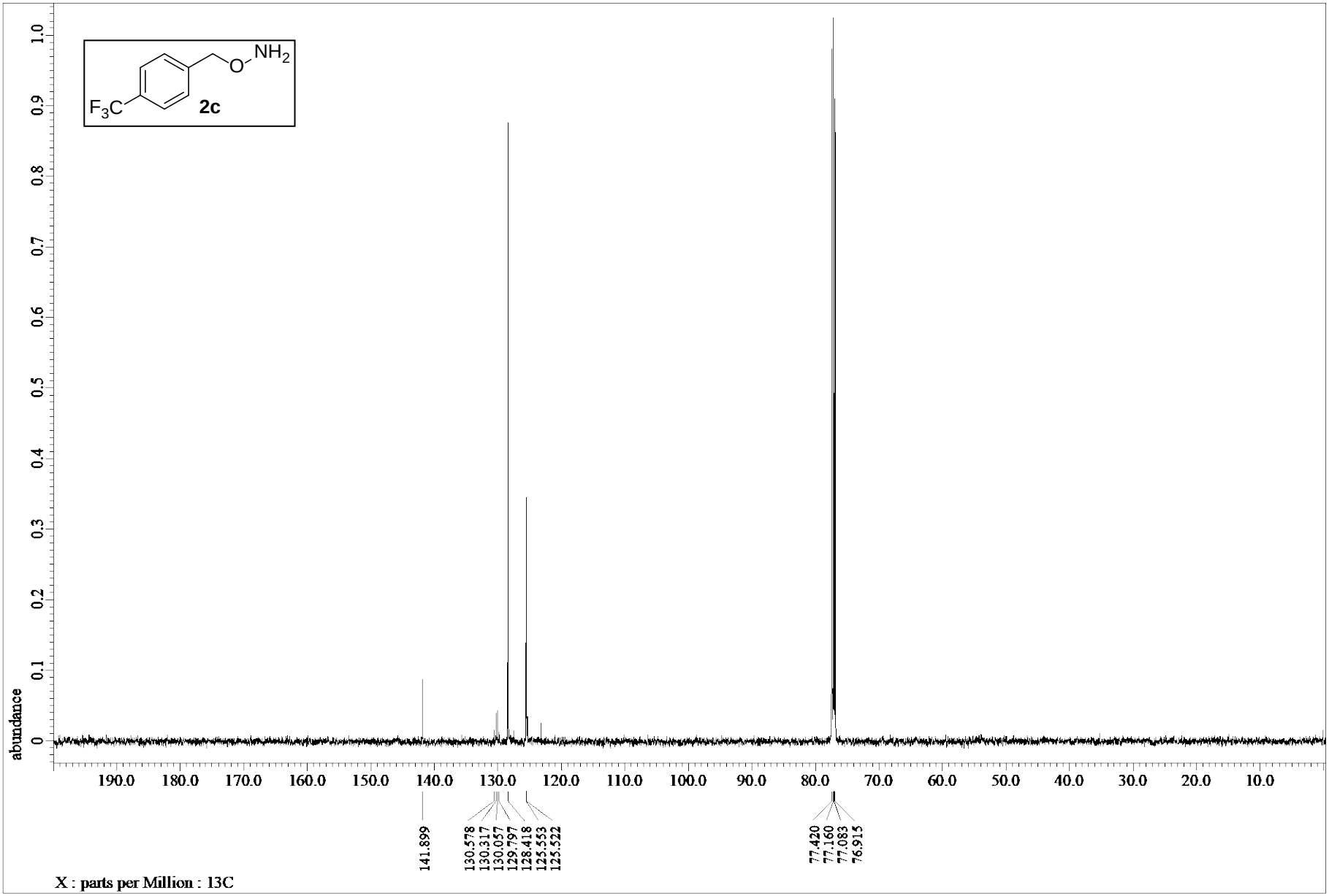
NH2
O
F3C
2c
abundance
1.0
0.9
0.8
0.7
0.6
0.5
0.4
0.3
0.2
0.1
0
190.0
180.0
170.0
160.0
150.0
140.0
130.0
120.0
110.0
100.0
90.0
80.0
70.0
60.0
50.0
40.0
30.0
20.0
10.0
141.899
130.578
130.317
130.057
129.797
128.418
125.553
125.522
77.420
77.160
77.083
76.915
X : parts per Million : 13C

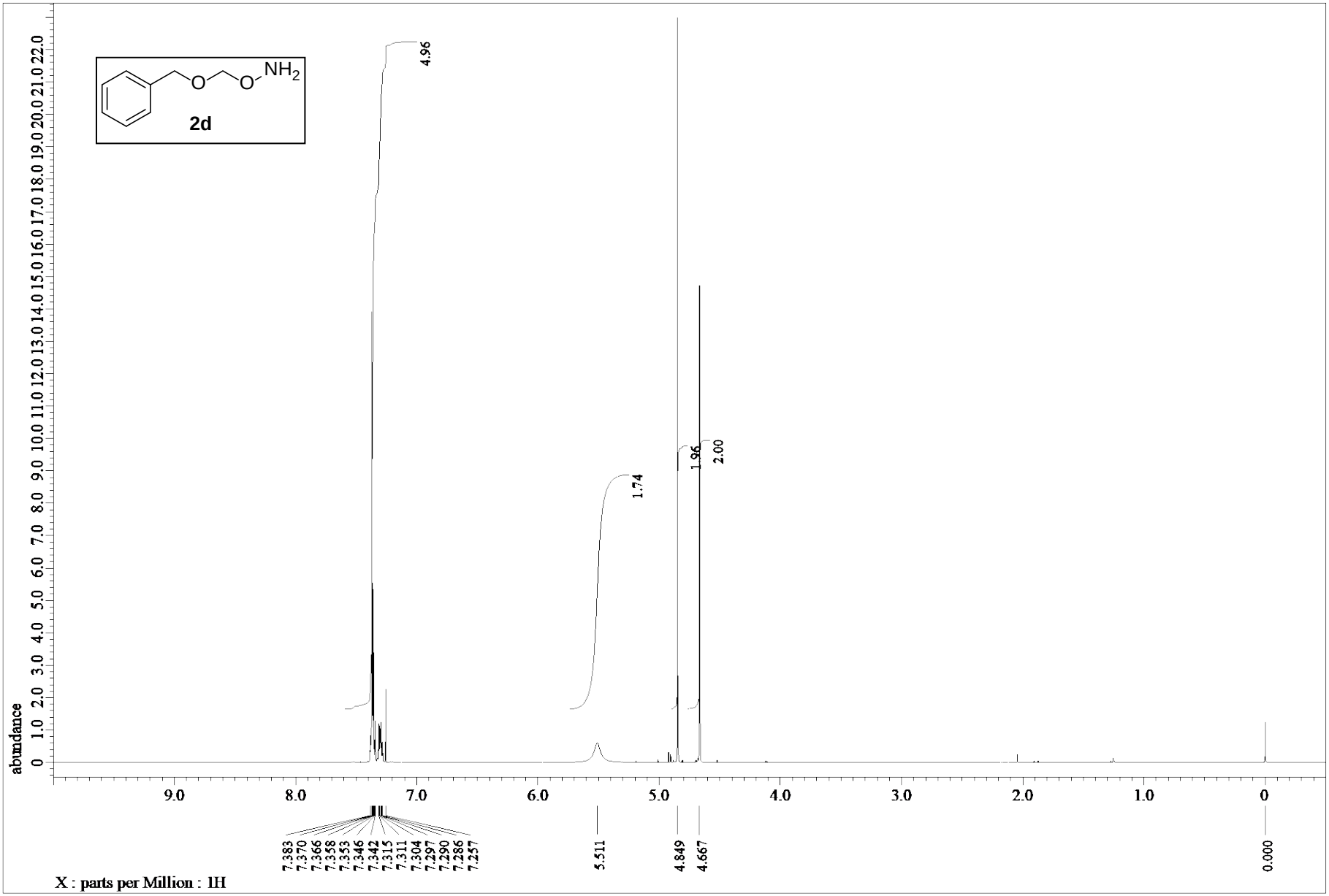
2d
NH2
O
O
4.96
1.74
1.96
2.00
abundance
0 1.0 2.0 3.0 4.0 5.0 6.0 7.0 8.0 9.0 10.0 11.0 12.0 13.0 14.0 15.0 16.0 17.0 18.0 19.0 20.0 21.0 22.0
9.0
8.0
7.0
6.0
5.0
4.0
3.0
2.0
1.0
0
7.383
7.370
7.366
7.358
7.353
7.346
7.342
7.315
7.311
7.304
7.297
7.290
7.286
7.257
5.511
4.849
4.667
0.000
X : parts per Million : 1H

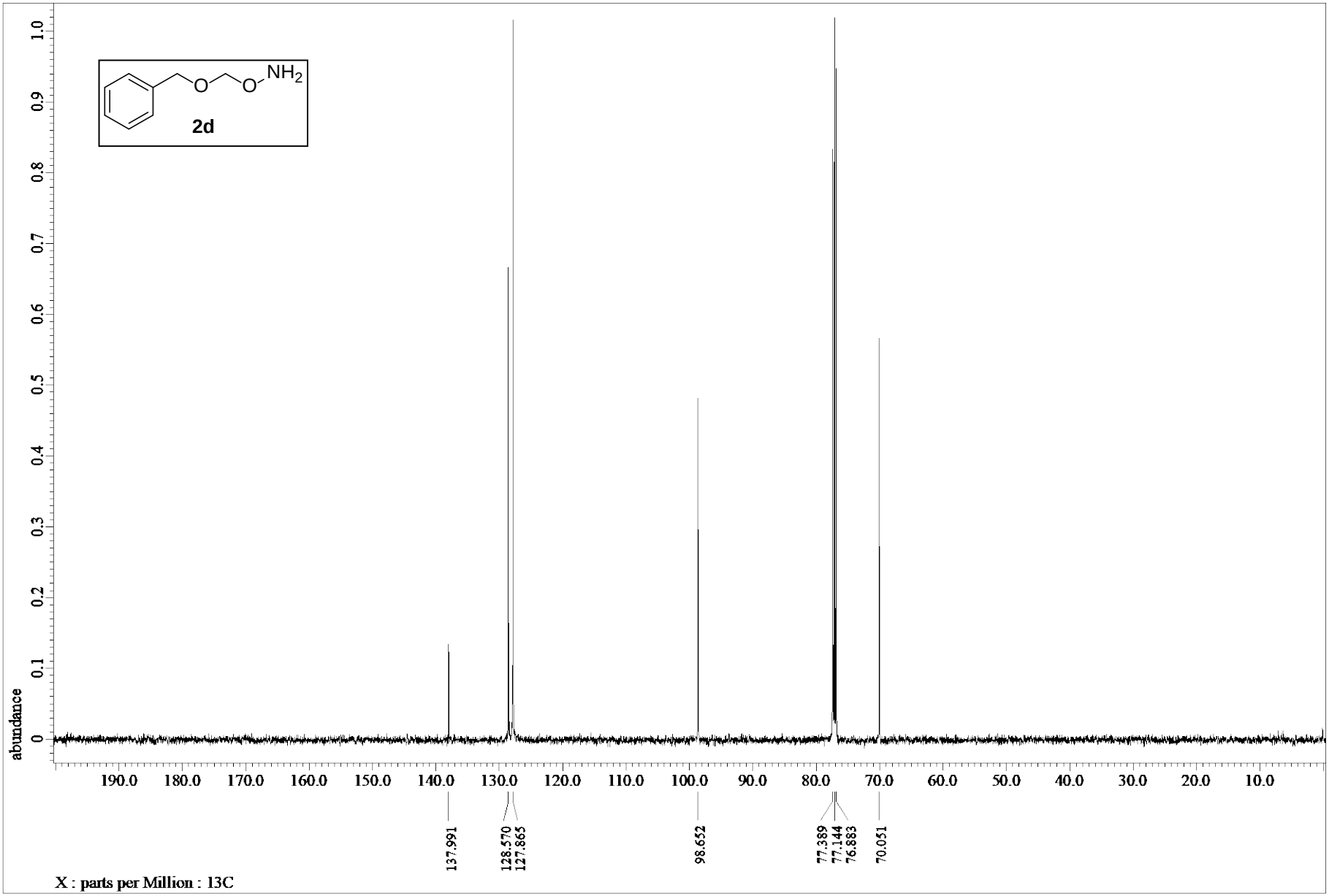
2d
abundance
X : parts per Million : 13C
137.991
128.570
127.865
98.652
77.389
77.144
76.883
70.051

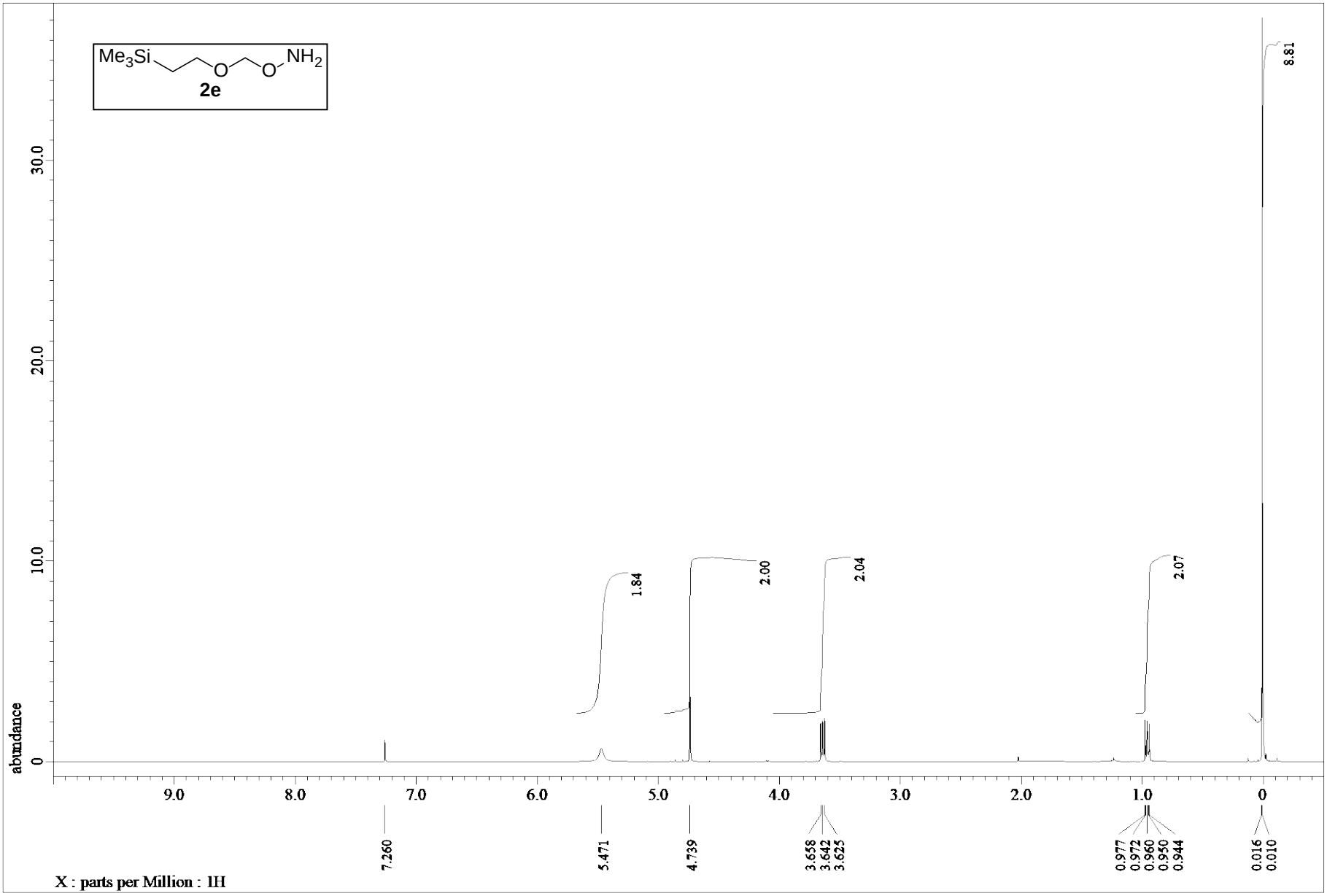
Me3Si
O
O
NH2
2e
30.0
20.0
10.0
0
abundance
1.84
2.00
2.04
2.07
8.81
9.0
8.0
7.0
6.0
5.0
4.0
3.0
2.0
1.0
0
7.260
5.471
4.739
3.658
3.642
3.625
0.977
0.972
0.960
0.950
0.944
0.016
0.010
X : parts per Million : 1H

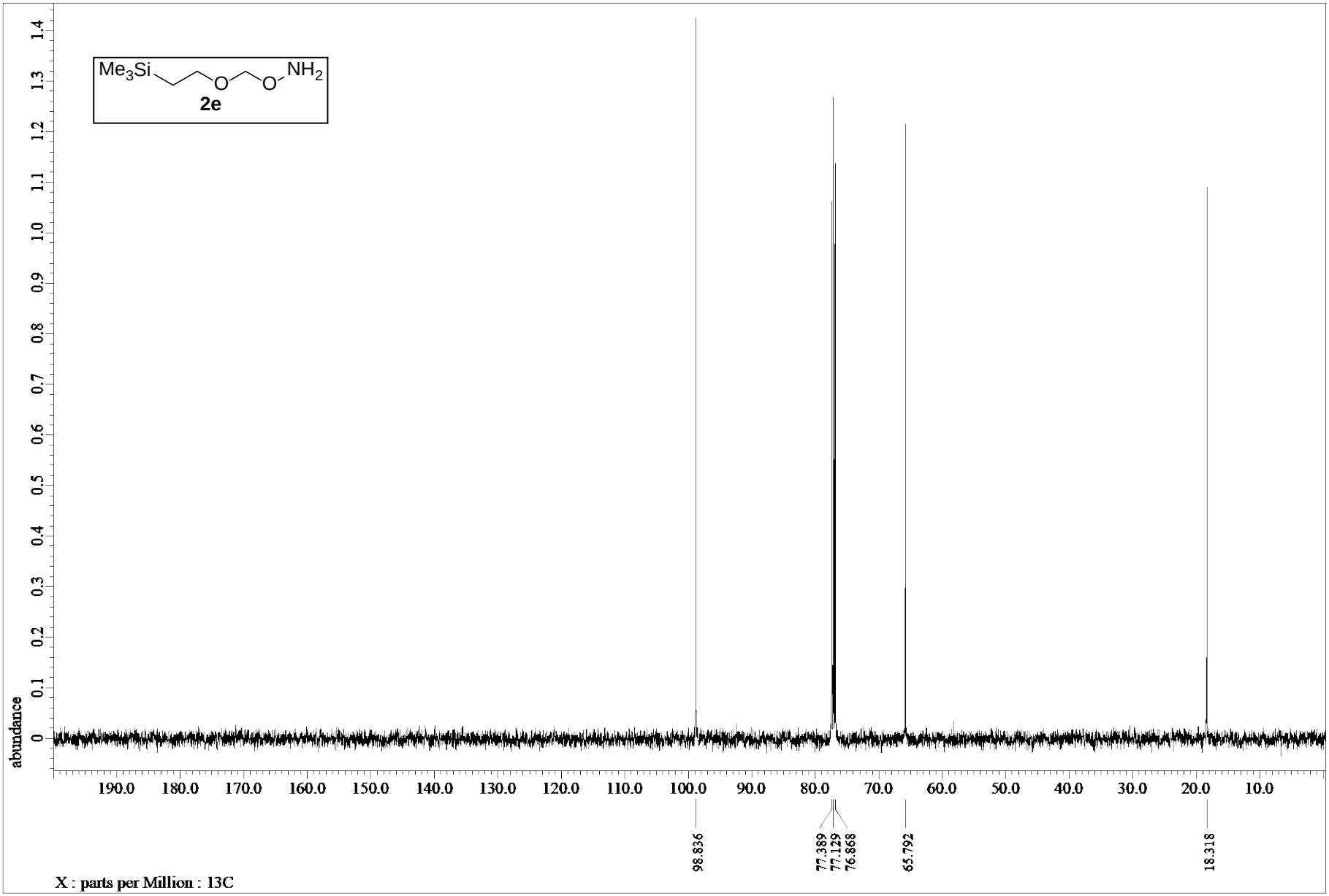
Me3Si
O
O
NH2
2e
abundance
0
0.1
0.2
0.3
0.4
0.5
0.6
0.7
0.8
0.9
1.0
1.1
1.2
1.3
1.4
190.0
180.0
170.0
160.0
150.0
140.0
130.0
120.0
110.0
100.0
90.0
80.0
70.0
60.0
50.0
40.0
30.0
20.0
10.0
98.836
77.389
77.129
76.868
65.792
18.318
X : parts per Million : 13C

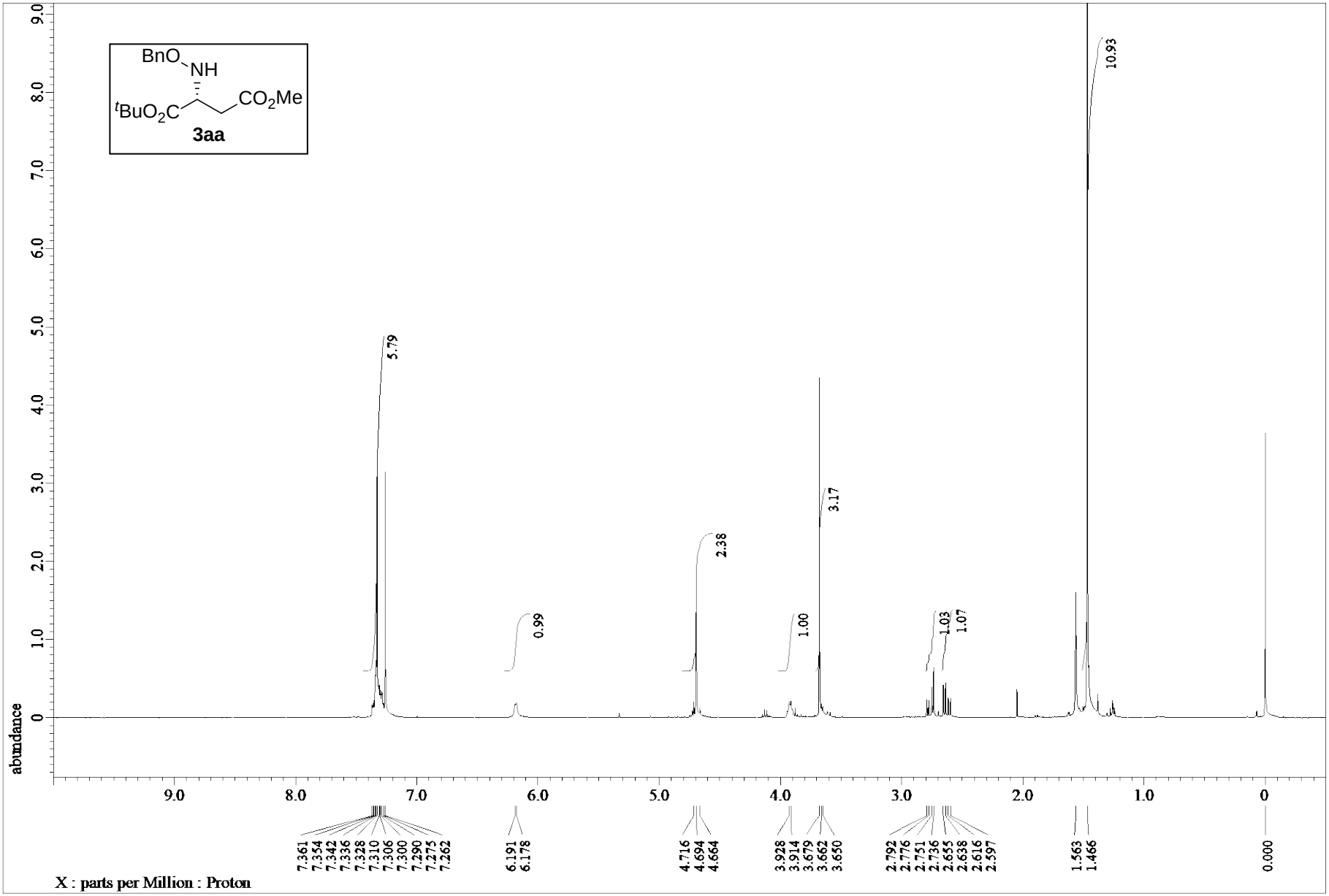
BnO
NH
tBuO2C
CO2Me
3aa
abundance
X : parts per Million : Proton
10.93
5.79
2.38
3.17
0.99
1.00
1.03
1.07
7.361
7.354
7.342
7.336
7.328
7.310
7.306
7.300
7.290
7.275
7.262
6.191
6.178
4.716
4.694
4.664
3.928
3.914
3.679
3.662
3.650
2.792
2.776
2.751
2.736
2.655
2.638
2.616
2.597
1.563
1.466
0.000

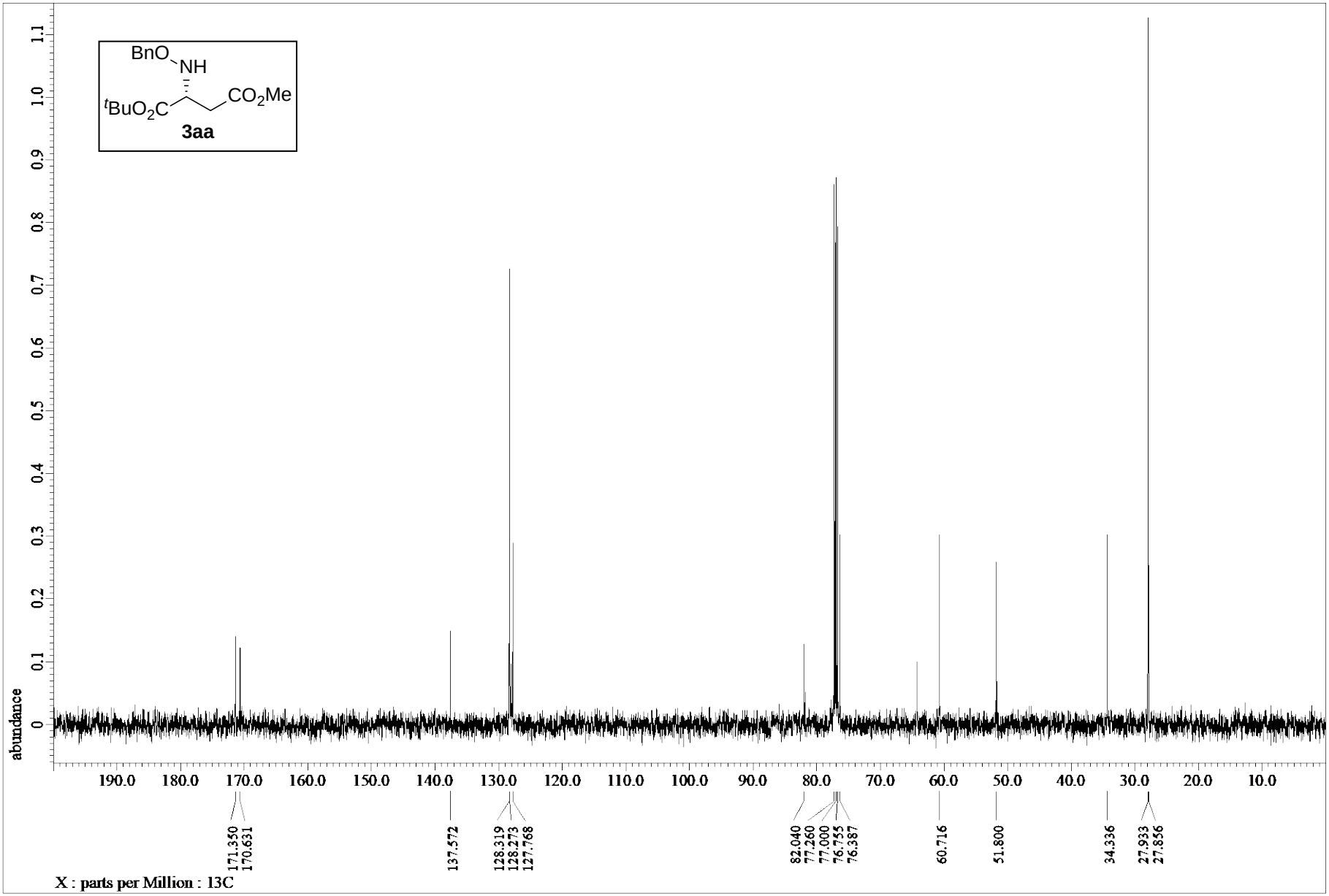
BnO
NH
tBuO2C
CO2Me
3aa
abundance
X : parts per Million : 13C
171.350
170.631
137.572
128.319
128.273
127.768
82.040
77.260
77.000
76.755
76.387
60.716
51.800
34.336
27.933
27.856

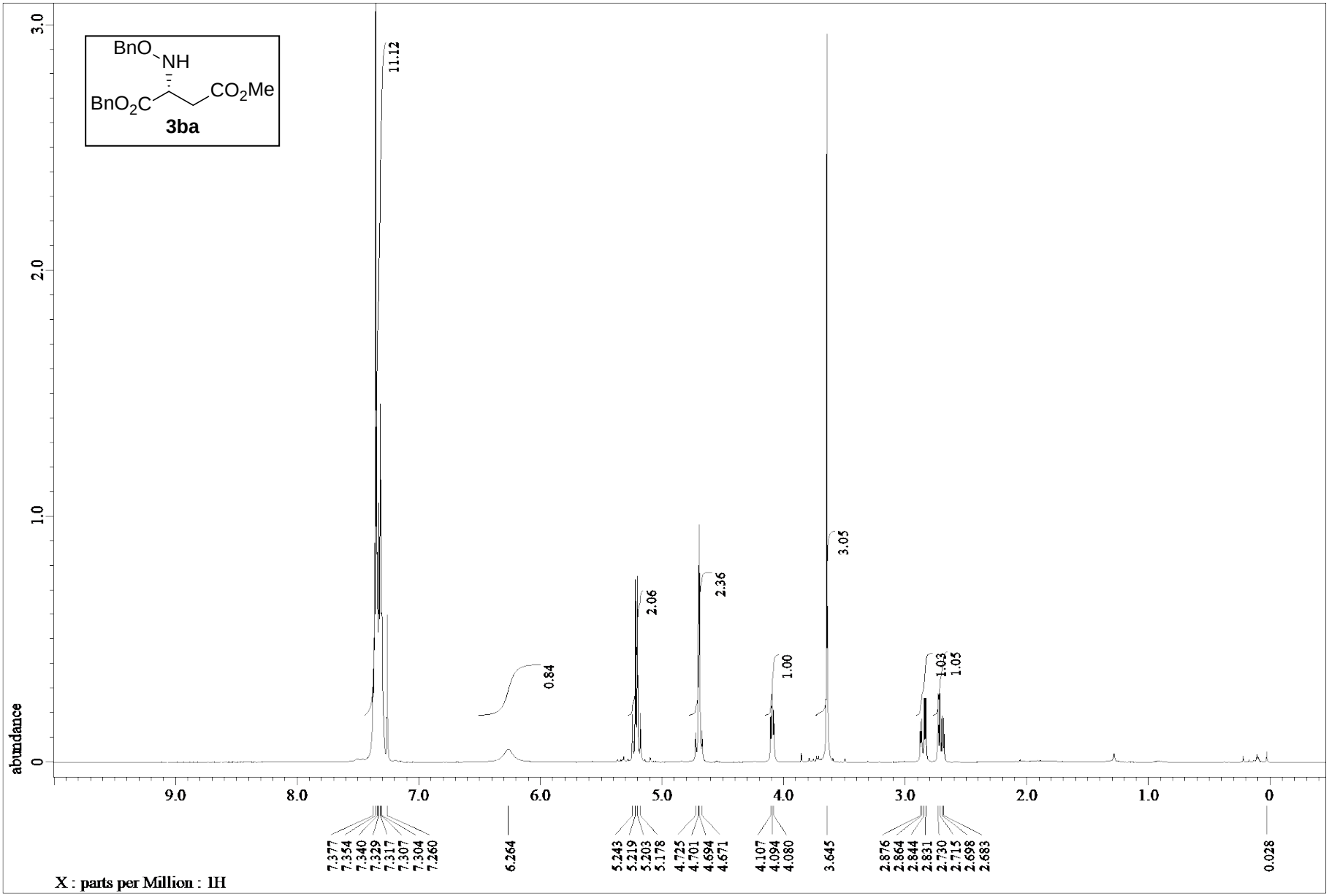
BnO
NH
BnO2C
CO2Me
3ba
11.12
0.84
2.06
2.36
1.00
3.05
1.03
1.05
abundance
X : parts per Million : 1H
7.377
7.354
7.340
7.329
7.317
7.307
7.304
7.260
6.264
5.243
5.219
5.203
5.178
4.725
4.701
4.694
4.671
4.107
4.094
4.080
3.645
2.876
2.864
2.844
2.831
2.730
2.715
2.698
2.683
0.028

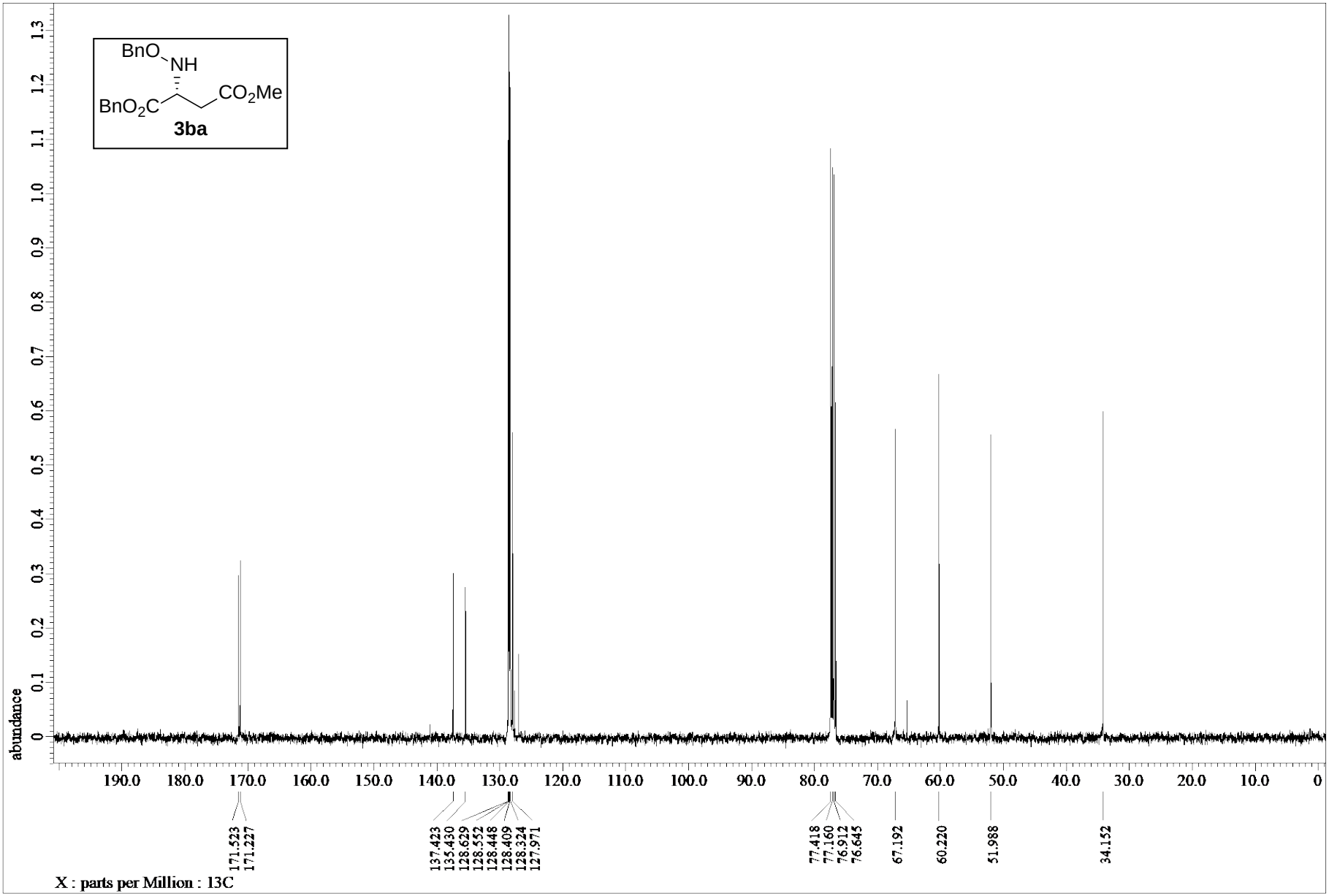
BnO
NH
BnO2C
CO2Me
3ba
abundance
X : parts per Million : 13C
171.523
171.227
137.423
135.430
128.629
128.552
128.448
128.409
128.324
127.971
77.418
77.160
76.912
76.645
67.192
60.220
51.988
34.152

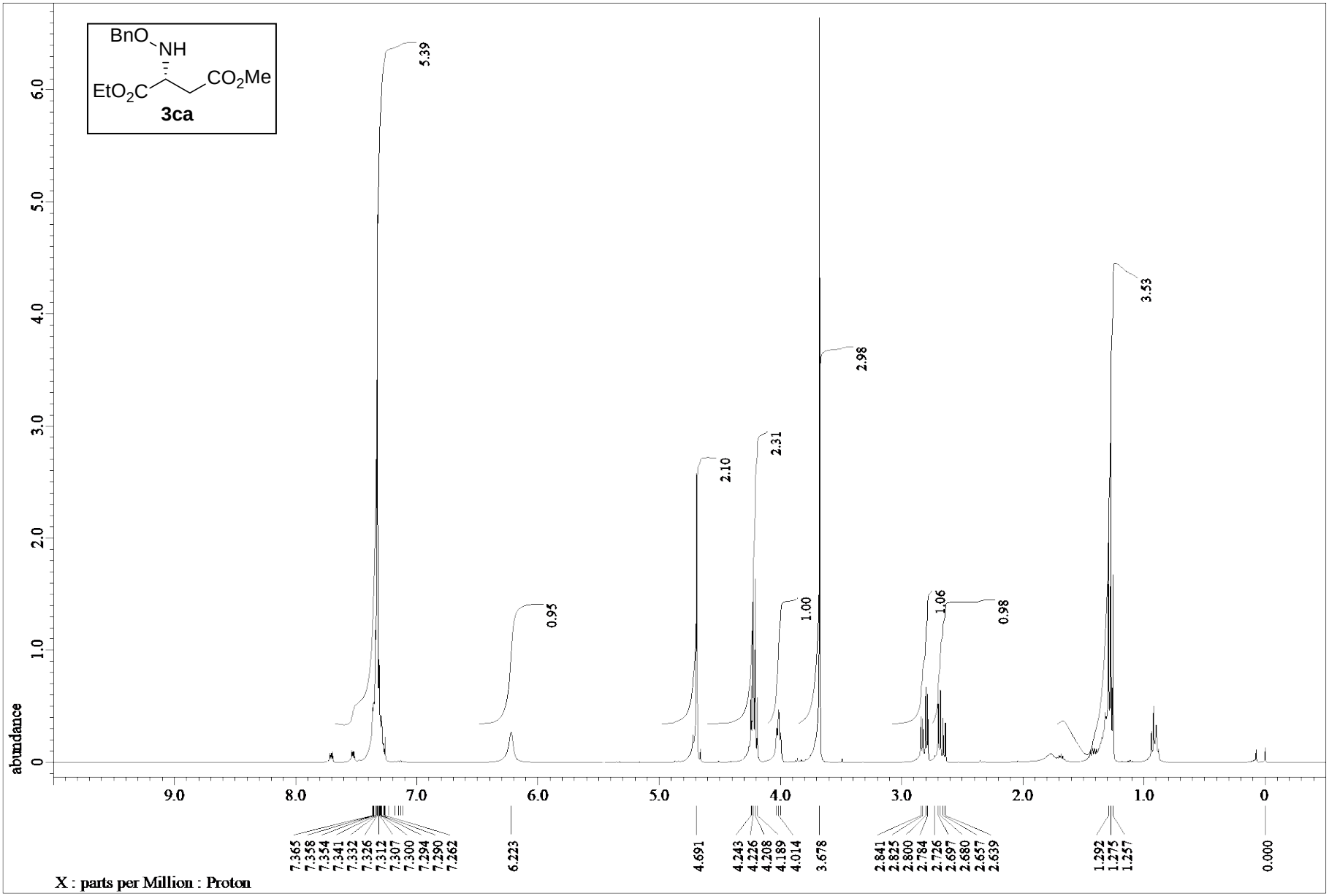
BnO
NH
EtO2C
CO2Me
3ca
abundance
X : parts per Million : Proton
5.39
0.95
2.10
2.31
1.00
2.98
1.06
0.98
3.53
7.365
7.358
7.354
7.341
7.332
7.326
7.312
7.307
7.300
7.294
7.290
7.262
6.223
4.691
4.243
4.226
4.208
4.189
4.014
3.678
2.841
2.825
2.800
2.784
2.726
2.697
2.680
2.657
2.639
1.292
1.275
1.257
0.000

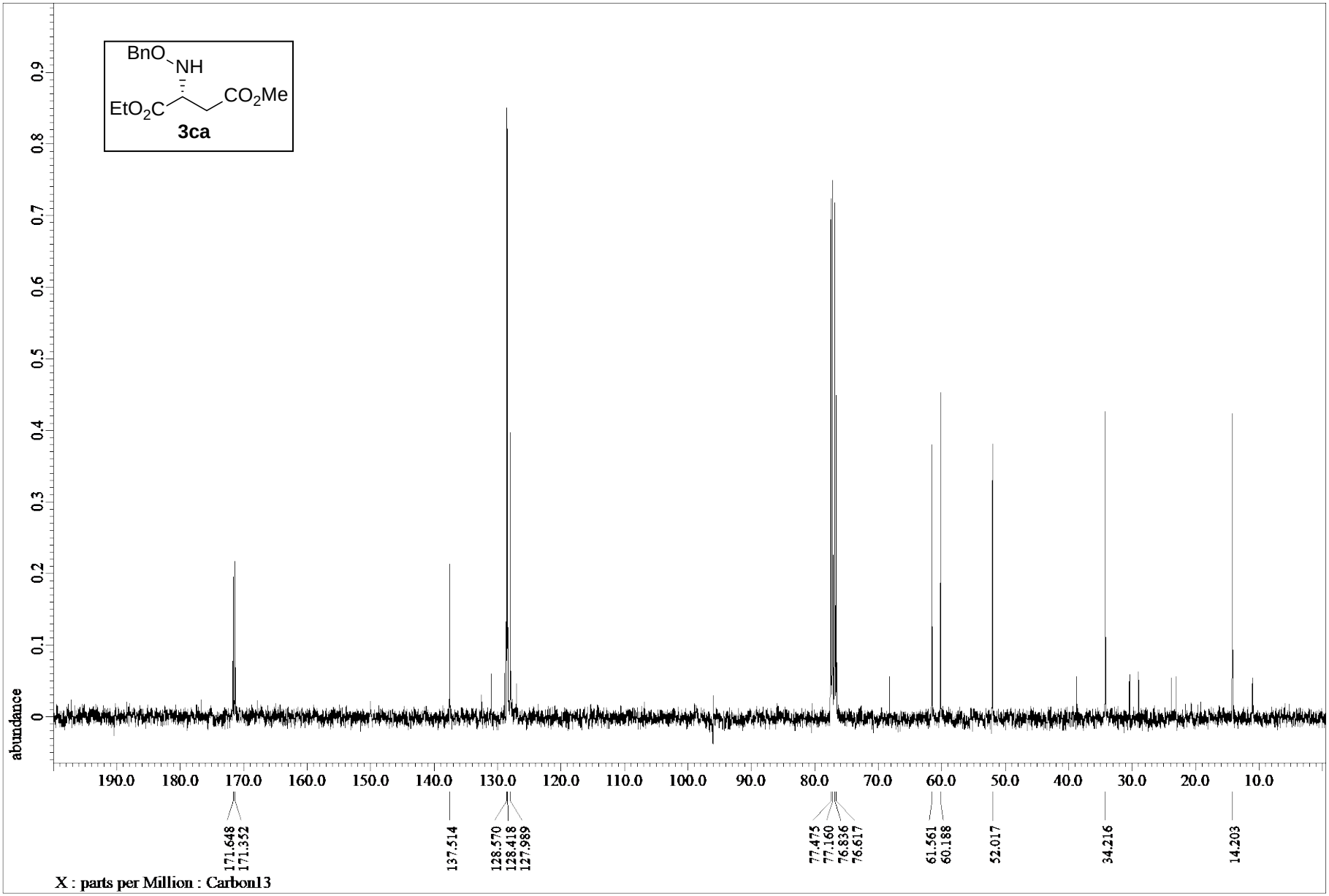
BnO
NH
EtO2C
CO2Me
3ca
abundance
0
0.1
0.2
0.3
0.4
0.5
0.6
0.7
0.8
0.9
190.0
180.0
170.0
160.0
150.0
140.0
130.0
120.0
110.0
100.0
90.0
80.0
70.0
60.0
50.0
40.0
30.0
20.0
10.0
171.648
171.352
137.514
128.570
128.418
127.989
77.475
77.160
76.836
76.617
61.561
60.188
52.017
34.216
14.203
X : parts per Million : Carbon13

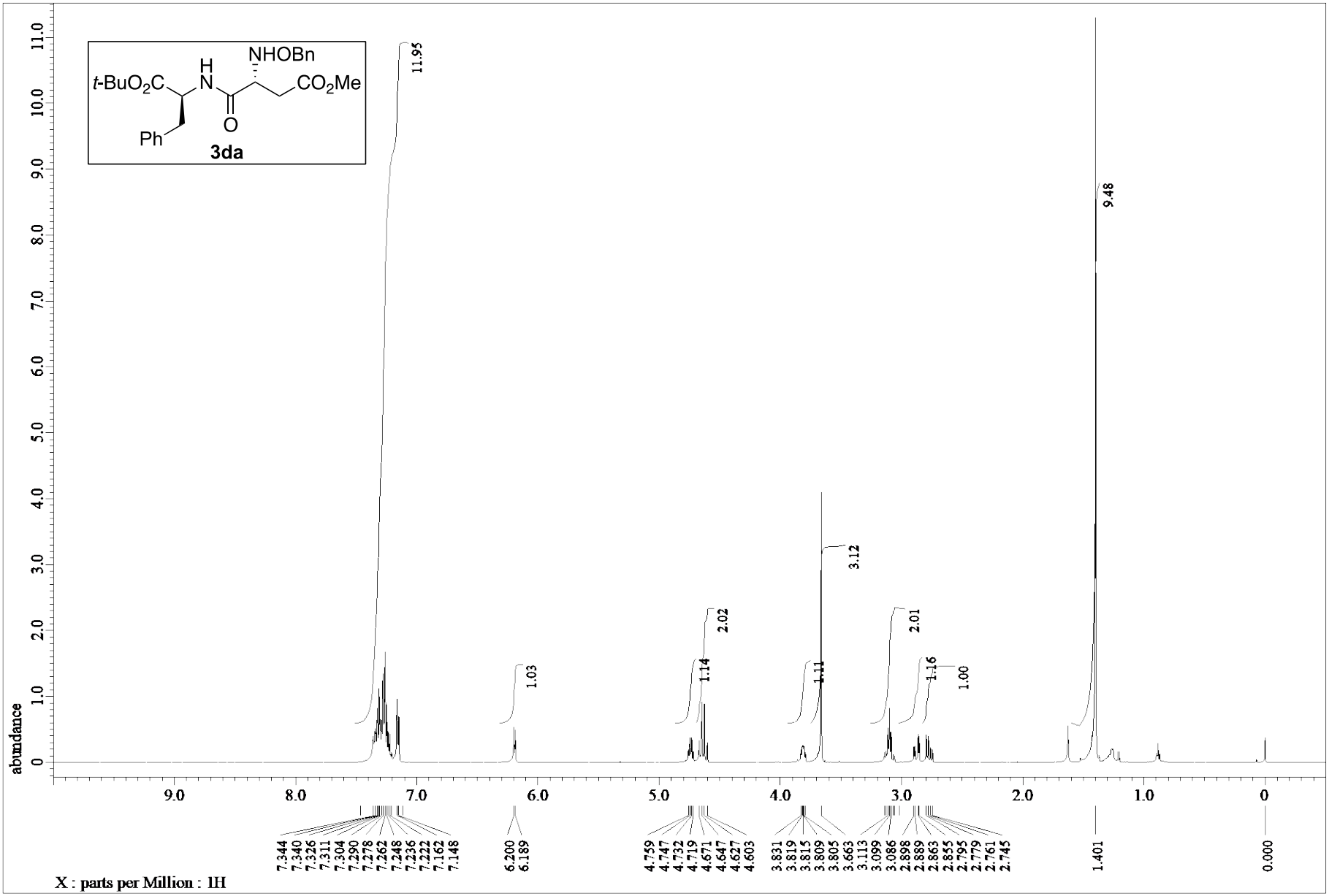
NHOBn
H
N
t-BuO2C
CO2Me
O
Ph
3da
abundance
X : parts per Million : 1H
11.95
9.48
3.12
2.02
2.01
1.14
1.11
1.16
1.03
1.00
7.344
7.340
7.326
7.311
7.304
7.290
7.278
7.262
7.248
7.236
7.222
7.162
7.148
6.200
6.189
4.759
4.747
4.732
4.719
4.671
4.647
4.627
4.603
3.831
3.819
3.815
3.809
3.805
3.663
3.113
3.099
3.086
2.898
2.889
2.863
2.855
2.795
2.779
2.761
2.745
1.401
0.000

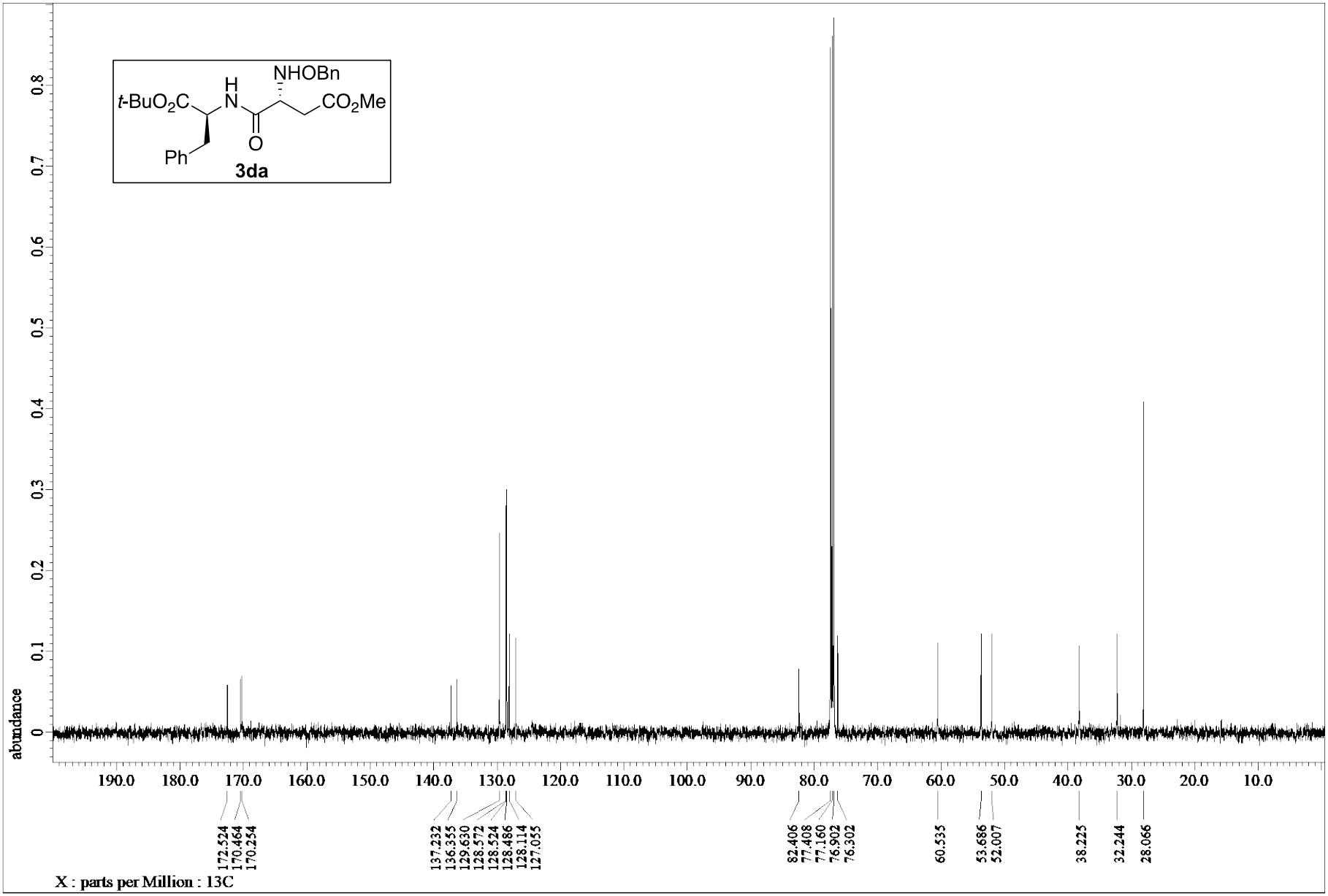
NHOBn
H
N
t-BuO2C
CO2Me
O
Ph
3da
abundance
0
0.1
0.2
0.3
0.4
0.5
0.6
0.7
0.8
190.0
180.0
170.0
160.0
150.0
140.0
130.0
120.0
110.0
100.0
90.0
80.0
70.0
60.0
50.0
40.0
30.0
20.0
10.0
172.524
170.464
170.254
137.232
136.355
129.630
128.572
128.524
128.486
128.114
127.055
82.406
77.408
77.160
76.902
76.302
60.535
53.686
52.007
38.225
32.244
28.066
X : parts per Million : 13C

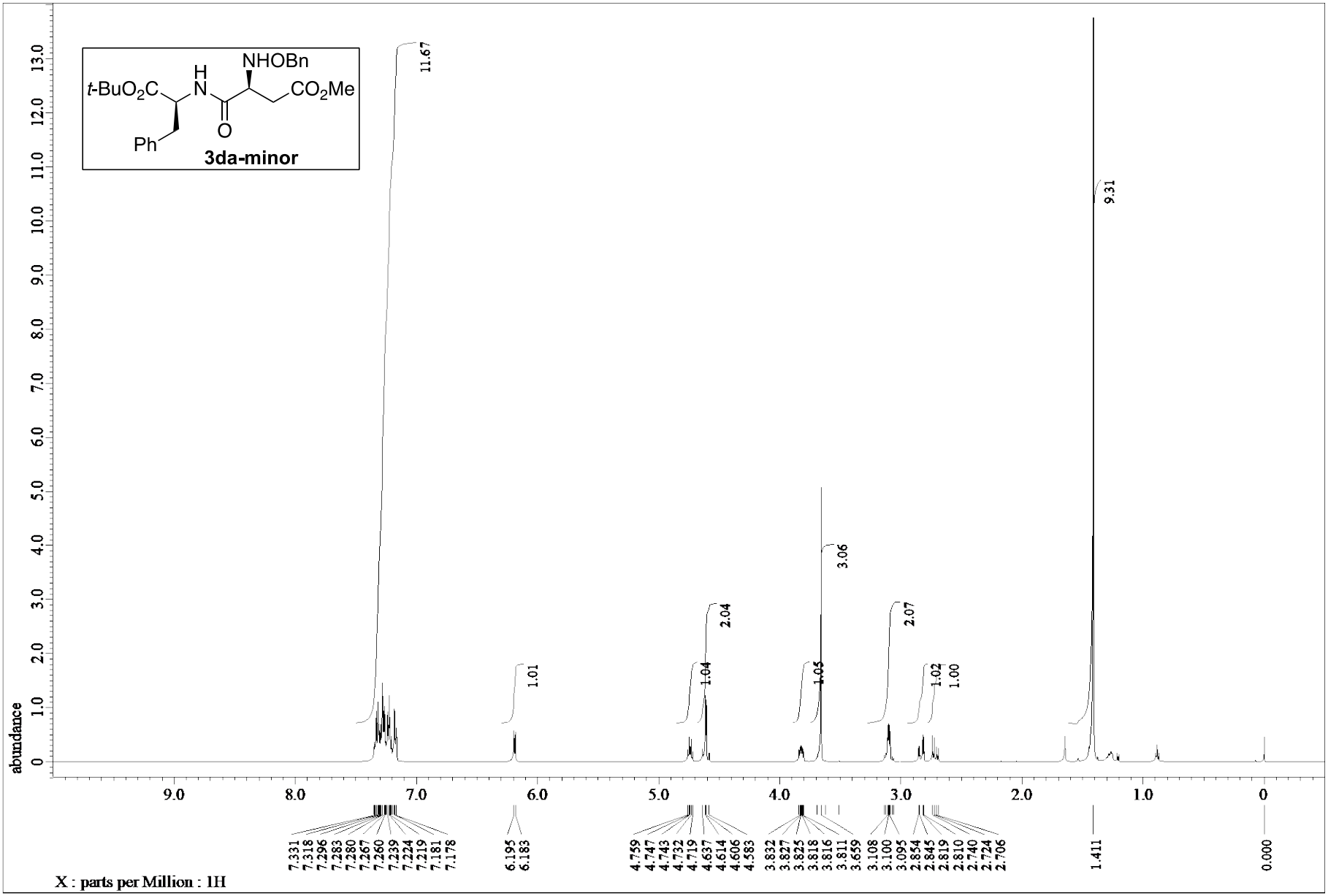
NHOBn
H
N
t-BuO2C
CO2Me
O
Ph
3da-minor
11.67
9.31
3.06
2.04
2.07
1.01
1.04
1.05
1.02
1.00
abundance
X : parts per Million : 1H
7.331
7.318
7.296
7.283
7.280
7.267
7.260
7.239
7.224
7.219
7.181
7.178
6.195
6.183
4.759
4.747
4.743
4.732
4.719
4.637
4.614
4.606
4.583
3.832
3.827
3.825
3.818
3.816
3.811
3.659
3.108
3.100
3.095
2.854
2.845
2.819
2.810
2.740
2.724
2.706
1.411
0.000

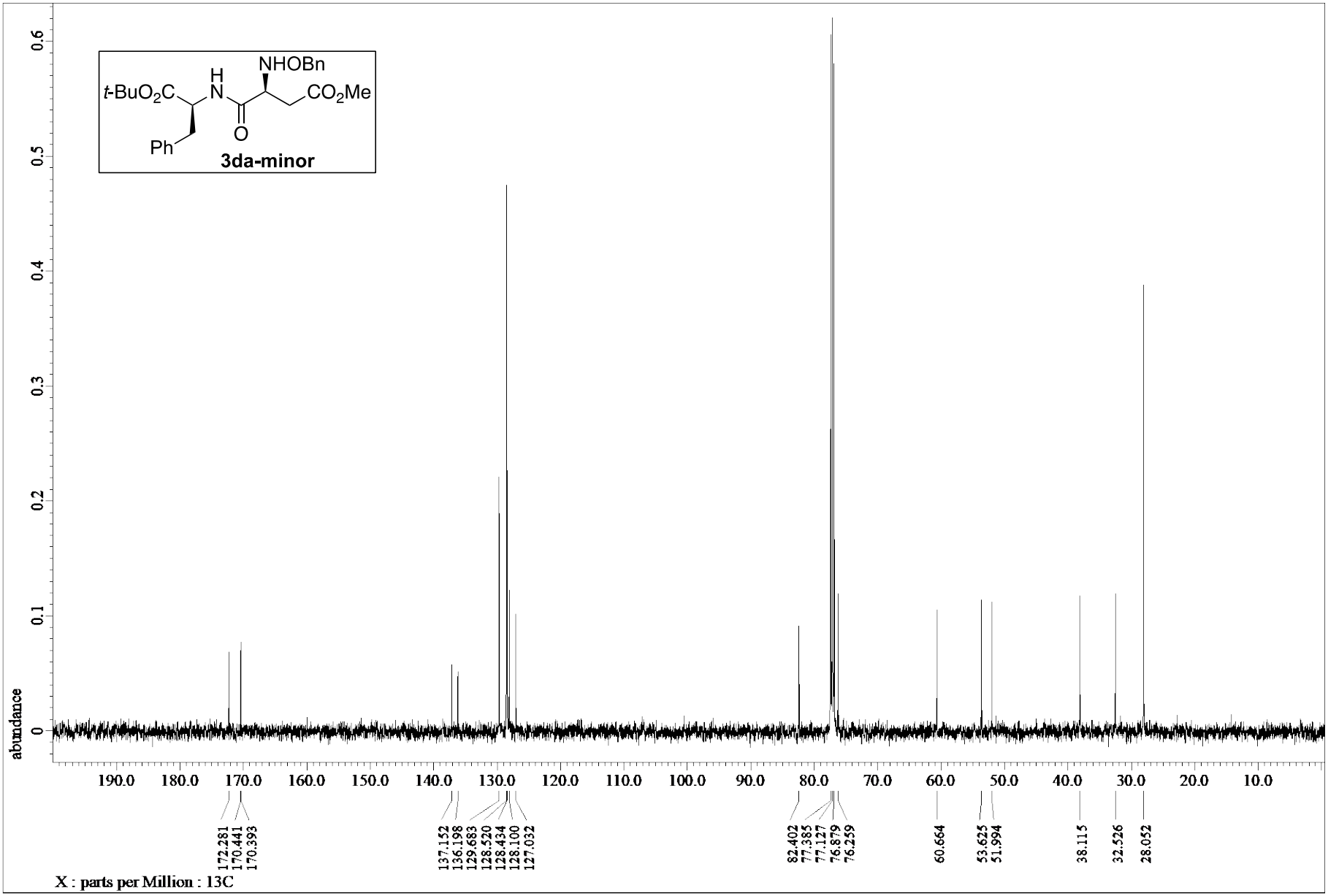
NHOBn
H
N
t-BuO2C
CO2Me
O
Ph
3da-minor
abundance
0.6
0.5
0.4
0.3
0.2
0.1
0
190.0
180.0
170.0
160.0
150.0
140.0
130.0
120.0
110.0
100.0
90.0
80.0
70.0
60.0
50.0
40.0
30.0
20.0
10.0
172.281
170.441
170.393
137.152
136.198
129.683
128.520
128.434
128.100
127.032
82.402
77.385
77.127
76.879
76.259
60.664
53.625
51.994
38.115
32.526
28.052
X : parts per Million : 13C

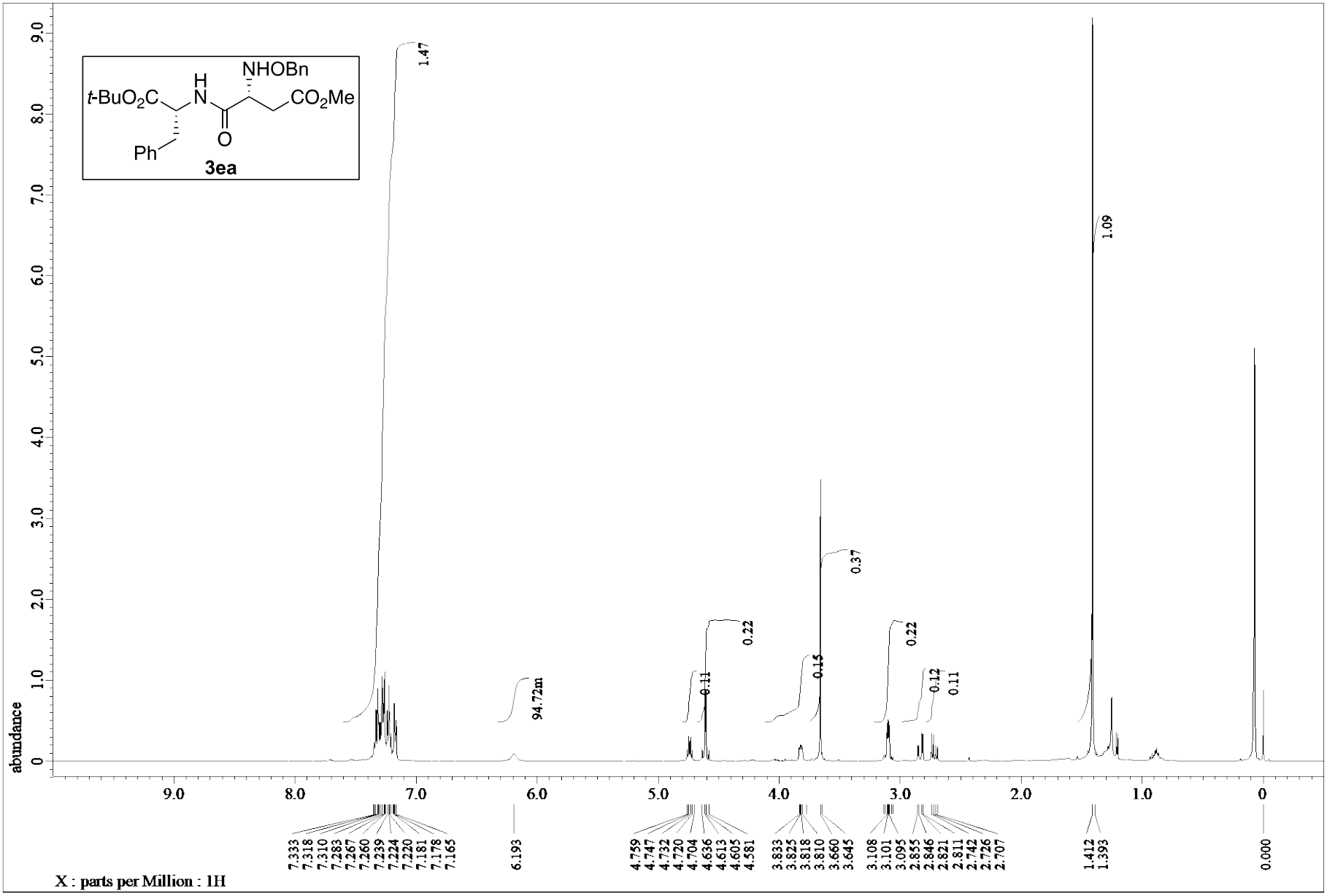
NHOBn
H
N
t-BuO2C
CO2Me
O
Ph
3ea
1.47
1.09
0.37
0.22
0.22
0.15
0.12
0.11
0.11
94.72m
abundance
X : parts per Million : 1H
7.333
7.318
7.310
7.283
7.267
7.260
7.239
7.224
7.220
7.181
7.178
7.165
6.193
4.759
4.747
4.732
4.720
4.704
4.636
4.613
4.605
4.581
3.833
3.825
3.818
3.810
3.660
3.645
3.108
3.101
3.095
2.855
2.846
2.821
2.811
2.742
2.726
2.707
1.412
1.393
0.000

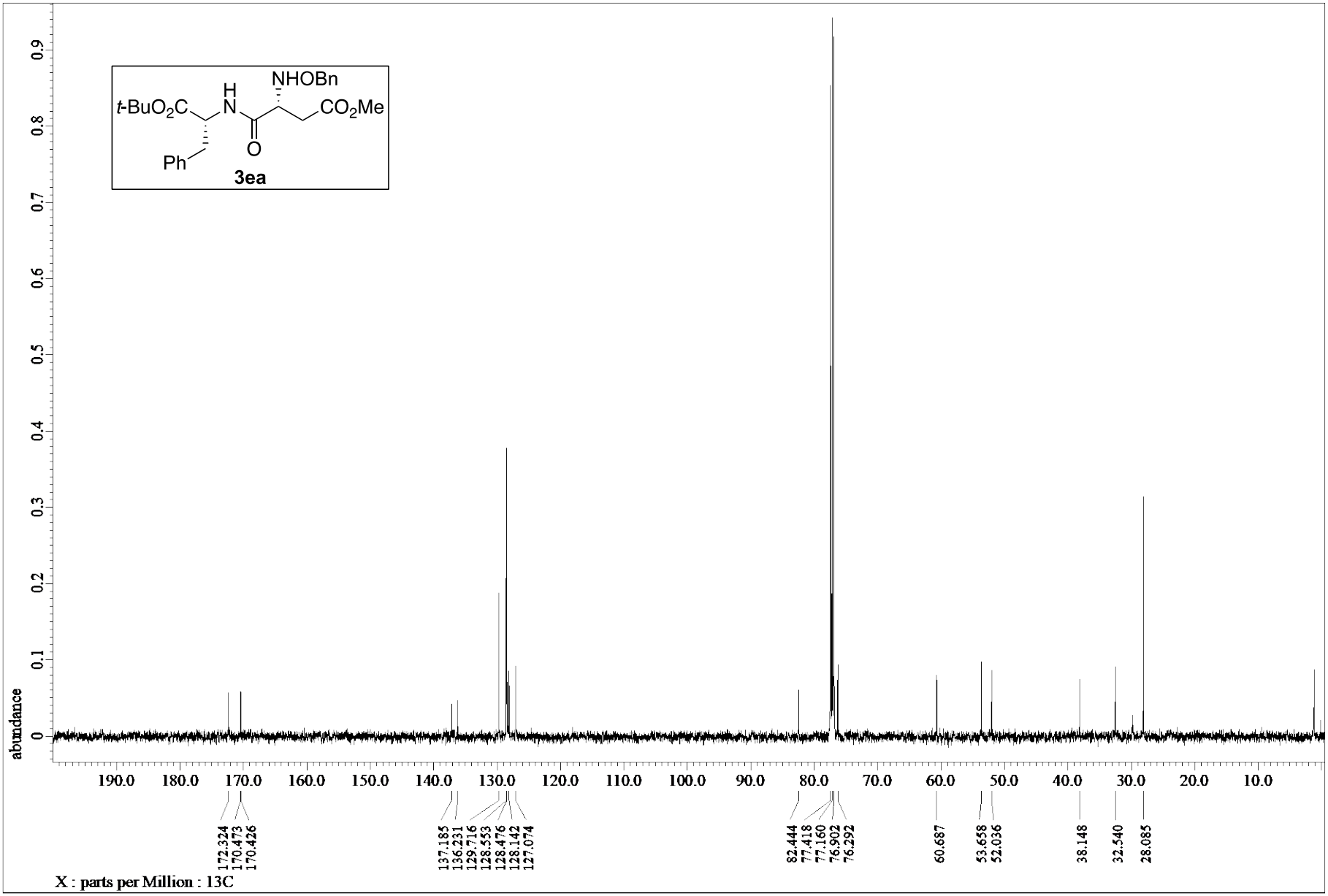
NHOBn
H
N
t-BuO2C
CO2Me
O
Ph
3ea
abundance
0
0.1
0.2
0.3
0.4
0.5
0.6
0.7
0.8
0.9
190.0
180.0
170.0
160.0
150.0
140.0
130.0
120.0
110.0
100.0
90.0
80.0
70.0
60.0
50.0
40.0
30.0
20.0
10.0
172.324
170.473
170.426
137.185
136.231
129.716
128.553
128.476
128.142
127.074
82.444
77.418
77.160
76.902
76.292
60.687
53.658
52.036
38.148
32.540
28.085
X : parts per Million : 13C

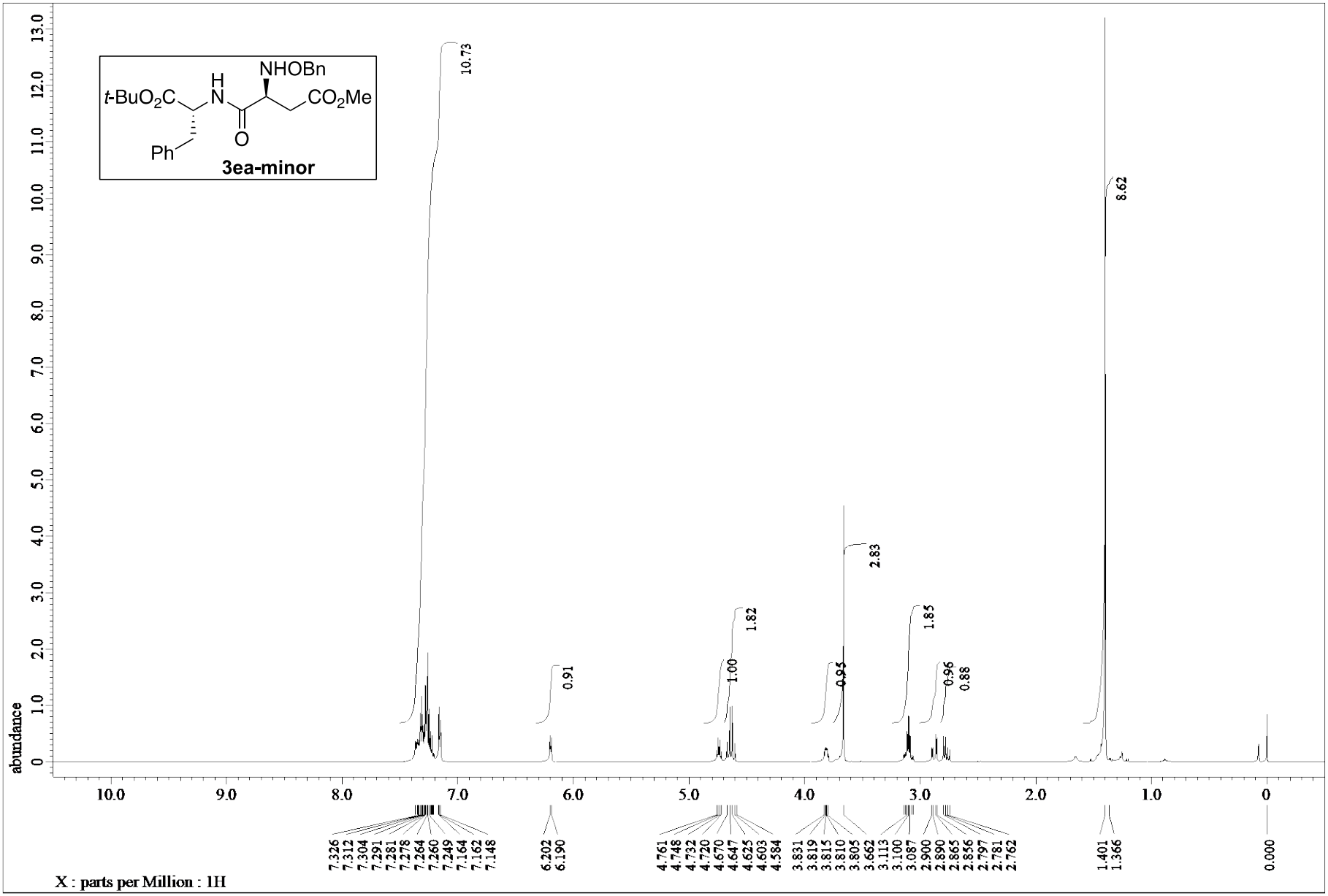
NHOBn
t-BuO2C
H
N
CO2Me
O
Ph
3ea-minor
10.73
8.62
2.83
1.82
1.85
1.00
0.91
0.95
0.96
0.88
abundance
X : parts per Million : 1H
7.326
7.312
7.304
7.291
7.281
7.278
7.264
7.260
7.249
7.164
7.162
7.148
6.202
6.190
4.761
4.748
4.732
4.720
4.670
4.647
4.625
4.603
4.584
3.831
3.819
3.815
3.810
3.805
3.662
3.113
3.100
3.087
2.900
2.890
2.865
2.856
2.797
2.781
2.762
1.401
1.366
0.000

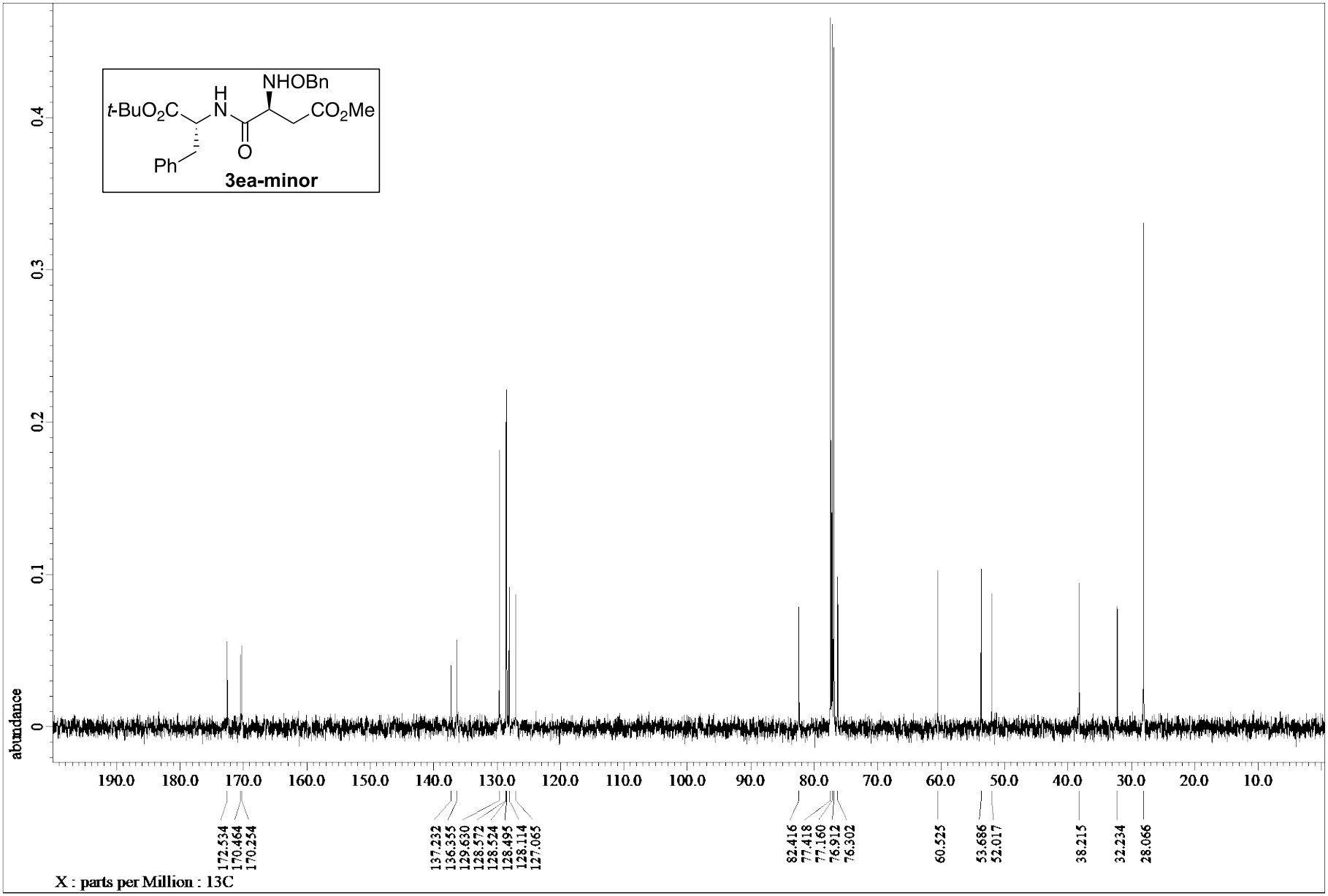
NHOBn
H
N
t-BuO2C
CO2Me
O
Ph
3ea-minor
abundance
0
0.1
0.2
0.3
0.4
190.0
180.0
170.0
160.0
150.0
140.0
130.0
120.0
110.0
100.0
90.0
80.0
70.0
60.0
50.0
40.0
30.0
20.0
10.0
172.534
170.464
170.254
137.232
136.355
129.630
128.572
128.524
128.495
128.114
127.065
82.416
77.418
77.160
76.912
76.302
60.525
53.686
52.017
38.215
32.234
28.066
X : parts per Million : 13C

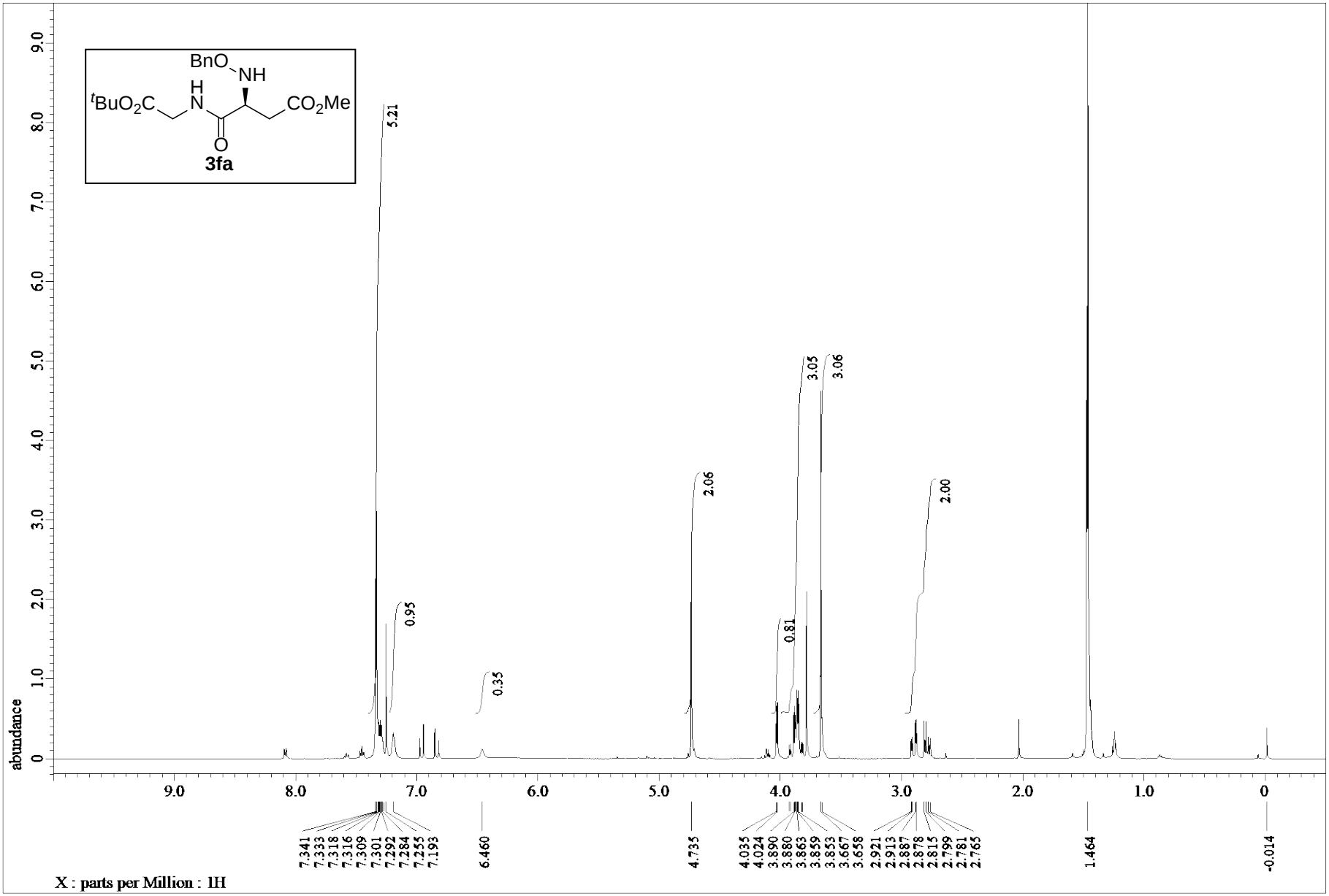
BnO
NH
H
N
tBuO2C
CO2Me
O
3fa
abundance
X : parts per Million : 1H
5.21
0.95
0.35
2.06
0.81
3.05
3.06
2.00
7.341
7.333
7.318
7.316
7.309
7.301
7.292
7.284
7.255
7.193
6.460
4.735
4.035
4.024
3.890
3.880
3.865
3.859
3.853
3.667
3.658
2.921
2.913
2.887
2.878
2.815
2.799
2.781
2.765
1.464
-0.014

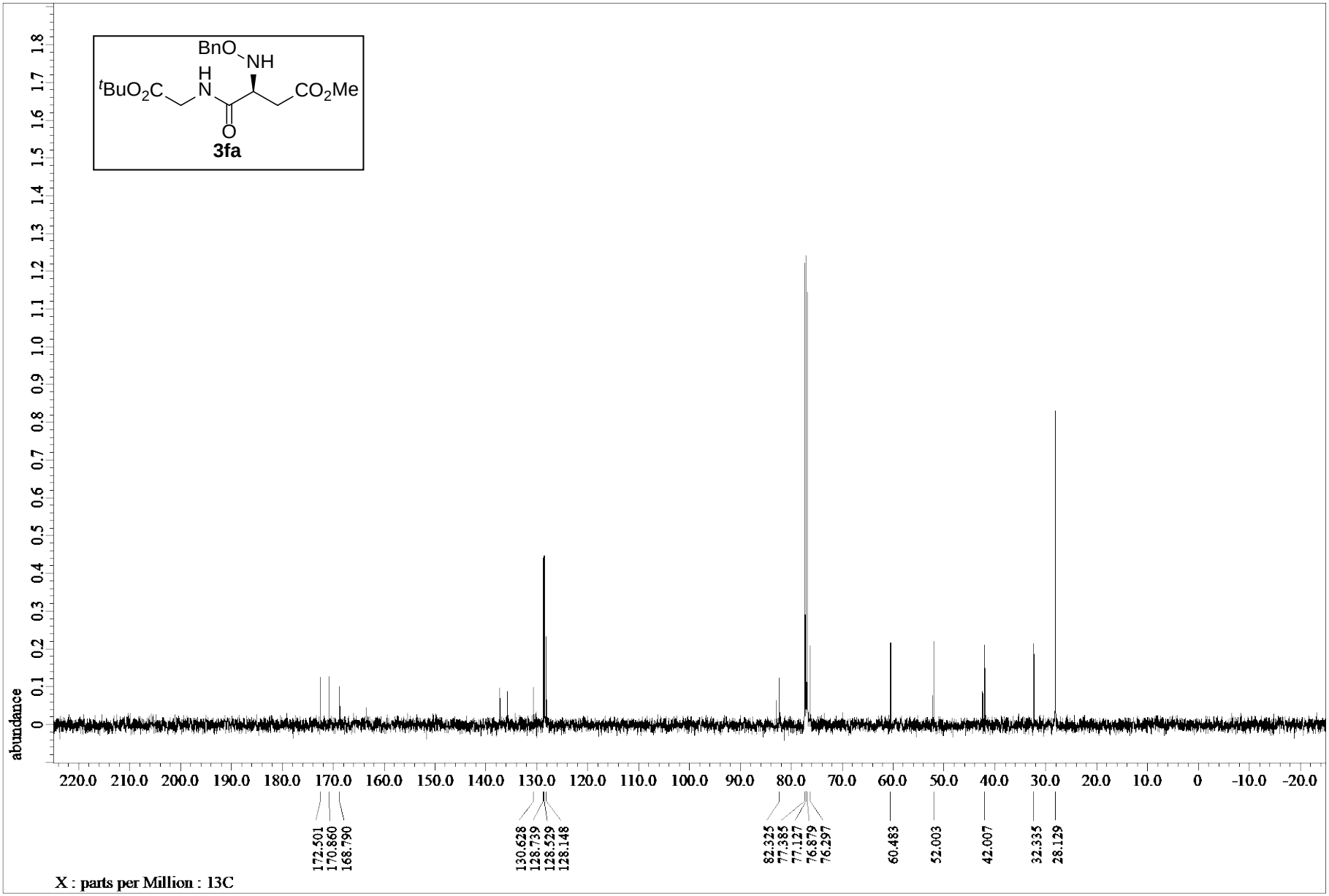
BnO
NH
H
N
tBuO2C
CO2Me
O
3fa
abundance
X : parts per Million : 13C
172.501
170.860
168.790
130.628
128.739
128.529
128.148
82.325
77.385
77.127
76.879
76.297
60.483
52.003
42.007
32.335
28.129

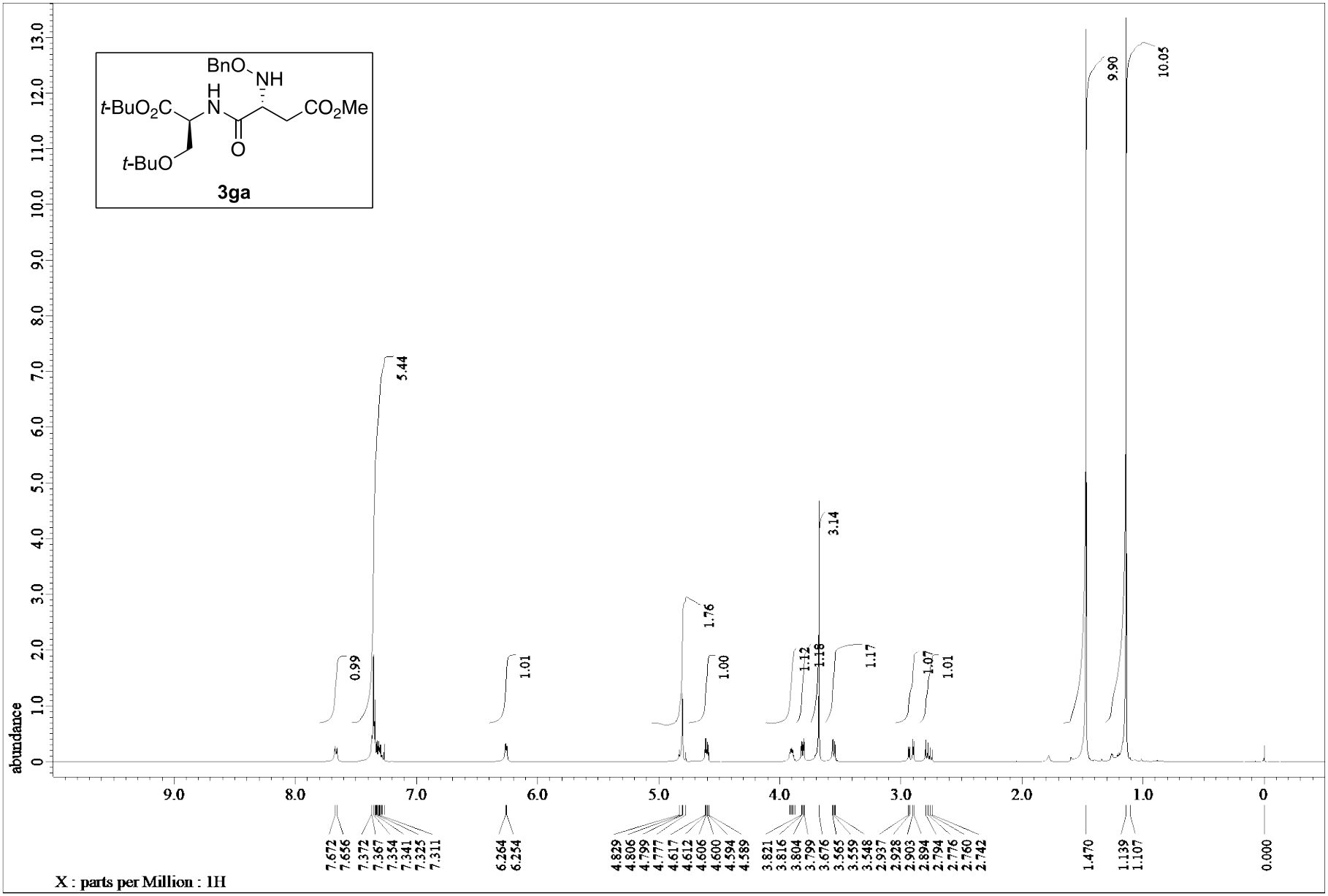
BnO
NH
H
N
t-BuO2C
CO2Me
O
t-BuO
3ga
abundance
X : parts per Million : 1H
9.90
10.05
5.44
3.14
1.76
0.99
1.01
1.00
1.12
1.18
1.17
1.07
1.01
7.672
7.656
7.372
7.367
7.354
7.341
7.325
7.311
6.264
6.254
4.829
4.806
4.799
4.777
4.617
4.612
4.606
4.600
4.594
4.589
3.821
3.816
3.804
3.799
3.676
3.565
3.559
3.548
2.937
2.928
2.903
2.894
2.794
2.776
2.760
2.742
1.470
1.139
1.107
0.000

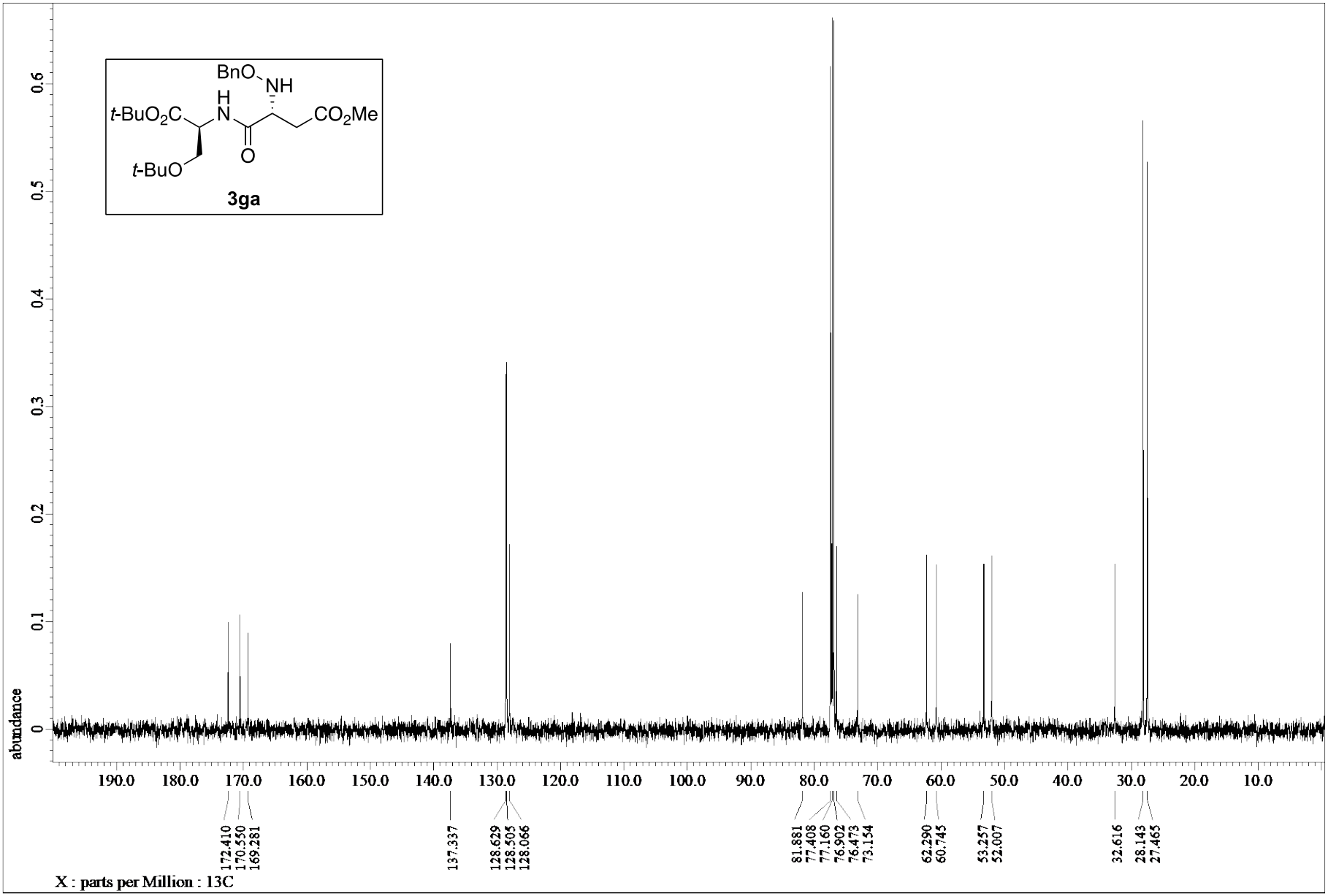
BnO
NH
H
N
t-BuO2C
CO2Me
O
t-BuO
3ga
abundance
0
0.1
0.2
0.3
0.4
0.5
0.6
190.0
180.0
170.0
160.0
150.0
140.0
130.0
120.0
110.0
100.0
90.0
80.0
70.0
60.0
50.0
40.0
30.0
20.0
10.0
172.410
170.550
169.281
137.337
128.629
128.505
128.066
81.881
77.408
77.160
76.902
76.473
73.154
62.290
60.745
53.257
52.007
32.616
28.143
27.465
X : parts per Million : 13C

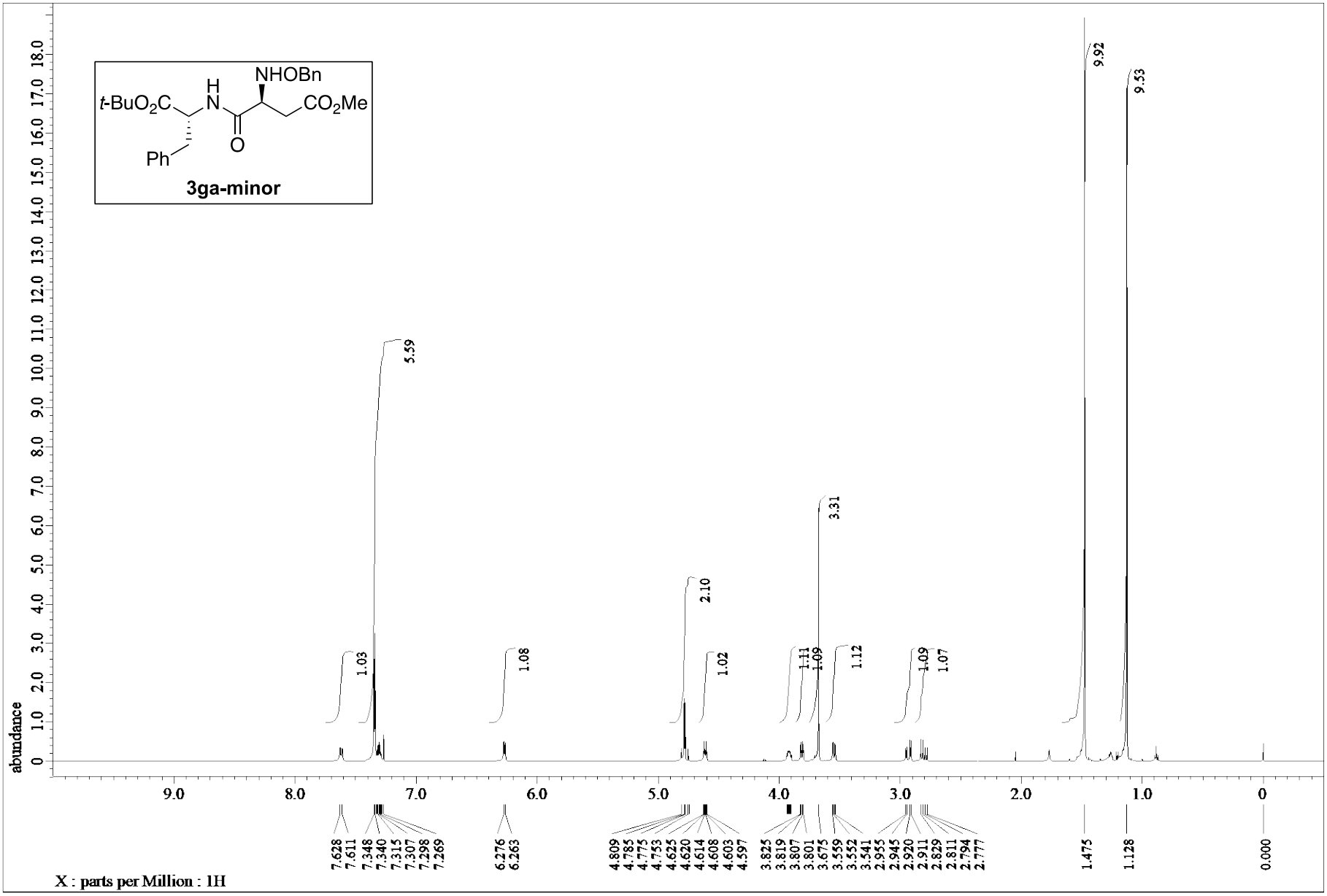
NHOBn
H
N
t-BuO2C
CO2Me
O
Ph
3ga-minor
abundance
X : parts per Million : 1H
9.92
9.53
5.59
3.31
2.10
1.03
1.08
1.02
1.11
1.09
1.12
1.09
1.07
7.628
7.611
7.348
7.340
7.315
7.307
7.298
7.269
6.276
6.263
4.809
4.785
4.775
4.753
4.625
4.620
4.614
4.608
4.603
4.597
3.825
3.819
3.807
3.801
3.675
3.559
3.552
3.541
2.955
2.945
2.920
2.911
2.829
2.811
2.794
2.777
1.475
1.128
0.000

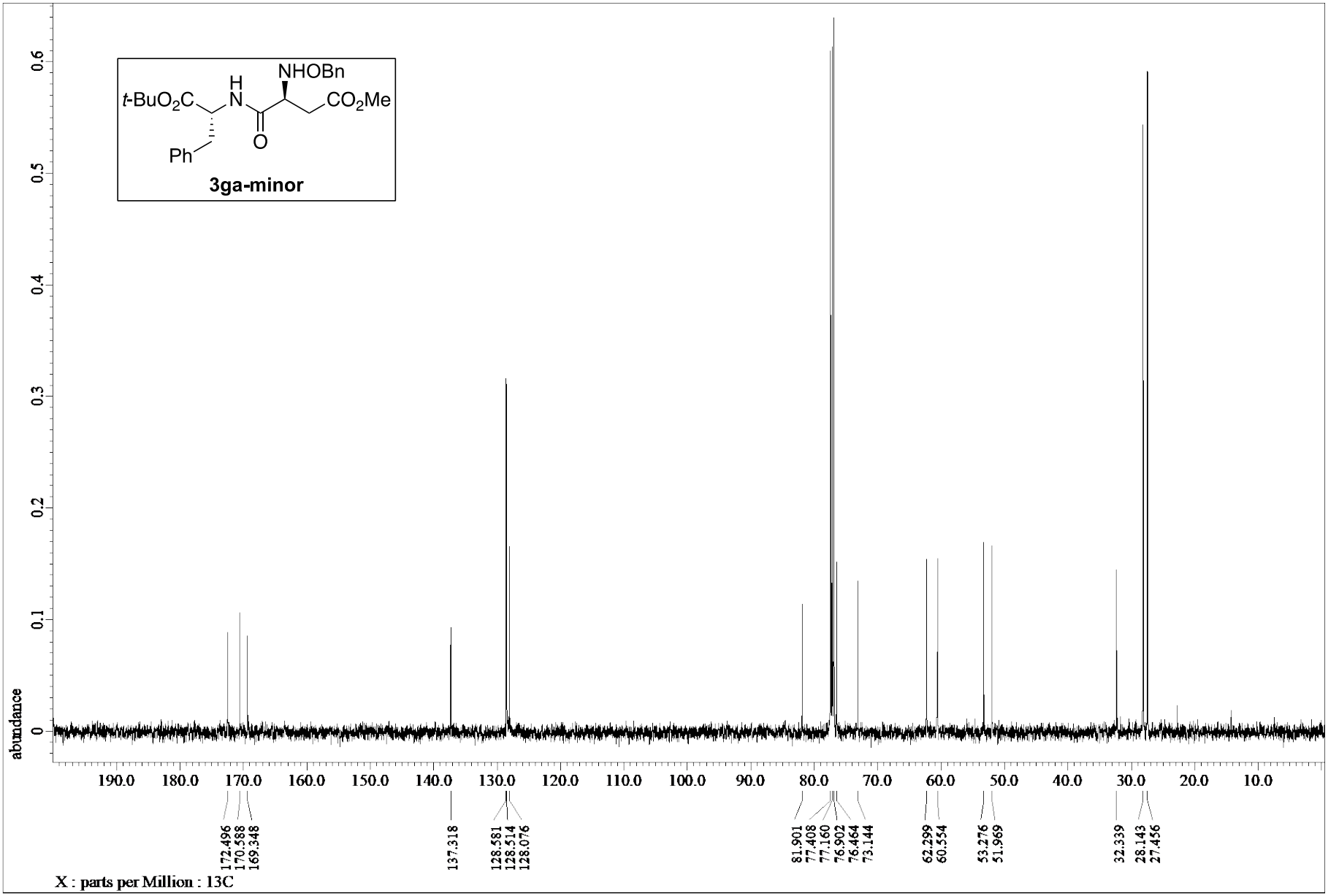
NHOBn
H
N
t-BuO2C
CO2Me
O
Ph
3ga-minor
abundance
0.6
0.5
0.4
0.3
0.2
0.1
0
190.0
180.0
170.0
160.0
150.0
140.0
130.0
120.0
110.0
100.0
90.0
80.0
70.0
60.0
50.0
40.0
30.0
20.0
10.0
172.496
170.588
169.348
137.318
128.581
128.514
128.076
81.901
77.408
77.160
76.902
76.464
73.144
62.299
60.554
53.276
51.969
32.339
28.143
27.456
X : parts per Million : 13C

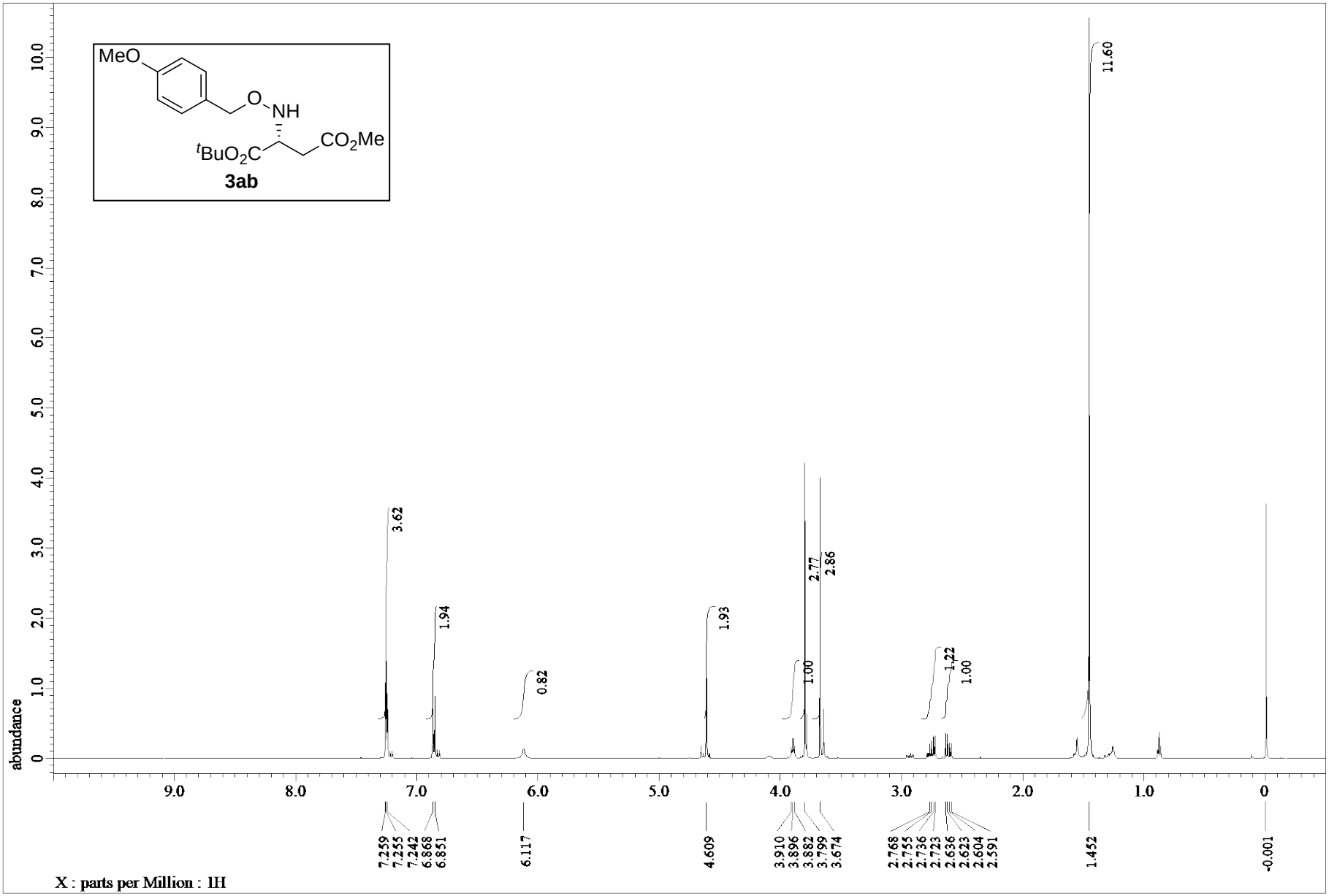
MeO
O
NH
^{t}BuO$_2$C
CO$_2$Me
3ab
abundance
X : parts per Million : 1H
3.62
1.94
0.82
1.93
1.00
2.77
2.86
1.22
1.00
11.60
7.259
7.255
7.242
6.868
6.851
6.117
4.609
3.910
3.896
3.882
3.799
3.674
2.768
2.755
2.736
2.723
2.636
2.623
2.604
2.591
1.452
-0.001

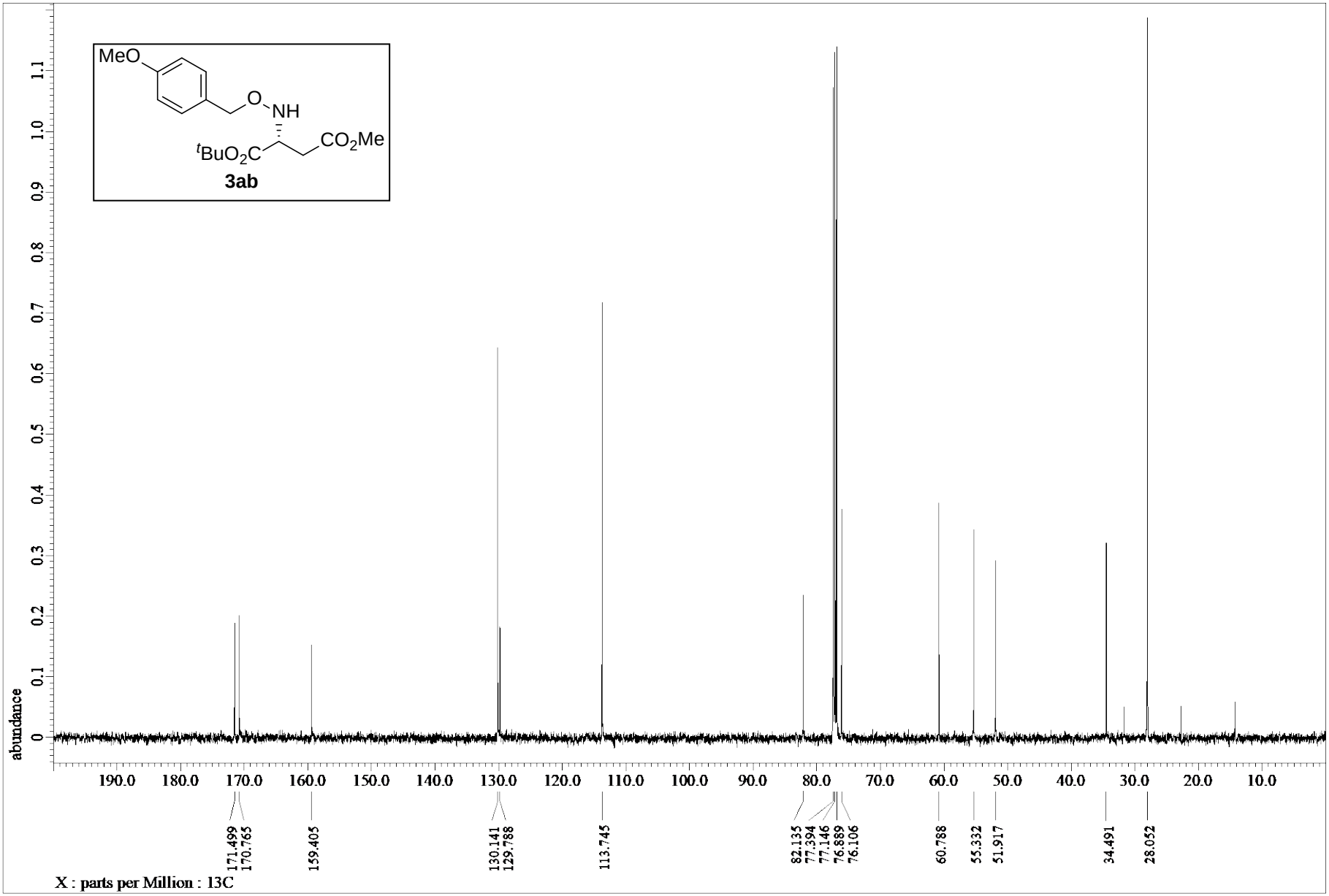
MeO
O
NH
^{t}BuO$_2$C
CO$_2$Me
3ab
abundance
0
0.1
0.2
0.3
0.4
0.5
0.6
0.7
0.8
0.9
1.0
1.1
190.0
180.0
170.0
160.0
150.0
140.0
130.0
120.0
110.0
100.0
90.0
80.0
70.0
60.0
50.0
40.0
30.0
20.0
10.0
171.499
170.765
159.405
130.141
129.788
113.745
82.135
77.394
77.146
76.889
76.106
60.788
55.332
51.917
34.491
28.052
X : parts per Million : 13C

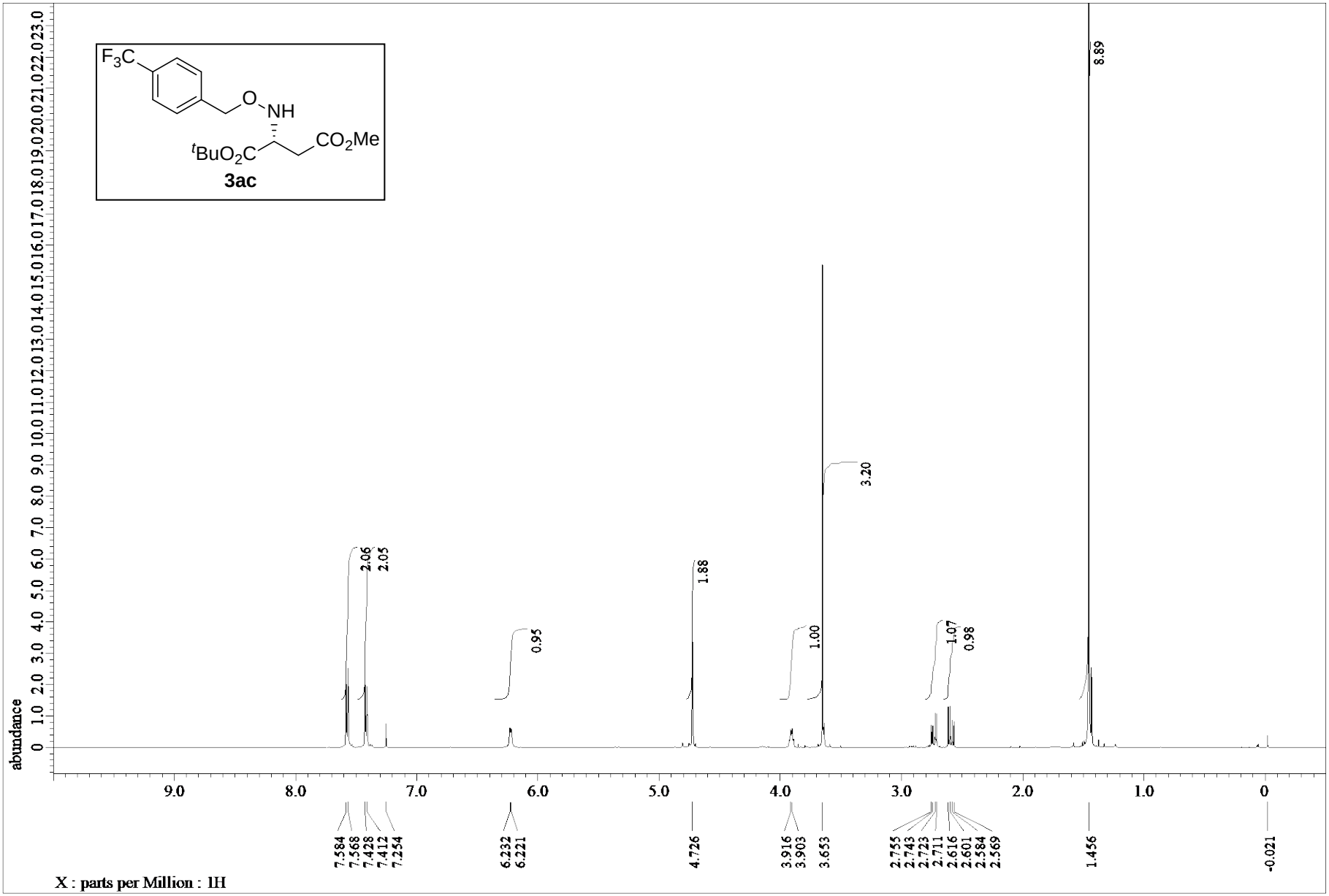
F3C
O
NH
tBuO2C
CO2Me
3ac
abundance
X : parts per Million : 1H
8.89
3.20
2.06
2.05
1.88
0.95
1.00
1.07
0.98
7.584
7.568
7.428
7.412
7.254
6.232
6.221
4.726
3.916
3.903
3.653
2.755
2.743
2.723
2.711
2.616
2.601
2.584
2.569
1.456
-0.021

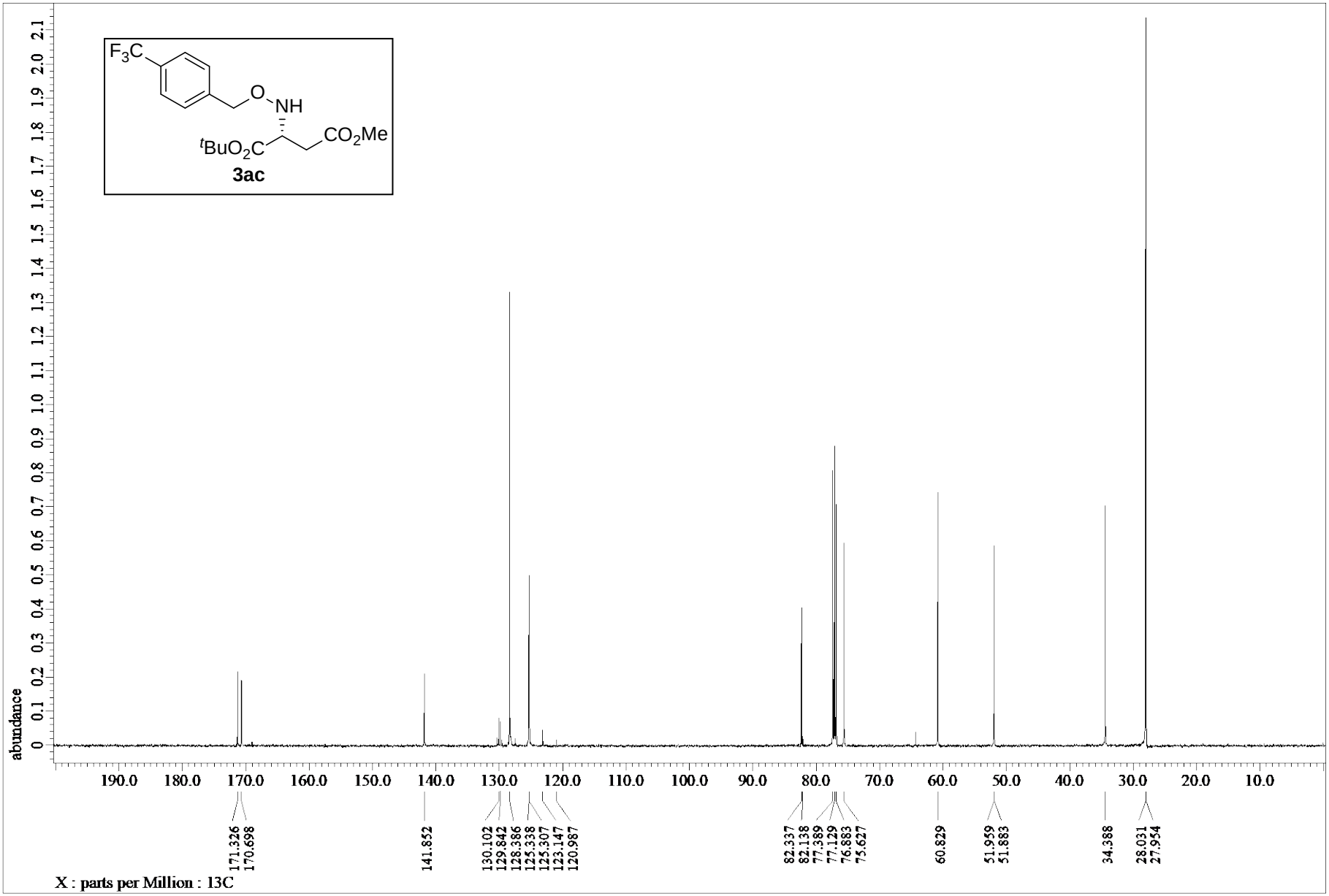
F3C
O
NH
tBuO2C
CO2Me
3ac
abundance
0 0.1 0.2 0.3 0.4 0.5 0.6 0.7 0.8 0.9 1.0 1.1 1.2 1.3 1.4 1.5 1.6 1.7 1.8 1.9 2.0 2.1
190.0 180.0 170.0 160.0 150.0 140.0 130.0 120.0 110.0 100.0 90.0 80.0 70.0 60.0 50.0 40.0 30.0 20.0 10.0
171.326
170.698
141.852
130.102
129.842
128.386
125.338
125.307
123.147
120.987
82.337
82.138
77.389
77.129
76.883
75.627
60.829
51.959
51.883
34.388
28.031
27.954
X : parts per Million : 13C

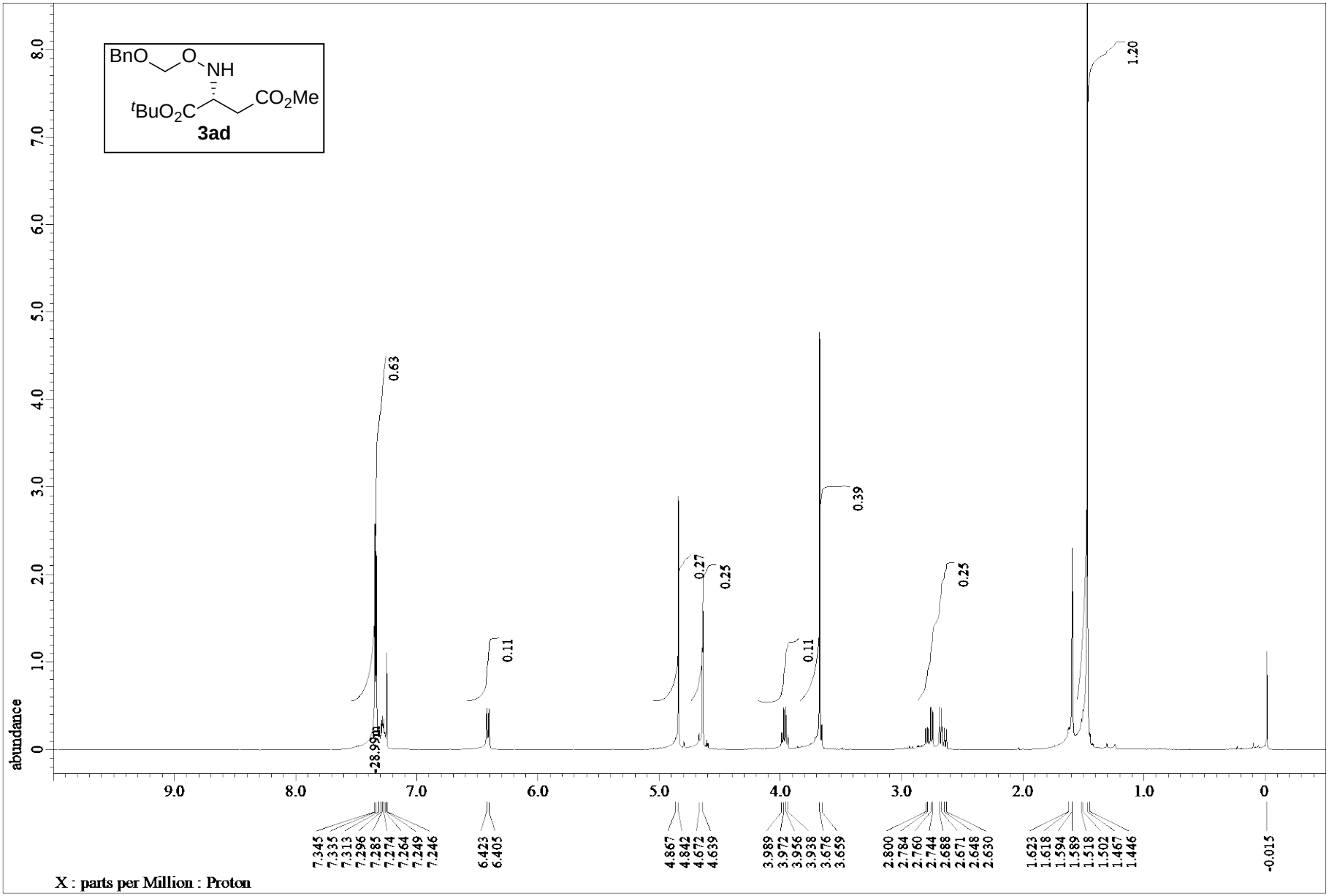
BnO
O
NH
tBuO2C
CO2Me
3ad
abundance
X : parts per Million : Proton
1.20
0.63
0.11
0.27
0.25
0.11
0.39
0.25
7.345
7.335
7.313
7.296
7.285
7.274
7.264
7.249
7.246
6.423
6.405
4.867
4.842
4.672
4.639
3.989
3.972
3.956
3.938
3.676
3.659
2.800
2.784
2.760
2.744
2.688
2.671
2.648
2.630
1.623
1.618
1.594
1.589
1.518
1.502
1.467
1.446
-0.015

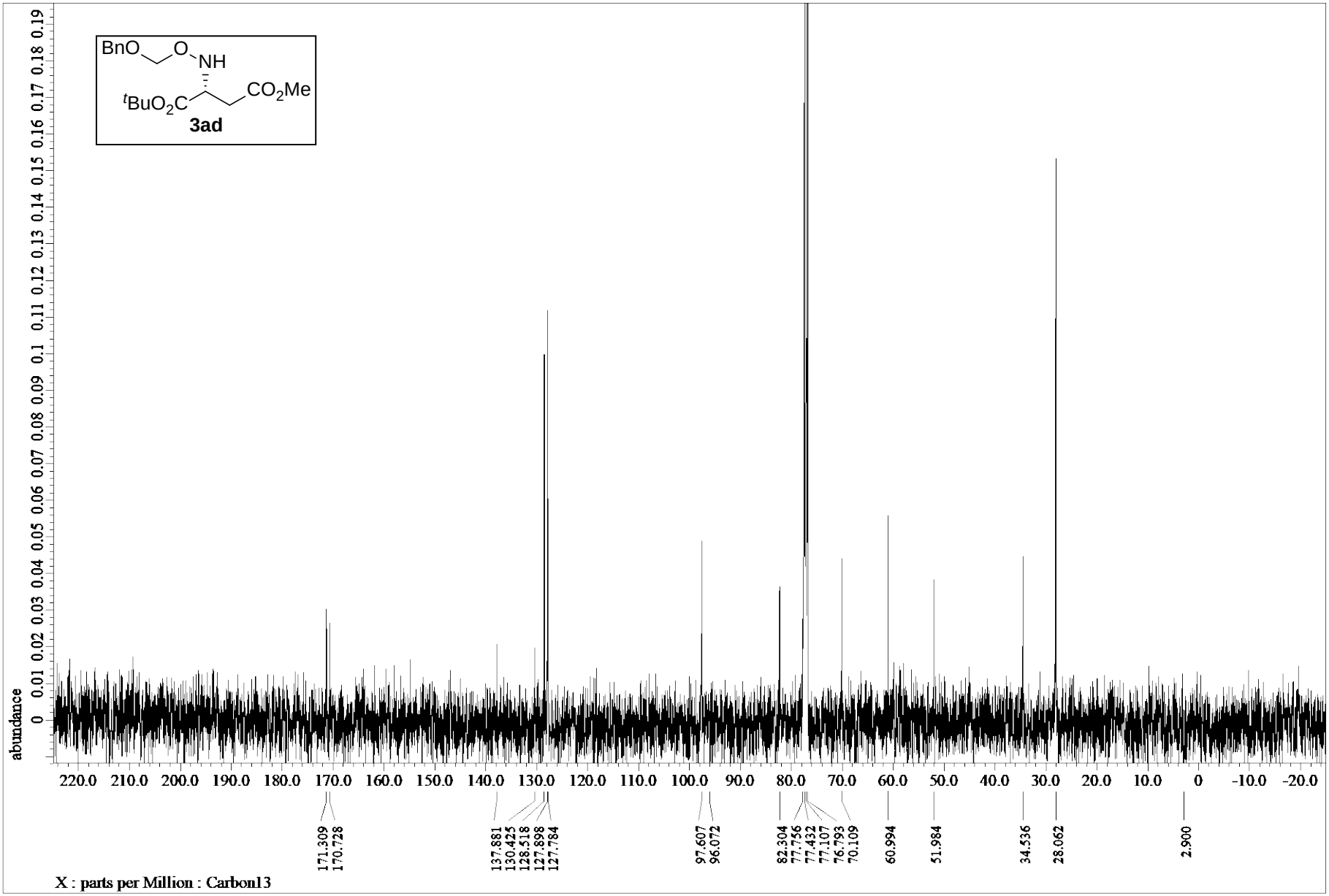
BnO
O
NH
tBuO2C
CO2Me
3ad
abundance
0 0.01 0.02 0.03 0.04 0.05 0.06 0.07 0.08 0.09 0.1 0.11 0.12 0.13 0.14 0.15 0.16 0.17 0.18 0.19
220.0 210.0 200.0 190.0 180.0 170.0 160.0 150.0 140.0 130.0 120.0 110.0 100.0 90.0 80.0 70.0 60.0 50.0 40.0 30.0 20.0 10.0 0 -10.0 -20.0
171.309
170.728
137.881
130.425
128.518
127.898
127.784
97.607
96.072
82.304
77.756
77.432
77.107
76.793
70.109
60.994
51.984
34.536
28.062
2.900
X : parts per Million : Carbon13

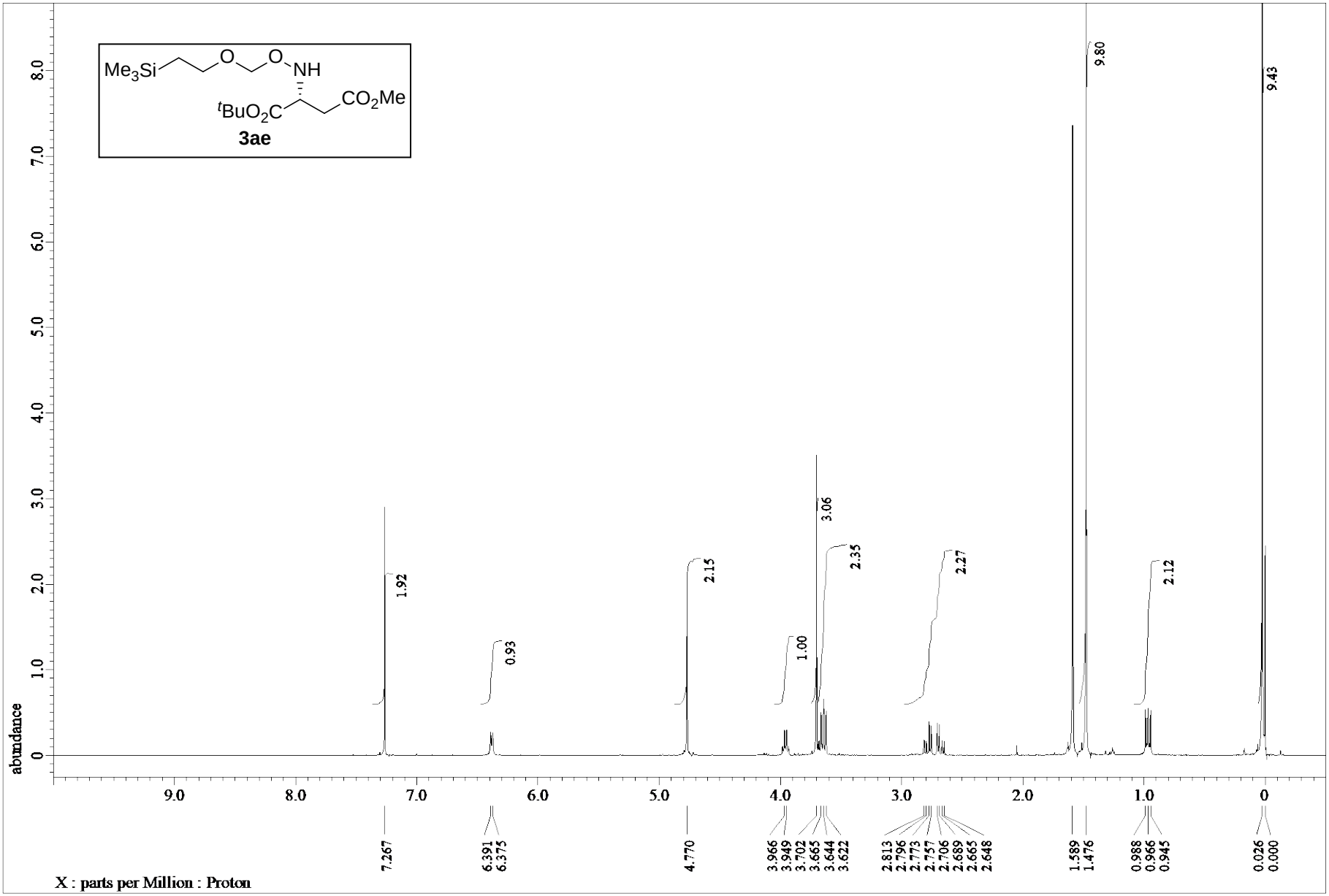
Me3Si
O
O
NH
tBuO2C
CO2Me
3ae
abundance
X : parts per Million : Proton
9.80
9.43
1.92
0.93
2.15
1.00
3.06
2.35
2.27
2.12
7.267
6.391
6.375
4.770
3.966
3.949
3.702
3.665
3.644
3.622
2.813
2.796
2.773
2.757
2.706
2.689
2.665
2.648
1.589
1.476
0.988
0.966
0.945
0.026
0.000

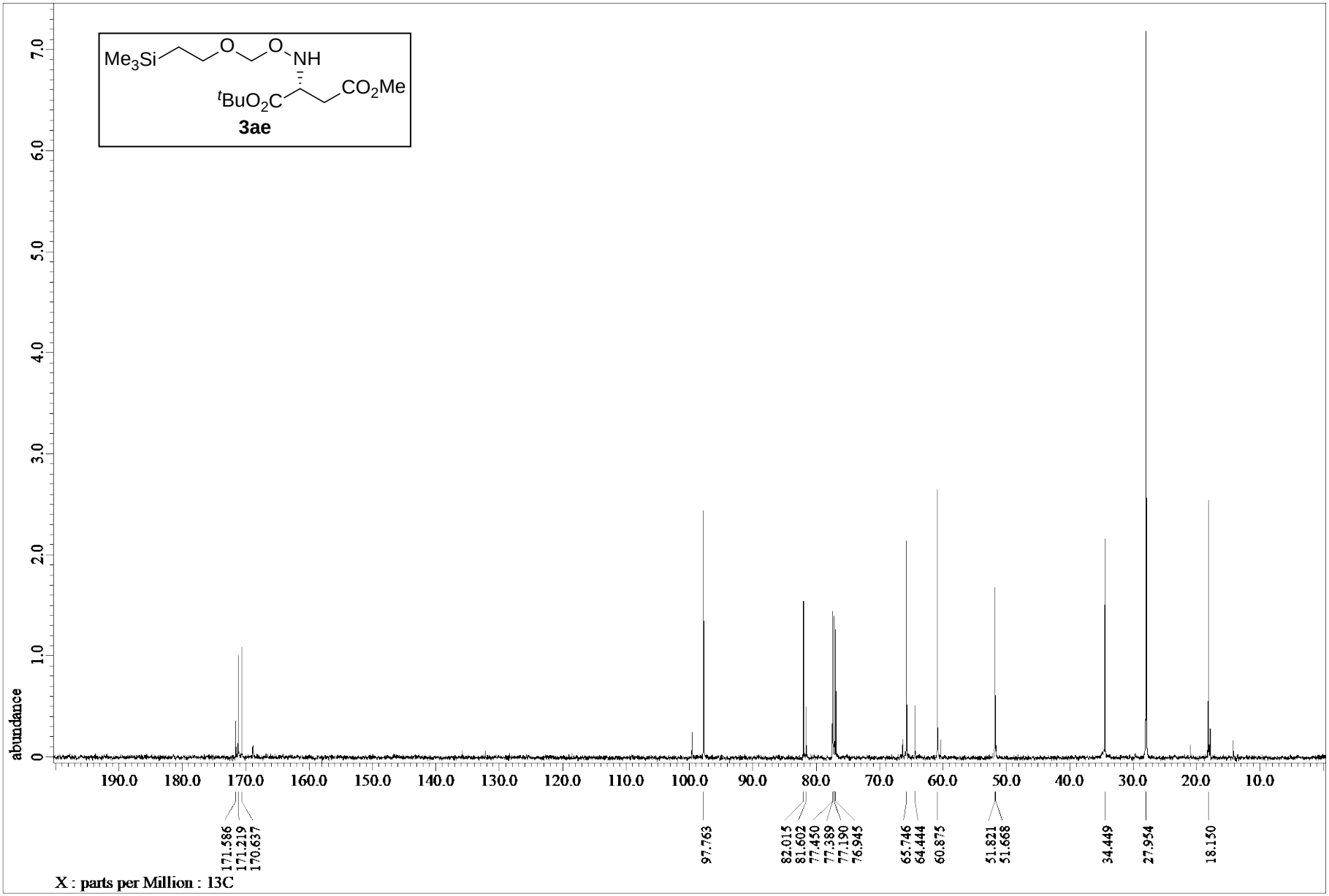
Me3Si
O
O
NH
tBuO2C
CO2Me
3ae
abundance
0
1.0
2.0
3.0
4.0
5.0
6.0
7.0
190.0
180.0
170.0
160.0
150.0
140.0
130.0
120.0
110.0
100.0
90.0
80.0
70.0
60.0
50.0
40.0
30.0
20.0
10.0
171.586
171.219
170.637
97.763
82.015
81.602
77.450
77.389
77.190
76.945
65.746
64.444
60.875
51.821
51.668
34.449
27.954
18.150
X : parts per Million : 13C

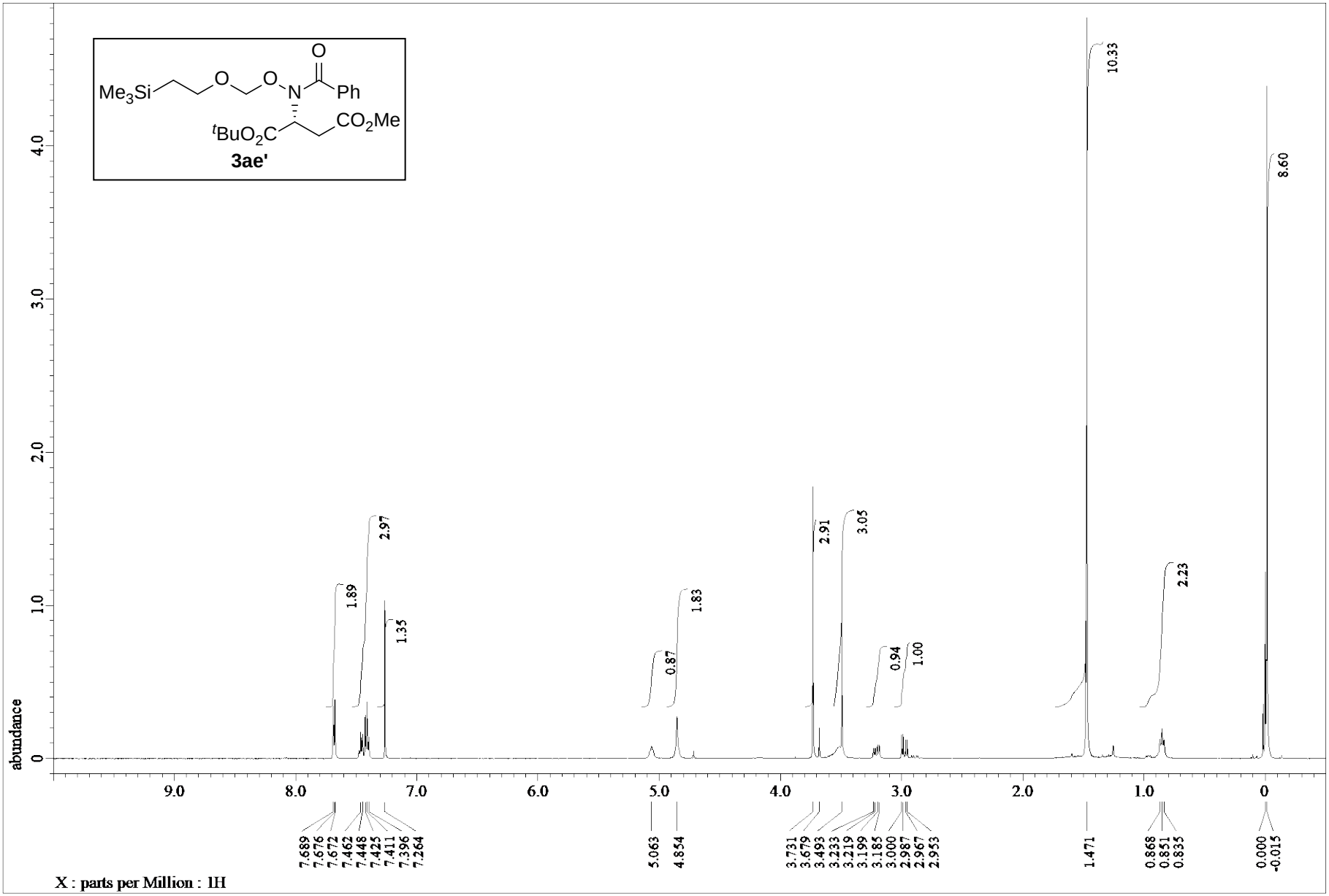
Me3Si
O
O
O
N
Ph
tBuO2C
CO2Me
3ae'
abundance
X : parts per Million : 1H
10.33
8.60
2.97
2.91
3.05
2.23
1.89
1.83
1.35
0.87
0.94
1.00
7.689
7.676
7.672
7.462
7.448
7.425
7.411
7.396
7.264
5.063
4.854
3.731
3.679
3.493
3.233
3.219
3.199
3.185
3.000
2.987
2.967
2.953
1.471
0.868
0.851
0.835
0.000
-0.015

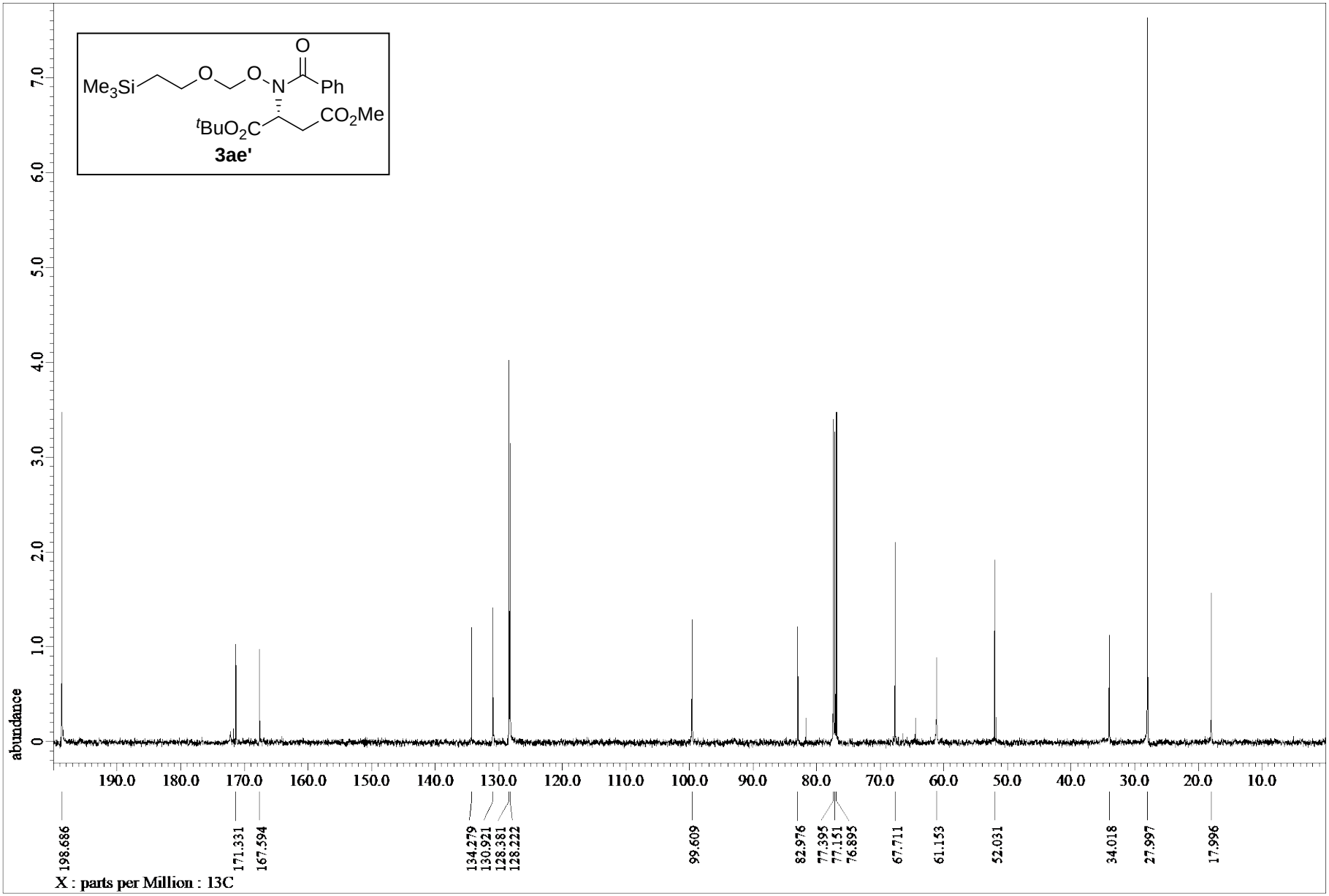
Me3Si
O
O
O
N
Ph
tBuO2C
CO2Me
3ae'
abundance
0
1.0
2.0
3.0
4.0
5.0
6.0
7.0
190.0
180.0
170.0
160.0
150.0
140.0
130.0
120.0
110.0
100.0
90.0
80.0
70.0
60.0
50.0
40.0
30.0
20.0
10.0
198.686
171.331
167.594
134.279
130.921
128.381
128.222
99.609
82.976
77.395
77.151
76.895
67.711
61.153
52.031
34.018
27.997
17.996
X : parts per Million : 13C

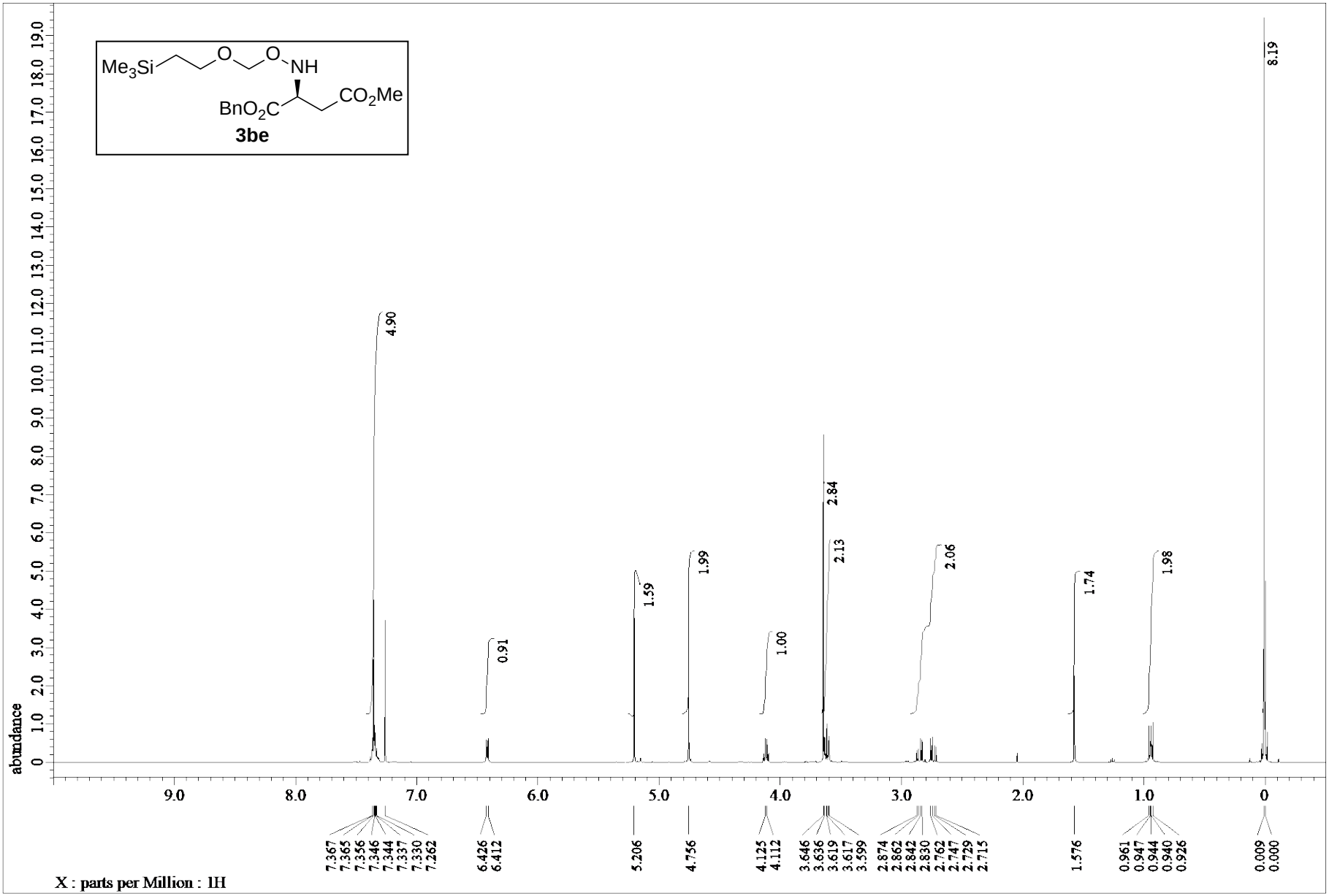
Me3Si
O
O
NH
BnO2C
CO2Me
3be
abundance
X : parts per Million : 1H
8.19
4.90
2.84
2.13
2.06
1.99
1.98
1.74
1.59
1.00
0.91
7.367
7.365
7.356
7.346
7.344
7.337
7.330
7.262
6.426
6.412
5.206
4.756
4.125
4.112
3.646
3.636
3.619
3.617
3.599
2.874
2.862
2.842
2.830
2.762
2.747
2.729
2.715
1.576
0.961
0.947
0.944
0.940
0.926
0.009
0.000

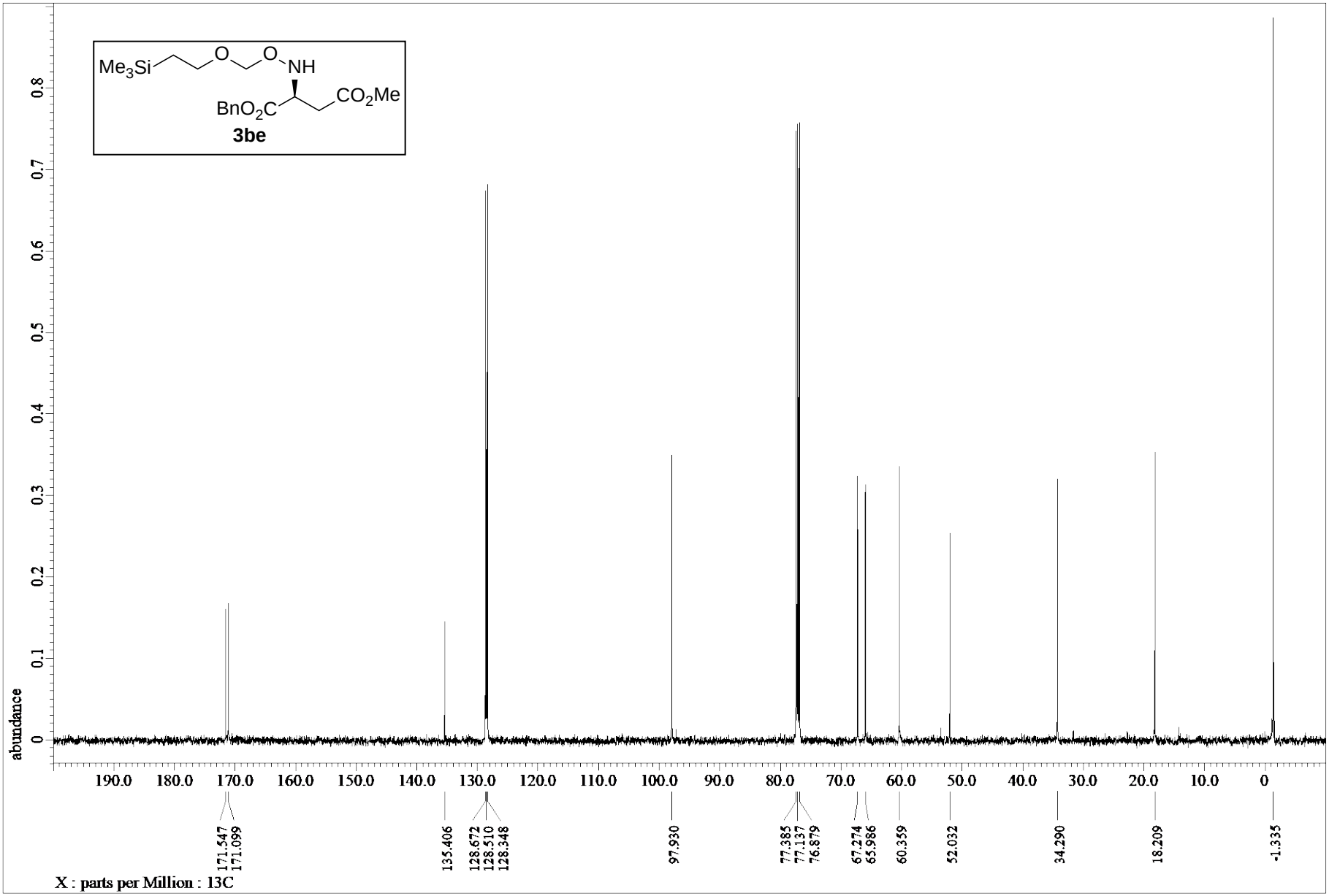
Me3Si
O
O
NH
BnO2C
CO2Me
3be
abundance
0
0.1
0.2
0.3
0.4
0.5
0.6
0.7
0.8
190.0
180.0
170.0
160.0
150.0
140.0
130.0
120.0
110.0
100.0
90.0
80.0
70.0
60.0
50.0
40.0
30.0
20.0
10.0
0
171.547
171.099
135.406
128.672
128.510
128.348
97.930
77.385
77.137
76.879
67.274
65.986
60.359
52.032
34.290
18.209
-1.335
X : parts per Million : 13C

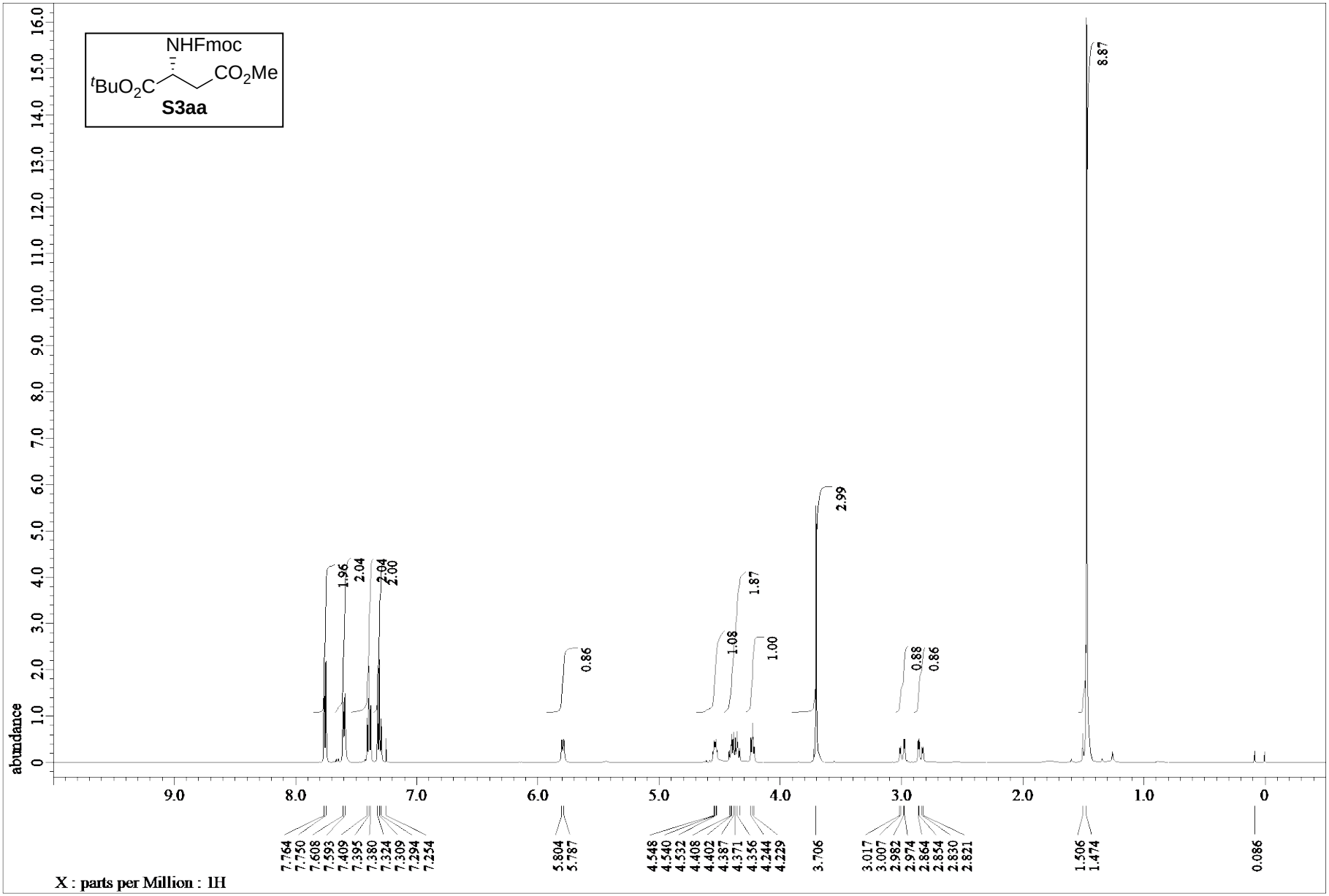
NHFmoc
tBuO2C
CO2Me
S3aa
abundance
X : parts per Million : 1H
8.87
2.99
1.96
2.04
2.04
2.00
1.87
1.08
1.00
0.86
0.88
0.86
7.764
7.750
7.608
7.593
7.409
7.395
7.380
7.324
7.309
7.294
7.254
5.804
5.787
4.548
4.540
4.532
4.408
4.402
4.387
4.371
4.356
4.244
4.229
3.706
3.017
3.007
2.982
2.974
2.864
2.854
2.830
2.821
1.506
1.474
0.086

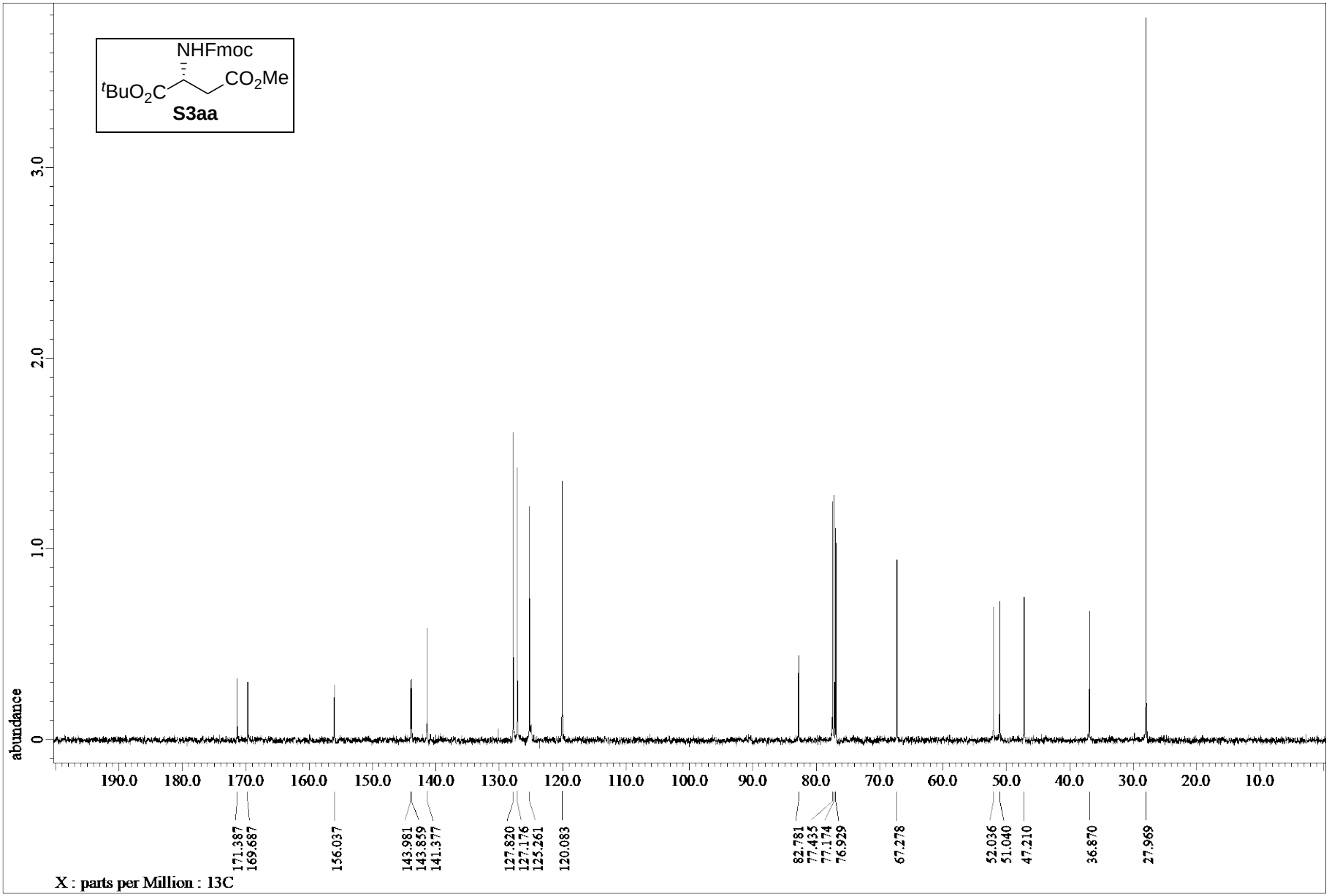
NHFmoc
tBuO2C
CO2Me
S3aa
abundance
3.0
2.0
1.0
0
190.0
180.0
170.0
160.0
150.0
140.0
130.0
120.0
110.0
100.0
90.0
80.0
70.0
60.0
50.0
40.0
30.0
20.0
10.0
171.387
169.687
156.037
143.981
143.859
141.377
127.820
127.176
125.261
120.083
82.781
77.435
77.174
76.929
67.278
52.036
51.040
47.210
36.870
27.969
X : parts per Million : 13C

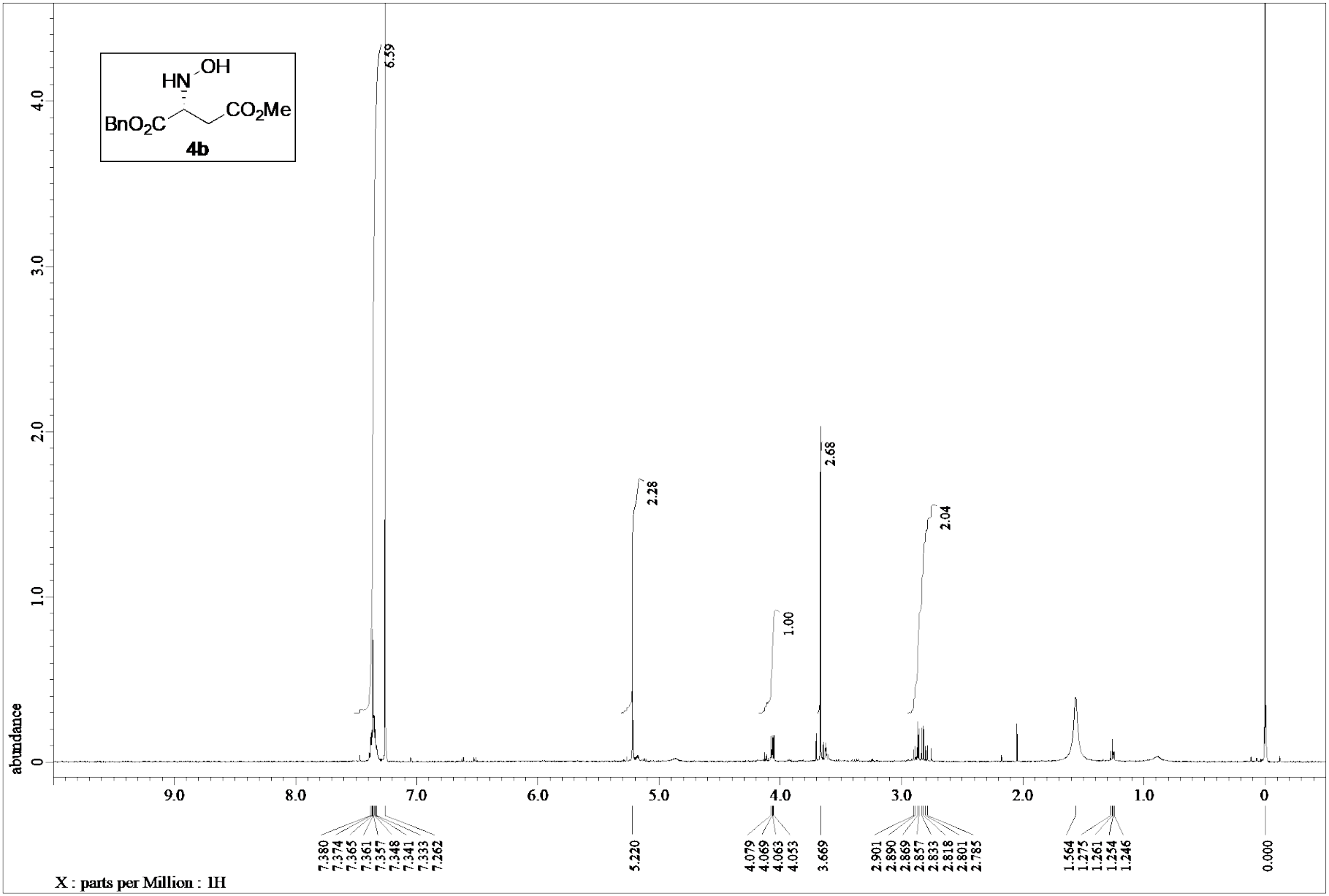
HN
OH
BnO2C
CO2Me
4b
6.59
2.28
1.00
2.68
2.04
abundance
4.0
3.0
2.0
1.0
0
9.0
8.0
7.0
6.0
5.0
4.0
3.0
2.0
1.0
0
7.380
7.374
7.365
7.361
7.357
7.348
7.341
7.333
7.262
5.220
4.079
4.069
4.063
4.053
3.669
2.901
2.890
2.869
2.857
2.833
2.818
2.801
2.785
1.564
1.275
1.261
1.254
1.246
0.000
X : parts per Million : 1H

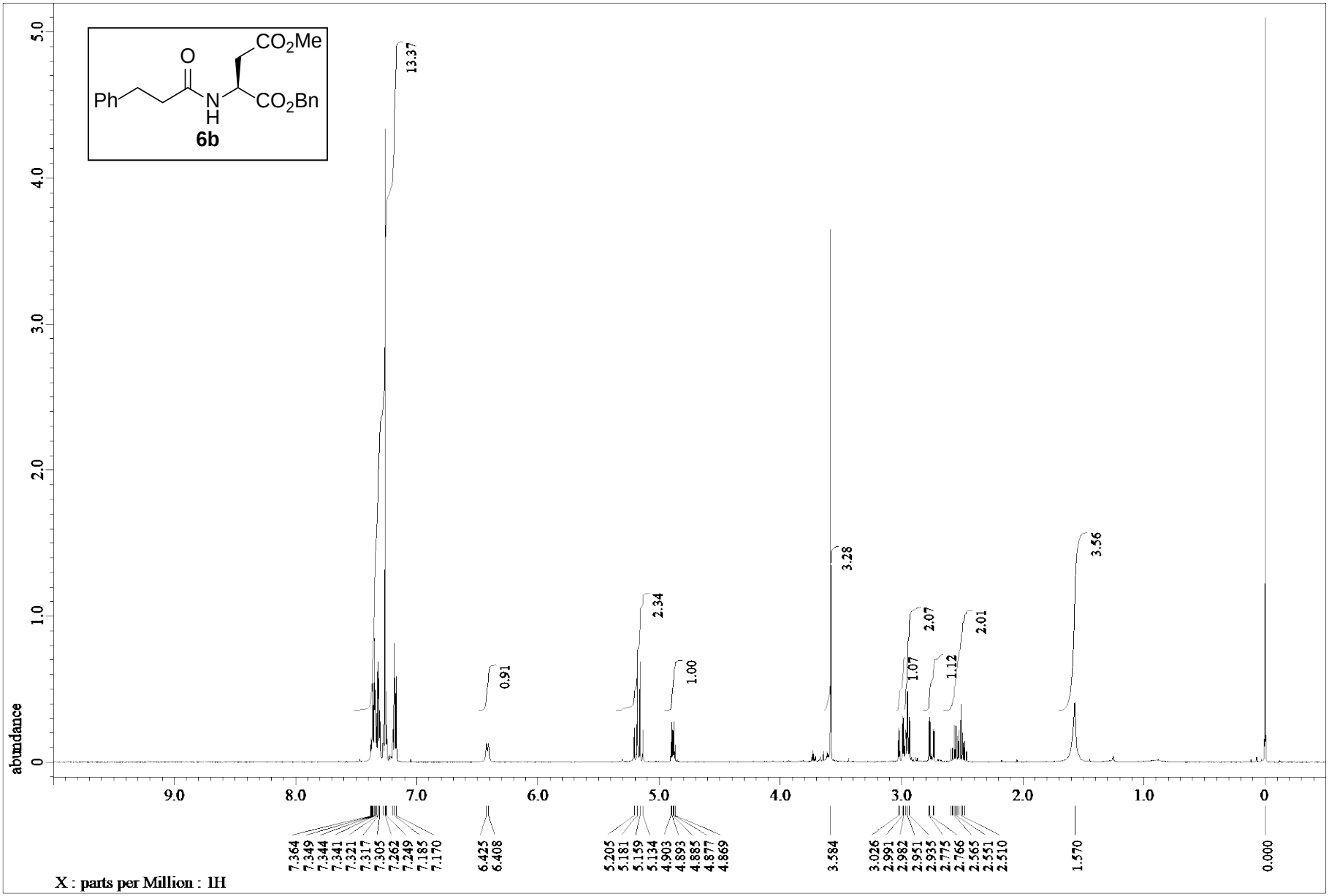
CO2Me
O
Ph
N
H
CO2Bn
6b
13.37
0.91
2.34
1.00
3.28
1.07
2.07
1.12
2.01
3.56
abundance
X : parts per Million : 1H
7.364
7.349
7.344
7.341
7.321
7.317
7.305
7.262
7.249
7.185
7.170
6.425
6.408
5.205
5.181
5.159
5.134
4.903
4.893
4.885
4.877
4.869
3.584
3.026
2.991
2.982
2.951
2.935
2.775
2.766
2.565
2.551
2.510
1.570
0.000

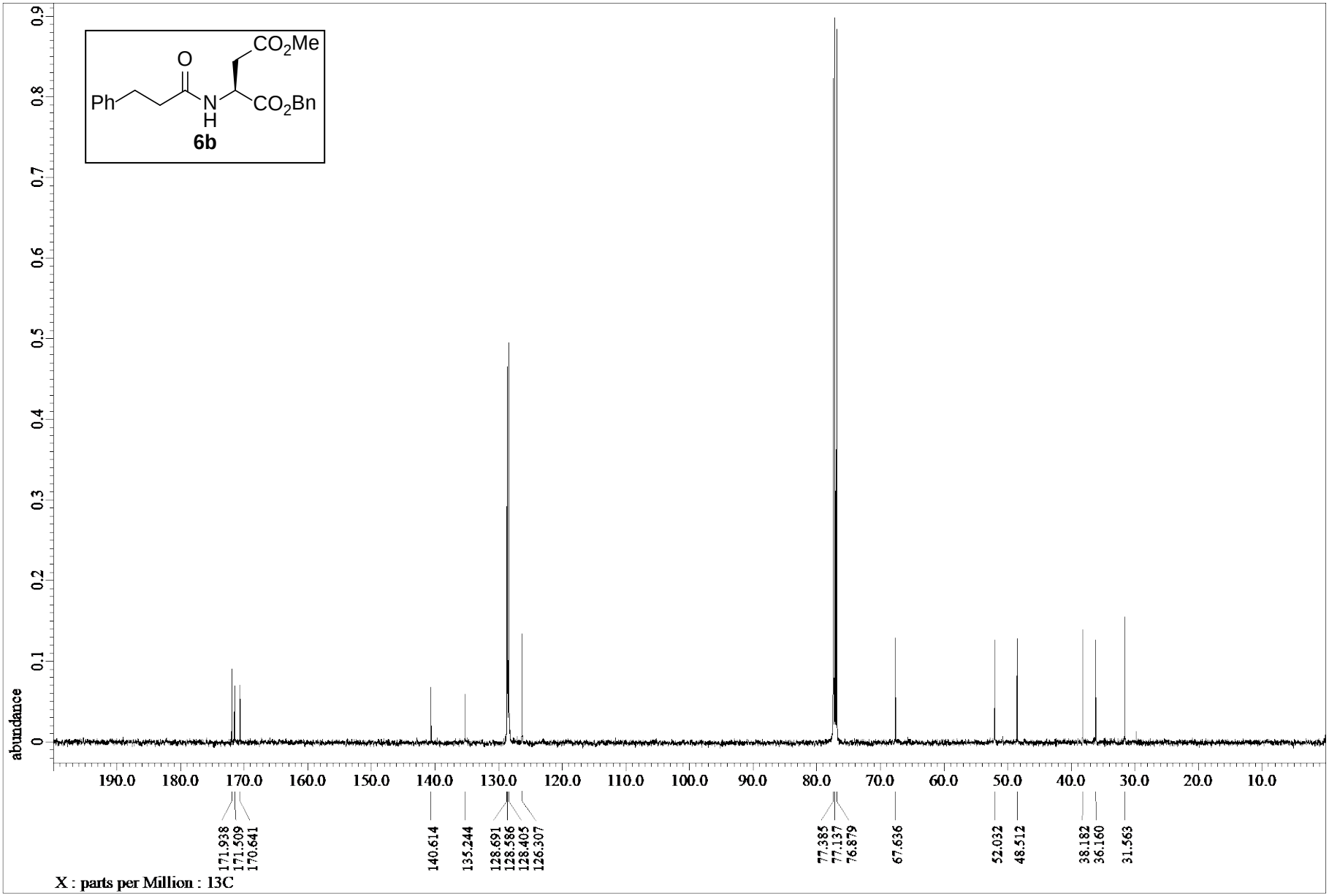
CO2Me
O
Ph
N
H
CO2Bn
6b
abundance
0
0.1
0.2
0.3
0.4
0.5
0.6
0.7
0.8
0.9
190.0
180.0
170.0
160.0
150.0
140.0
130.0
120.0
110.0
100.0
90.0
80.0
70.0
60.0
50.0
40.0
30.0
20.0
10.0
171.938
171.509
170.641
140.614
135.244
128.691
128.586
128.405
126.307
77.385
77.137
76.879
67.636
52.032
48.512
38.182
36.160
31.563
X : parts per Million : 13C

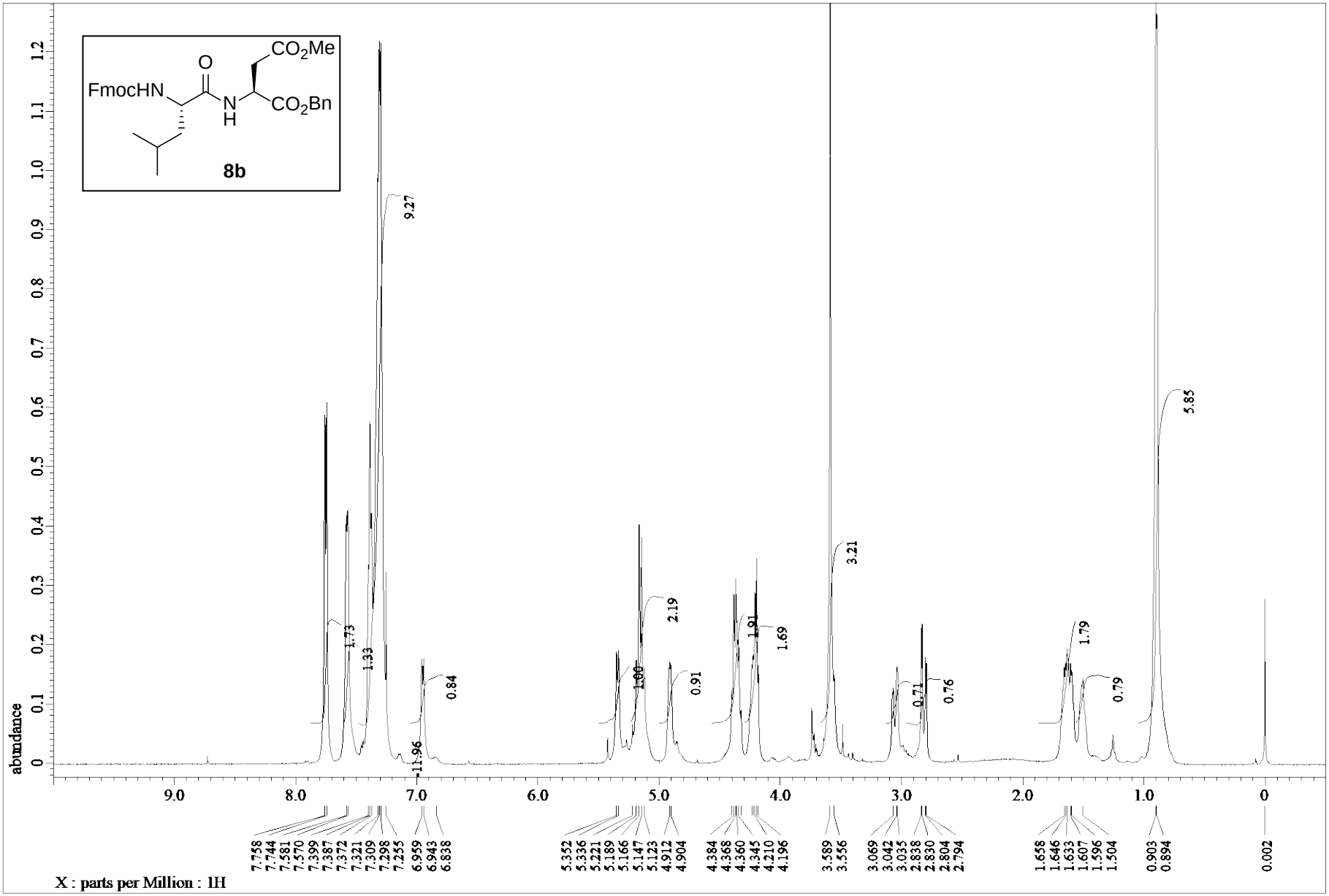
FmocHN
O
N
H
CO2Me
CO2Bn
8b
abundance
X : parts per Million : 1H
9.27
1.73
1.33
0.84
11.96
2.19
1.00
0.91
1.91
1.69
3.21
0.71
0.76
1.79
0.79
5.85
7.758
7.744
7.581
7.570
7.399
7.387
7.372
7.321
7.309
7.298
7.255
6.959
6.943
6.838
5.352
5.336
5.221
5.189
5.166
5.147
5.123
4.912
4.904
4.384
4.368
4.360
4.345
4.210
4.196
3.589
3.556
3.069
3.042
3.035
2.838
2.830
2.804
2.794
1.658
1.646
1.633
1.607
1.596
1.504
0.903
0.894
0.002

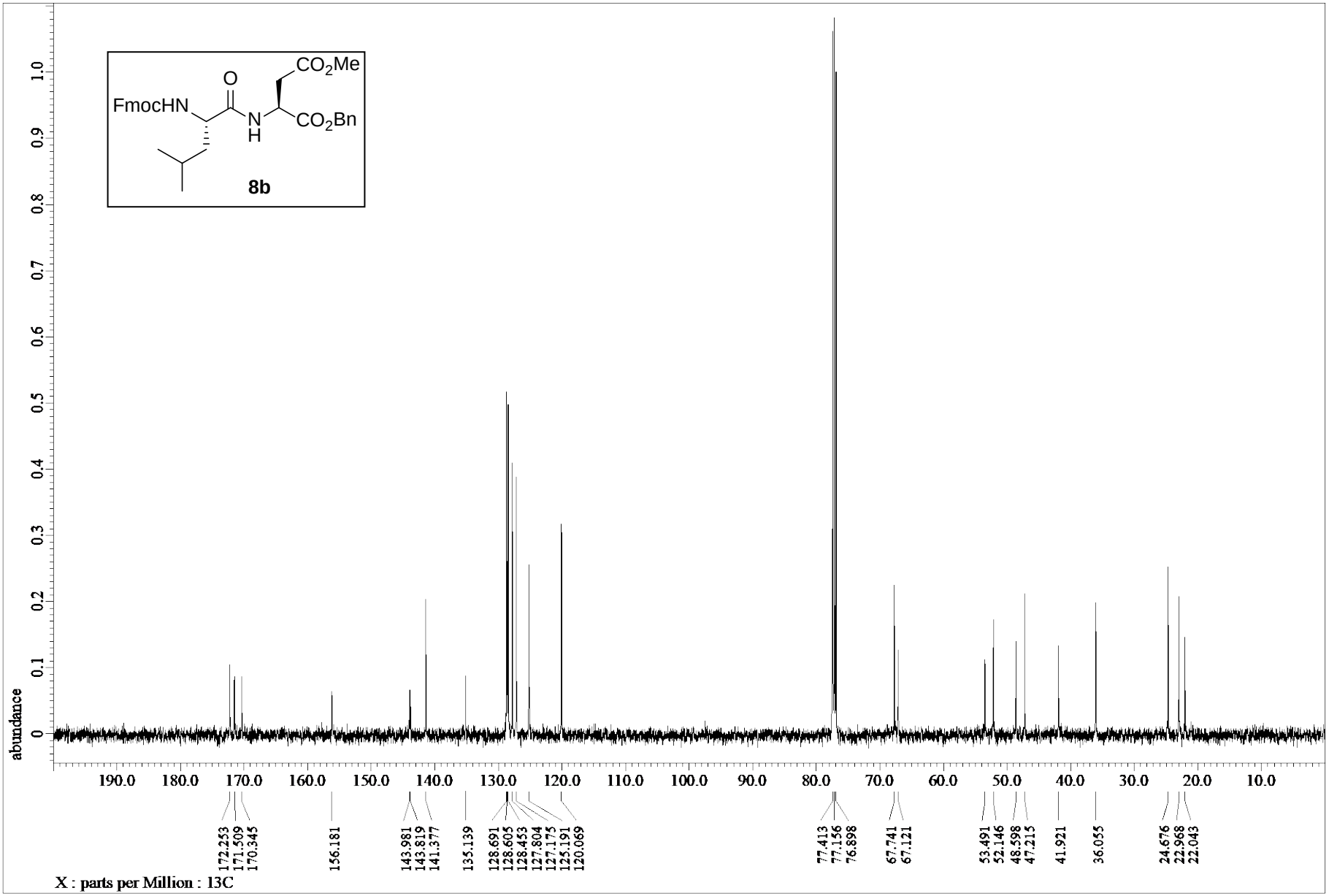
FmocHN
O
N
H
CO2Me
CO2Bn
8b
abundance
X : parts per Million : 13C
172.253
171.509
170.345
156.181
143.981
143.819
141.377
135.139
128.691
128.605
128.453
127.804
127.175
125.191
120.069
77.413
77.156
76.898
67.741
67.121
53.491
52.146
48.598
47.215
41.921
36.055
24.676
22.968
22.043

(G) HPLC Traces

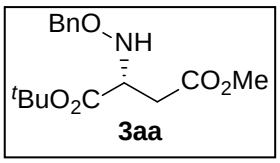

3aa

<Chromatogram>

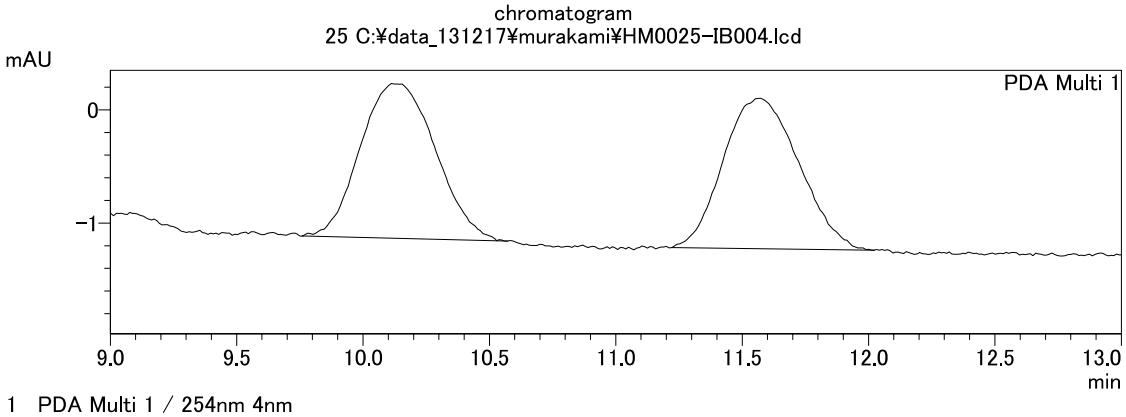

1 PDA Multi 1 / 254nm 4nm

<Peak Report>

peak table C:¥data_131217¥murakami¥HM0025-IB004.lcd

PDA Ch1 254nm 4nm

peak#	retention time (min)	area	area (%)
1	10.110	28220	50.566
2	11.563	27589	49.434

<Chromatogram>

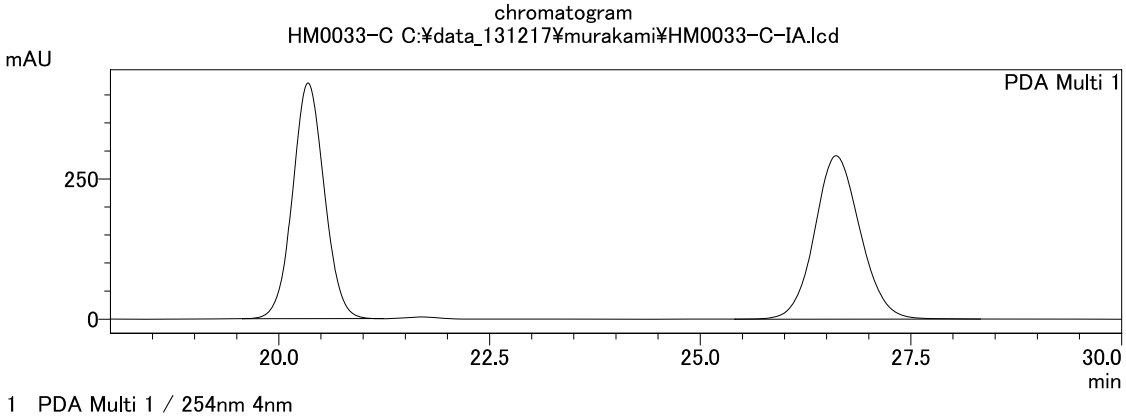

1 PDA Multi 1 / 254nm 4nm

<Peak Report>

peak table C:¥data_131217¥murakami¥HM0033-C-IA.lcd

PDA Ch1 254nm 4nm

peak#	retention time (min)	area	area (%)
1	20.340	11004240	50.134
2	26.606	10945554	49.866

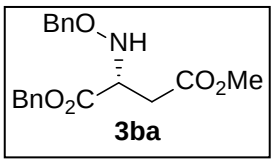

3ba

<Chromatogram>

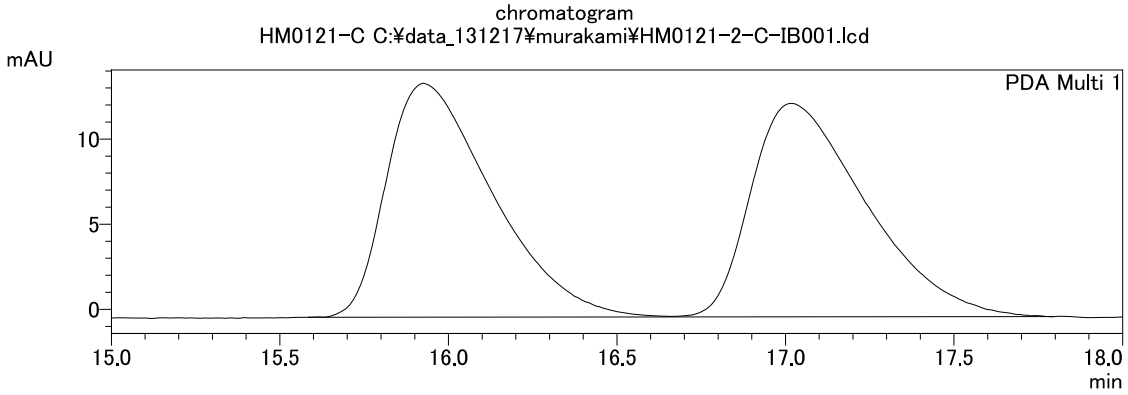

1 PDA Multi 1 / 254nm 4nm

<Peak Report>

peak table C:¥data_131217¥murakami¥HM0121-2-C-IB001.lcd

PDA Ch1 254nm 4nm

peak#	retention time (min)	area	area (%)
1	15.920	300238	50.167
2	17.012	298243	49.833

<Chromatogram>

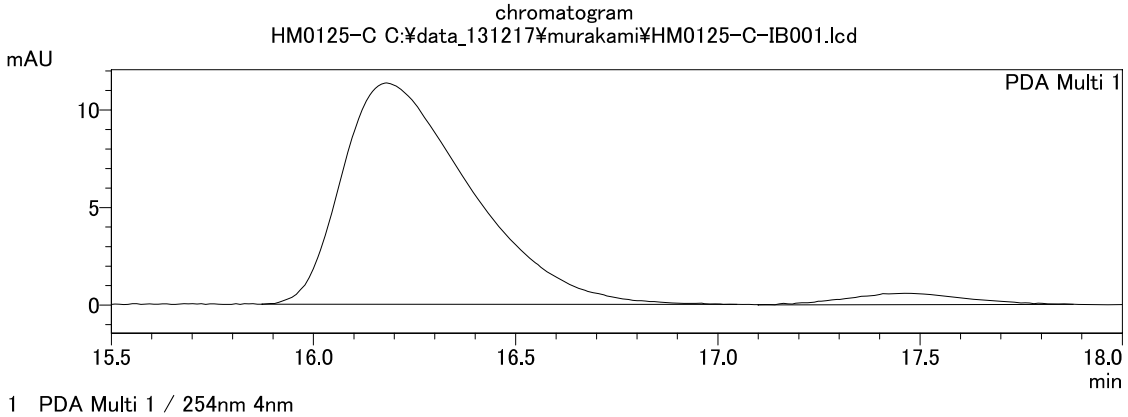

1 PDA Multi 1 / 254nm 4nm

<Peak Report>

peak table C:¥data_131217¥murakami¥HM0125-C-IB001.lcd

PDA Ch1 254nm 4nm

peak#	retention time (min)	area	area (%)
1	16.175	249368	95.468
2	17.454	11837	4.532

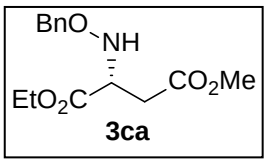

3ca

<Chromatogram>

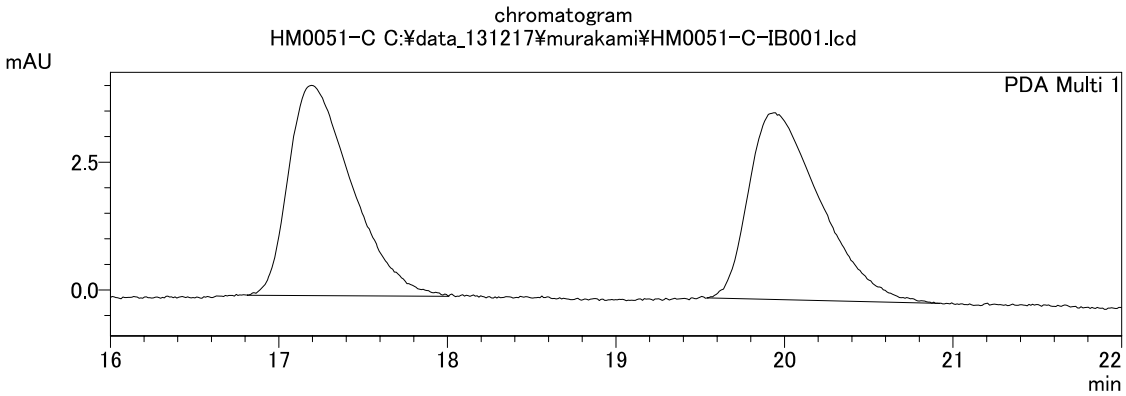

1 PDA Multi 1 / 254nm 4nm

<Peak Report>

peak table C:¥data_131217¥murakami¥HM0051-C-IB001.lcd

PDA Ch1 254nm 4nm

peak#	retention time (min)	area	area (%)
1	17.190	107411	49.860
2	19.936	108013	50.140

<Chromatogram>

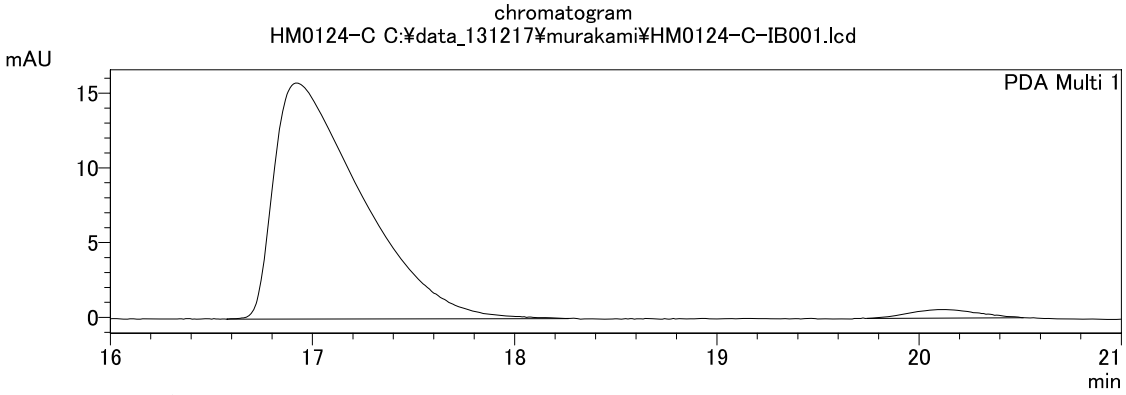

1 PDA Multi 1 / 254nm 4nm

<Peak Report>

peak table C:¥data_131217¥murakami¥HM0124-C-IB001.lcd

PDA Ch1 254nm 4nm

peak#	retention time (min)	area	area (%)
1	16.916	476565	97.175
2	20.131	13852	2.825

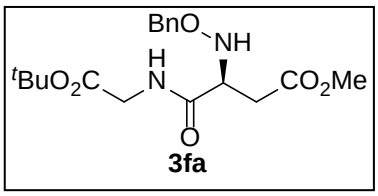

3fa

<Chromatogram>

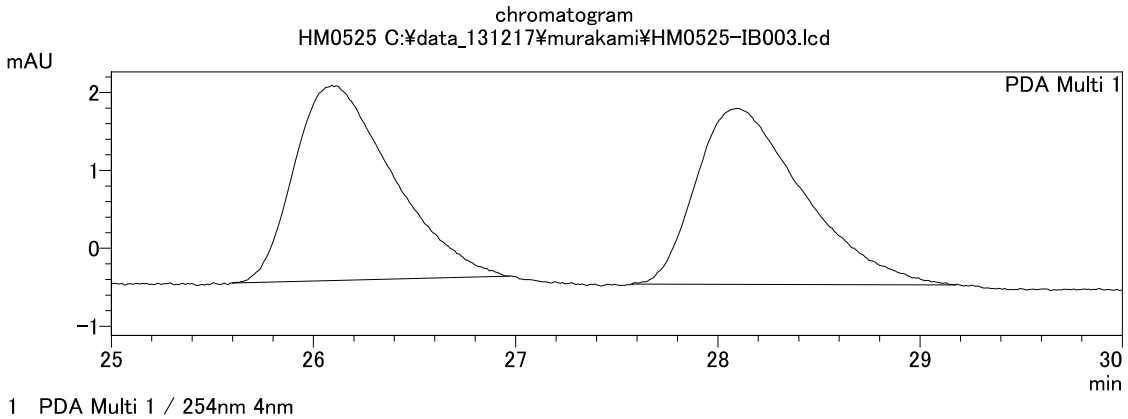

1 PDA Multi 1 / 254nm 4nm

<Peak Report>

peak table C:¥data_131217¥murakami¥HM0525-IB003.lcd

PDA Ch1 254nm 4nm

peak#	retention time (min)	area	area (%)
1	26.085	84655	50.344
2	28.090	83498	49.656

<Chromatogram>

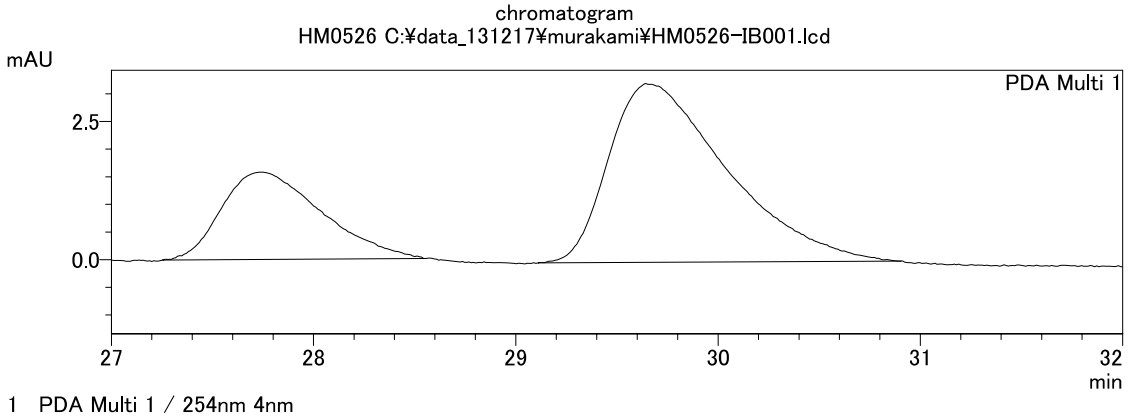

1 PDA Multi 1 / 254nm 4nm

<Peak Report>

peak table C:¥data_131217¥murakami¥HM0526-IB001.lcd

PDA Ch1 254nm 4nm

peak#	retention time (min)	area	area (%)
1	27.732	54324	29.314
2	29.637	130993	70.686

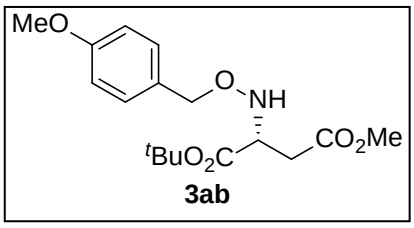

3ab

<Chromatogram>

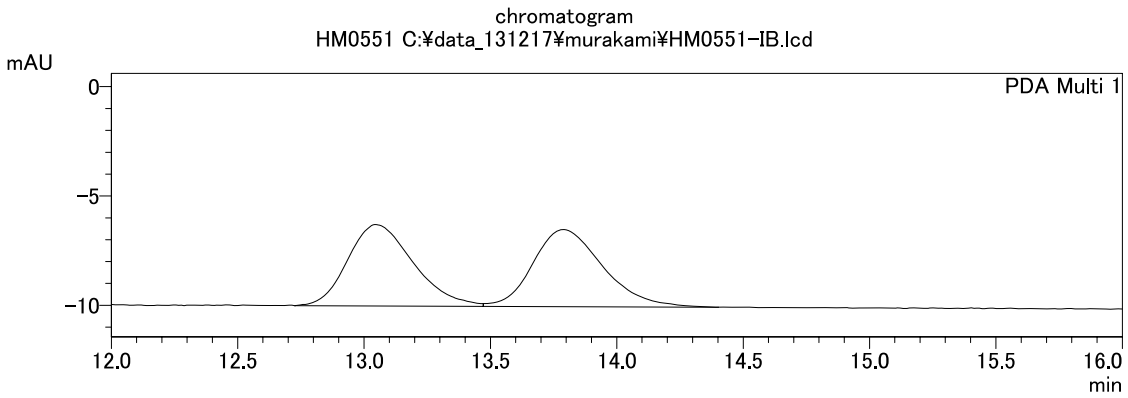

1 PDA Multi 1 / 254nm 4nm

<Peak Report>

peak table C:¥data_131217¥murakami¥HM0551-IB.lcd

PDA Ch1 254nm 4nm

peak#	retention time (min)	area	area (%)
1	13.040	67291	49.834
2	13.784	67740	50.166

<Chromatogram>

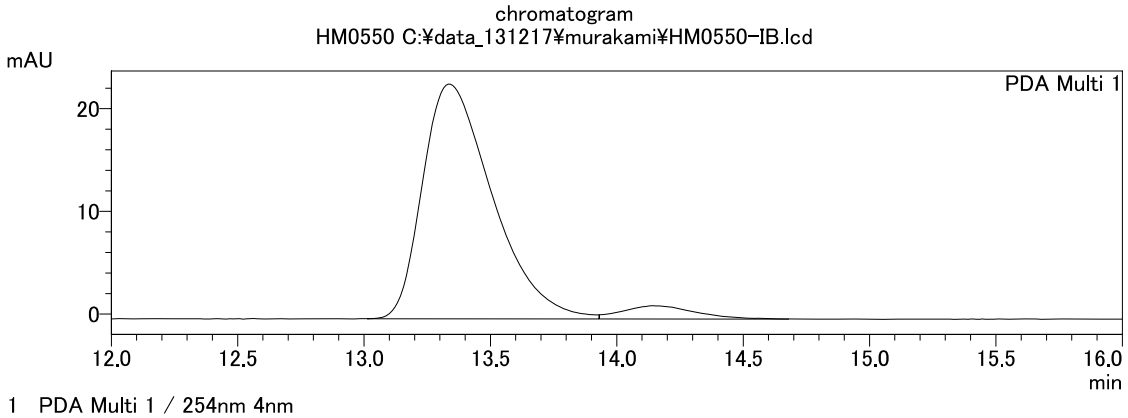

1 PDA Multi 1 / 254nm 4nm

<Peak Report>

peak table C:¥data_131217¥murakami¥HM0550-IB.lcd

PDA Ch1 254nm 4nm

peak#	retention time (min)	area	area (%)
1	13.332	440616	94.445
2	14.132	25918	5.555

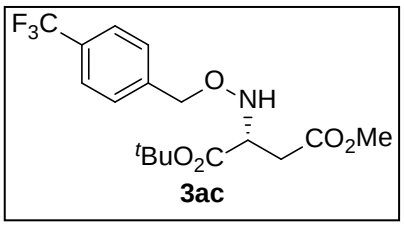

3ac

<Chromatogram>

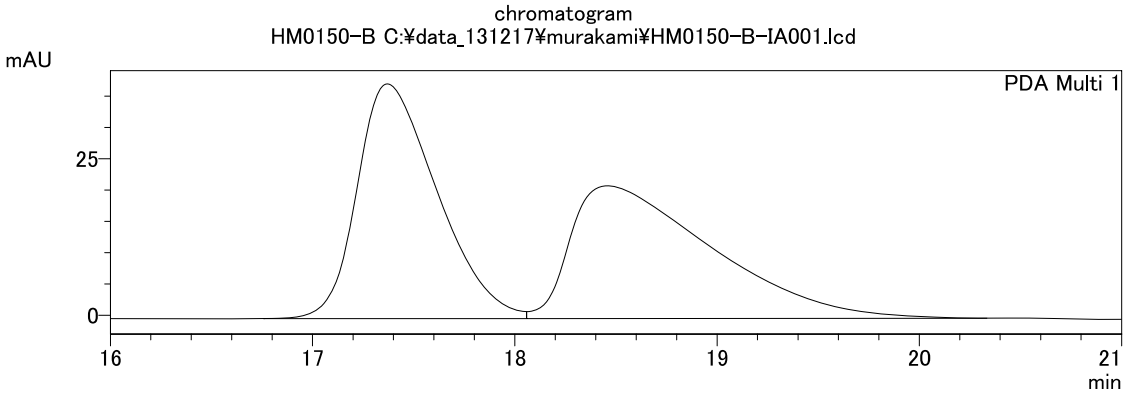

<Peak Report>

peak table C:¥data_131217¥murakami¥HM0150-B-IA001.lcd

PDA Ch1 254nm 4nm

peak#	retention time (min)	area	area (%)
1	17.363	1032118	50.070
2	18.456	1029236	49.930

<Chromatogram>

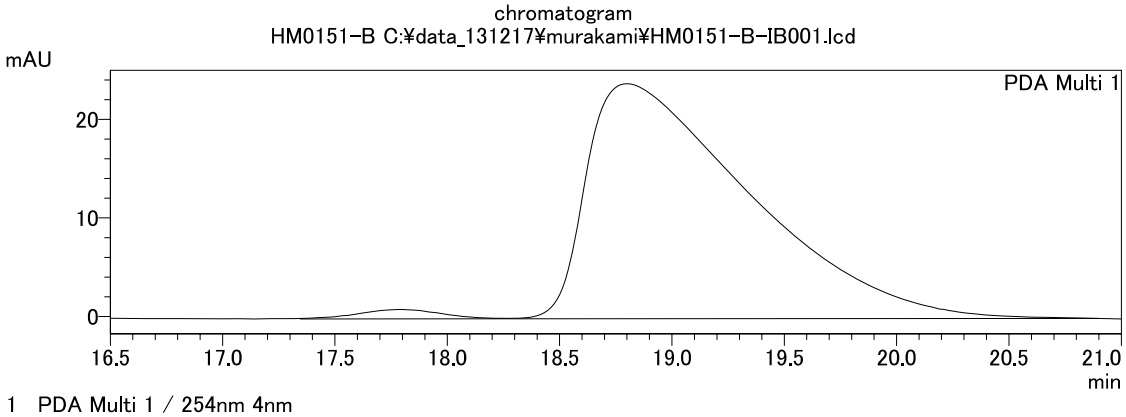

1 PDA Multi 1 / 254nm 4nm

<Peak Report>

peak table C:¥data_131217¥murakami¥HM0151-B-IB001.lcd

PDA Ch1 254nm 4nm

peak#	retention time (min)	area	area (%)
1	17.799	24343	1.981
2	18.800	1204526	98.019

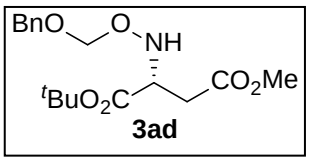

3ad

<Chromatogram>

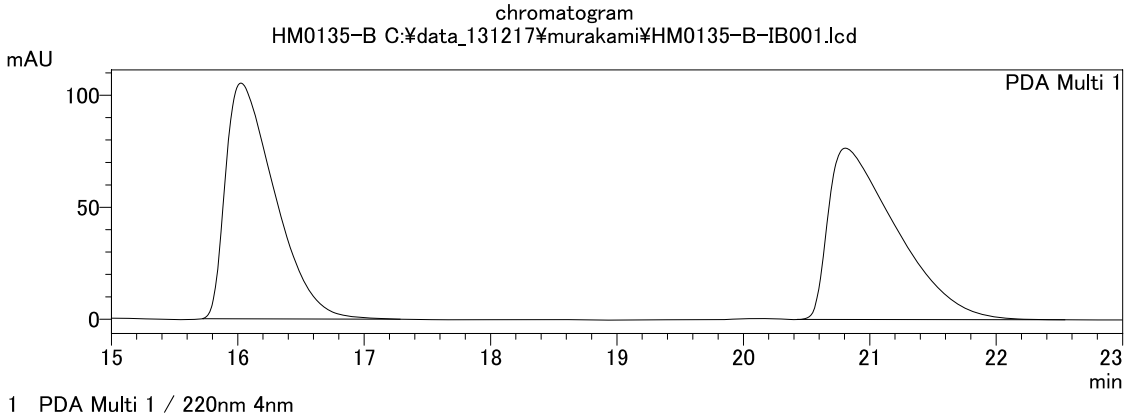

1 PDA Multi 1 / 220nm 4nm

<Peak Report>

peak table C:¥data_131217¥murakami¥HM0135-B-IB001.lcd

PDA Ch1 220nm 4nm

peak#	retention time (min)	area	area (%)
1	16.019	2851908	49.822
2	20.800	2872271	50.178

<Chromatogram>

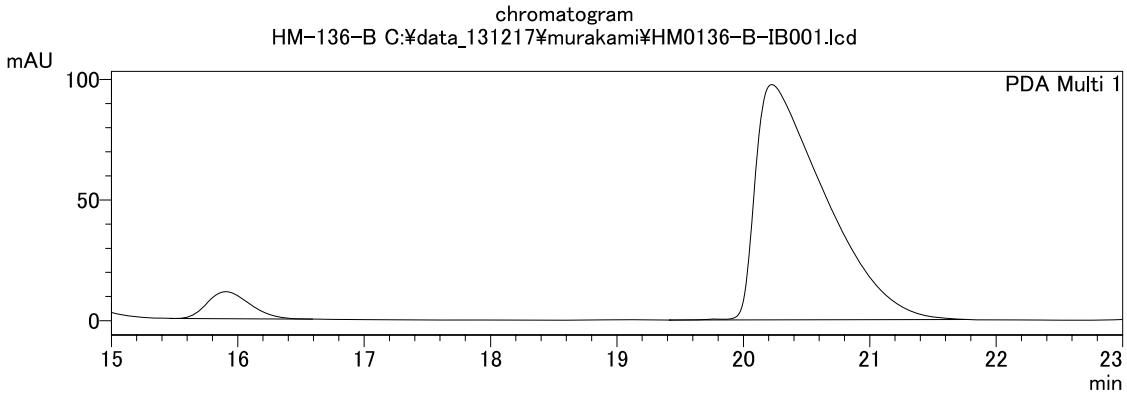

1 PDA Multi 1 / 220nm 4nm

<Peak Report>

peak table C:¥data_131217¥murakami¥HM0136-B-IB001.lcd

PDA Ch1 220nm 4nm

peak#	retention time (min)	area	area (%)
1	15.904	262510	6.579
2	20.219	3727434	93.421

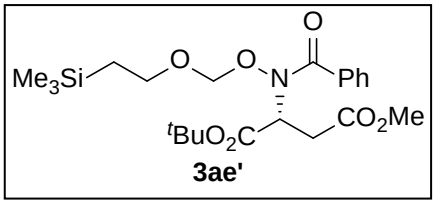

3ae'

<Chromatogram>

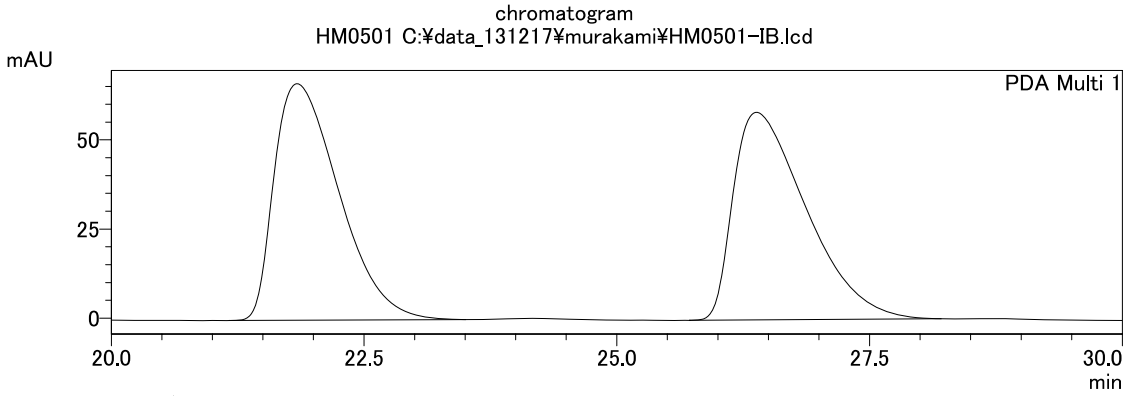

1 PDA Multi 1 / 254nm 4nm

<Peak Report>

peak table C:¥data_131217¥murakami¥HM0501-IB.lcd

PDA Ch1 254nm 4nm

peak#	retention time (min)	area	area (%)
1	21.830	2954870	50.255
2	26.375	2924865	49.745

<Chromatogram>

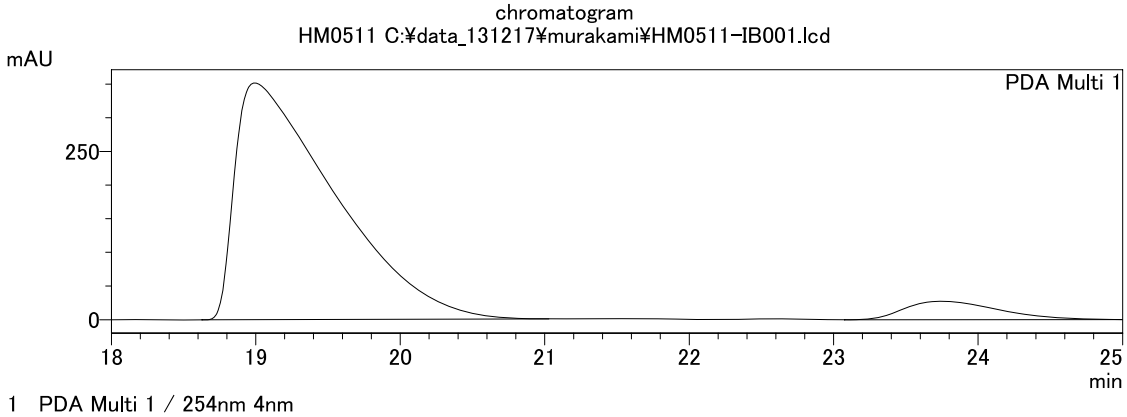

1 PDA Multi 1 / 254nm 4nm

<Peak Report>

peak table C:¥data_131217¥murakami¥HM0511-IB001.lcd

PDA Ch1 254nm 4nm

peak#	retention time (min)	area	area (%)
1	18.988	16853273	93.145
2	23.742	1240399	6.855

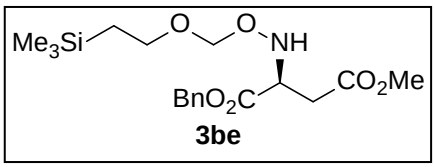

3be

<Chromatogram>

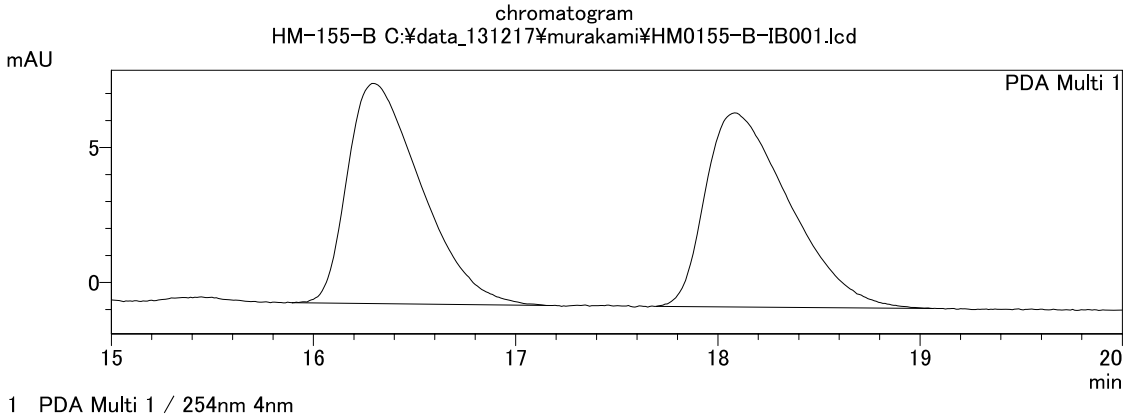

1 PDA Multi 1 / 254nm 4nm

<Peak Report>

peak table C:¥data_131217¥murakami¥HM0155-B-IB001.lcd

PDA Ch1 254nm 4nm

peak#	retention time (min)	area	area (%)
1	16.289	206655	49.880
2	18.079	207647	50.120

<Chromatogram>

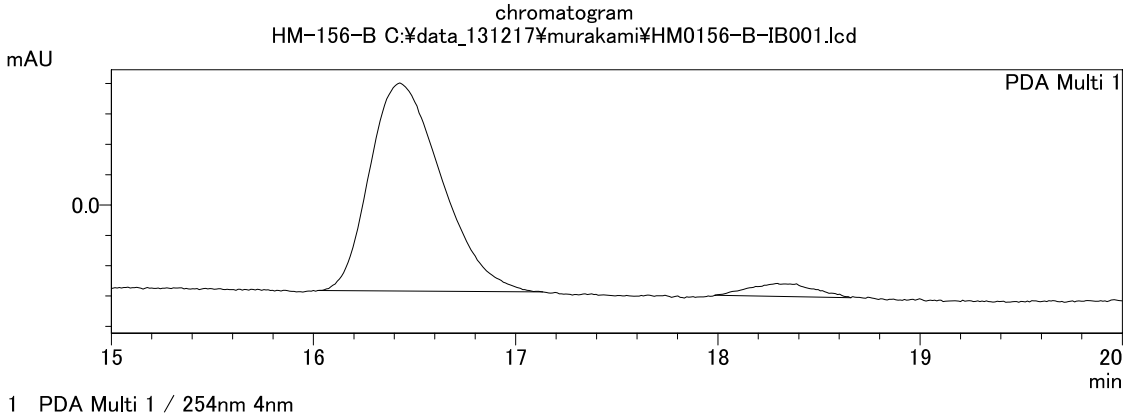

1 PDA Multi 1 / 254nm 4nm

<Peak Report>

peak table C:¥data_131217¥murakami¥HM0156-B-IB001.lcd

PDA Ch1 254nm 4nm

peak#	retention time (min)	area	area (%)
1	16.421	84529	94.632
2	18.287	4795	5.368

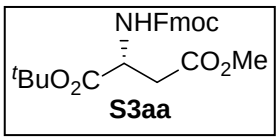

S3aa

<Chromatogram>

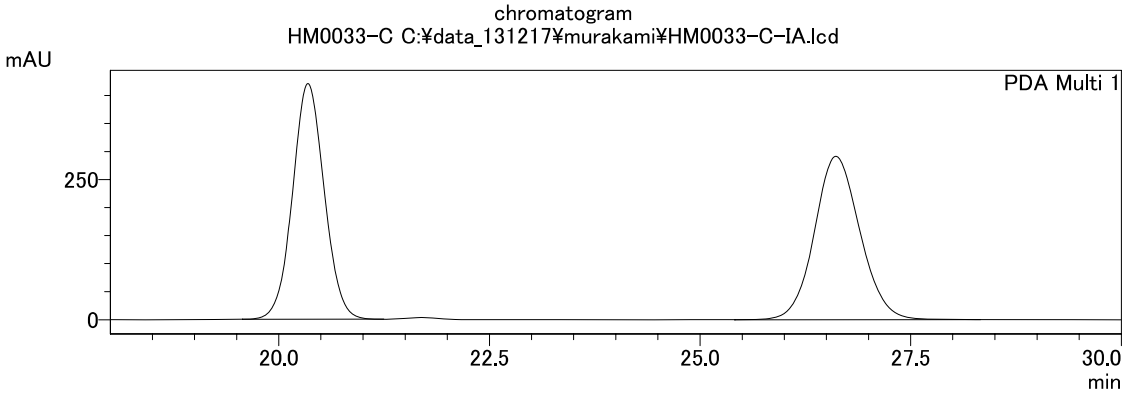

1 PDA Multi 1 / 254nm 4nm

<Peak Report>

peak table C:¥data_131217¥murakami¥HM0033-C-IA.lcd

PDA Ch1 254nm 4nm

peak#	retention time (min)	area	area (%)
1	20.340	11004240	50.134
2	26.606	10945554	49.866

<Chromatogram>

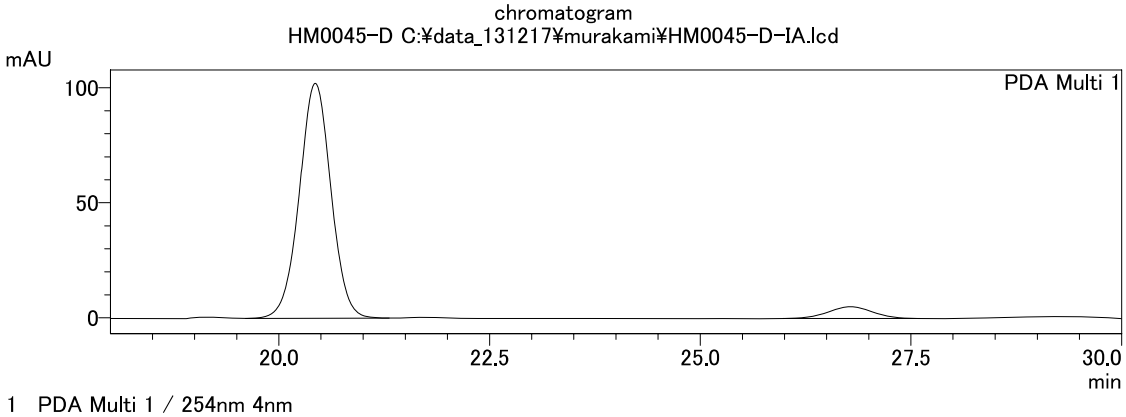

1 PDA Multi 1 / 254nm 4nm

<Peak Report>

peak table C:¥data_131217¥murakami¥HM0045-D-IA.lcd

PDA Ch1 254nm 4nm

peak#	retention time (min)	area	area (%)
1	20.425	2667915	93.426
2	26.772	187744	6.574

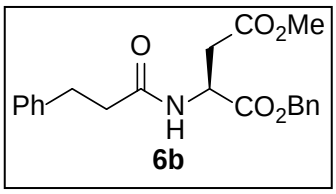

6b

<Chromatogram>

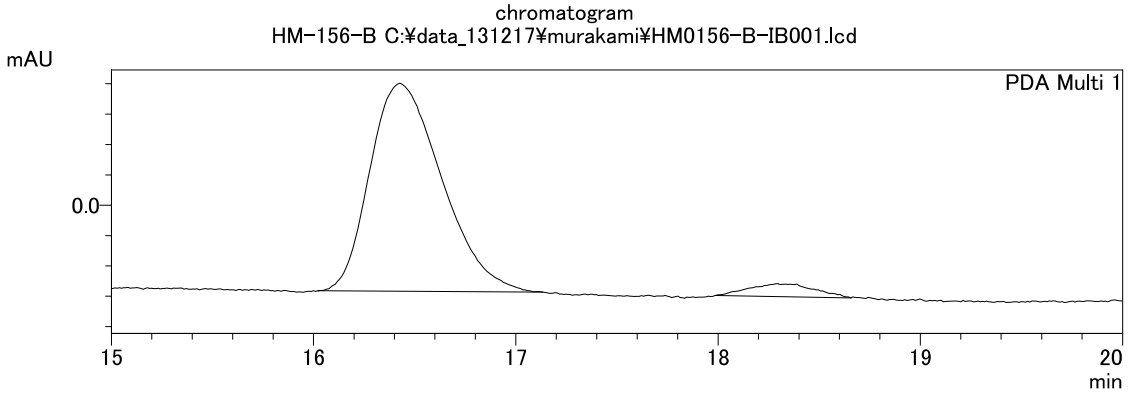

1 PDA Multi 1 / 254nm 4nm

<Peak Report>

peak table C:¥data_131217¥murakami¥HM0156-B-IB001.lcd

PDA Ch1 254nm 4nm

peak#	retention time (min)	area	area (%)
1	16.421	84529	94.632
2	18.287	4795	5.368

<Chromatogram>

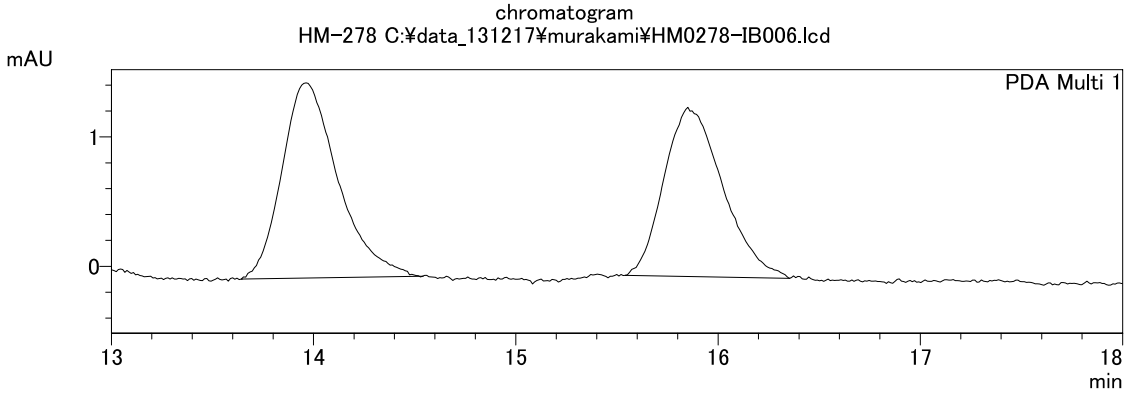

1 PDA Multi 1 / 254nm 4nm

<Peak Report>

peak table C:¥data_131217¥murakami¥HM0278-IB006.lcd

PDA Ch1 254nm 4nm

peak#	retention time (min)	area	area (%)
1	13.958	29089	52.465
2	15.844	26356	47.535